The Pennsylvania State University

The Graduate School

Department of Materials Science and Engineering

POLARIZATION SWITCHING AND FATIGUE ANISOTROPY IN RELAXOR-LEAD TITANATE FERROELECTRIC SINGLE CRYSTALS

A Thesis in

Materials Science and Engineering

by

Metin Ozgul

Submitted in Partial Fulfillment
of the Requirements
for the Degree of

Doctor of Philosophy

December 2003

The thesis of Metin Ozgul was reviewed and approved* by the following:

Clive A. Randall
Professor of Materials Science and Engineering
Thesis Co-Advisor
Co-Chair of Committee

Susan Trolier-McKinstry
Professor of Ceramic Science and Engineering
Thesis Co-Advisor
Co-Chair of Committee

L. Eric Cross
Evan Pugh Professor of Electrical Engineering

Darrell G. Schlom
Professor of Materials Science and Engineering

Venkatraman Gopalan
Assistant Professor of Materials Science and Engineering

James Runt
Professor of Polymer Science
Associate Head for Graduate Studies in Materials Science and Engineering

*Signatures are on file in the Graduate School

ABSTRACT

The hysteretic behavior of ferroelectrics relating polarization and electric field, is utilized for nonvolatile memory applications. Nonvolatile memories are attractive due to the ability to hold information without requiring an external field; i.e., a buck-up battery. One of the critical features of nonvolatile memory devices is typically destructive reading, requiring the ferroelectric to endure large number of electrical cycles during operation. However, decrease of switching charge due to repeated polarization reversal, known as fatigue, is a common problem in bulk and thin film ferroelectrics. Fundamental studies of ferroelectric materials are essential in understanding the origin of fatigue mechanisms. There have been a number of advances to overcome fatigue in ferroelectric films, such as the utilization of oxide electrodes, or using layered type ferroelectrics that exhibit fatigue-free behavior. There still exist certain issues which need to be solved when employing these strategies.

In this study, fatigue anisotropy was discovered in rhombohedral $Pb(Zn_{1/3}Nb_{2/3})O_3$–$PbTiO_3$ (PZN-PT) single crystals. When the electric field is applied along $[001]_C$ or $[110]_C$ orientations, single crystals do not fatigue, while normal fatigue occurs along $[111]_C$ orientations. Further studies focused on the study of the origin of fatigue anisotropy in PZN-PT and other ferroelectric systems. Experiments consistently showed that if a ferroelectric to ferroelectric phase transition occurs (i.e, rhombohedral ---->tetragonal) through composition, temperature, and field strength, fatigue reappears in otherwise “fatigue-free” orientations. These results indicated that the fatigue rates depend on both the ferroelectric phase and crystallographic orientation. Fatigue

anisotropy was investigated also in several other ferroelectric systems including both relaxor based and normal ferroelectrics. Normal ferroelectric $BaTiO_3$ and its solid solutions with $BaZrO_3$ did not exhibit fatigue anisotropy in the rhombohedral phase in $[001]_C$ orientations. From these studies it seems a combination of engineered domain states (orientation) and relaxor nature is required for fatigue free orientations.

Given the relaxor ferroelectric nature of PZN-PT single crystals, the field and frequency dependence of switching and relaxation of sub-coercive field dc field excited polarization were studied as a function of fatigue history. A power law fit gives less field and frequency dependence for $[001]_C$. The behavior remains constant throughout cycling. However, strong field and frequency dependence was noted in $[111]_C$ as a function of fatigue. Polarization relaxation data was analyzed by a stretched exponential function. Fitting parameters indicate a broader time constant distribution for relaxation along $[001]_C$, meaning more diverse contribution to the switching process. These parameters also remained constant with cycling along $[001]_C$. On the other hand, a narrower time constant distribution with a higher stretched exponent was determined along $[111]_C$ direction. With fatigue evolution, changes occur along $[111]_C$. These observations are consistent with the progressive loss of the slower elements from the switched polarization signal, demonstrated in conventional *P-E* loops.

Finally, optical microscopy was performed in PZN-4.5PT single crystals along $[001]_C$ and $[111]_C$ orientations as a function of fatigue (cycling) history. With fatigue evolution, domains became more fractal (discontinuous) along $[111]_C$, whereas the presence of finer domains with a wide size range was noted along $[001]_C$. If these observations can be confirmed by a high magnification microscopy, the microscopic

domain pictures are consistent with the macroscopic electrical characterization findings. This would suggest that the presence of domain structure at a very fine scale in $[001]_C$ rhombohedral crystals may make it extremely difficult to effectively pin the polarization out on cycling. The result is considerable fatigue resistance.

TABLE OF CONTENTS

LIST OF FIGURES

LIST OF TABLES

ACKNOWLEDGMENTS

I am exceedingly grateful to my parents, Ali Osman and Fatma Ozgul, for their love, support, and sacrifice from the very first day of my journey of life. If it were not for their vision with respect to my education, I would have been perfecting my farming skills in the small village I was born in instead of discovering the mysteries of scientific life. . A successful journey starts with good preparation. I must acknowledge my brothers, Tekin and Mustafa, and sister, Nursen. Together with we made a great family, which I believe is the basis for a bright future. As I began my pursuit of higher dreams in State College, I found a great helper, a source of inspiration, and love which were prerequisites for completion of this dissertation. This was my wife, Amine. With a degree as a physical therapist, she would have chosen to build a career for herself. Instead, she was always there for me and walked through all the difficult aspects of life with me. I appreciate her great sacrifice for making my life more beautiful and meaningful and for postponing her own educational dreams for me and our two golden sons , Selman and Enes. I also extend my thanks to her parents, Ahmet and Naile, and family, Elif, Fevziye, and Erdal, for their trust in me as I took a part of them far away.

For the opportunity to study in the U.S., I owe huge thanks filled with gratefulness to the Turkish government and the Turkish nation. I am committed to do my best to share the knowledge and experience I have acquired here with members of this great country as well as all humanity.

Living abroad and having the chance to see and know people from other parts of the world is a privilege as well as a fundamental pillar of peace and a better world. The multi-cultural and peaceful society of State College made me believe with conviction that the concept of diversity can be realized. As a member of the Turkish Student Association (TSA), I had the chance to continue to fulfill my interests in literature and poetry with Turkuaz, a TSA student bulletin. I thank everyone in the Turkish community for their friendship and for making life easier.

It is my strong belief that academic success is closely related to the choice of the right mentors and advisors. I had the privilege and honor to pursue my Ph.D. studies under the guidance and direction of two outstanding professors, Dr. Clive A. Randall and Dr. Susan Trolier-McKinstry. At the end of this work, I have not only finished my Ph.D. but also become a "perfectionist." I am deeply thankful for their help, support, and patience in my progress of academic learning and exploration.

I also would like to express my gratitude to the rest of my committee members: Dr. L. Eric Cross, Dr. Darrell G. Schlom, and Dr. Venkatraman Gopalan for their invaluable, insightful comments and suggestions that improved the quality of this work.

I would also like to acknowledge the contribution of my friends and colleagues. Dr. K. Takemura and Dr. E. Furman deserve special thanks for their collaboration during this study. I also must acknowledge Dr. S. Zhang for his help with sample preparation and the experimental part of this work. My thanks also go to all my colleagues at the Materials Research Laboratory who provided essential help throughout the course of my study: (Dr. S.-E. Park, Dr. S. Priya, B. Jones, S. Atkinson, J. Long, P. Moses, S. Gaylord, J. Aller, B.

Davies). S. Ural is a friend I must thank in particular for his companionship and Sheetz trips for coffee breaks as I was struggling at the MRL for many long and sleepless nights.

My final words will be for the expression of my hope for the future. I wish I would have the chance to visit Penn State many years later with my sons and tell them about my stories as we walk around this beautiful campus.

Chapter 1

INTRODUCTION AND BACKGROUND

It is the intent of this chapter to provide a brief description of ferroelectricity with an emphasis on polarization switching and related issues. Because of their reorientable polarization, ferroelectric materials are being utilized for memory applications. However, continuous polarization reversals lead to several reliability issues, such as the reduction of the switchable polarization. This issue has been addressed in different ferroelectric systems and several mechanisms responsible for the decrease of switchable polarization (polarization fatigue) have been proposed. A brief review of the fatigue studies with major conclusions is provided to clarify the motivation and the focus of this work.

To bring a new insight into polarization fatigue research, relaxor-type ferroelectric compositions with a lead titanate ($PbTiO_3$) end member were chosen as model systems. Single crystals of such systems exhibit greatly anisotropic ferroelectric, piezoelectric, and dielectric properties. Polarization switching and fatigue behavior under electric field cycling can be studied as a function of orientation in light of such earlier explorations. To improve the clarity and understanding of the experimental work and follow-up discussions in this study, the basic characteristics of the relaxor-$PbTiO_3$ systems are also discussed from a structure-property relationship perspective. Specific attention is given to lead zinc niobate $Pb(Zn_{1/3}Nb_{2/3})O_3$-$PbTiO_3$ (PZN-PT) single crystals, as they were chosen for this study.

The order of the issues discussed in this chapter will be as follows;

-Review of ferroelectricity and polarization switching

-Polarization fatigue

-Crystal chemistry and related properties of relaxor based single crystals, i.e., PZN-PT.

1.1 Basic Definitions and Characteristics of Ferroelectric Phenomena

1.1.1 Ferroelectricity and Polarization

Ferroelectricity is a phenomenon which was discovered by Valasek in 1921.[1] Since then, many essential features of the ferroelectric phenomenon were studied and described. Chronological information is provided for the early ferroelectric crystals in Table 1.1**.** Now, many excellent books introducing ferroelectric crystals and explaining ferroelectricity (with a number of phenomenological theories) have been published.[2, 3,4 5, 6, 7, 8, 9, 10, 11, 12] Rochelle Salt ($NaKC_4H_4O_6 \cdot 4H_2O$) was the first material found to show ferroelectric properties, such as a reorientable *spontaneous polarization* ($\boldsymbol{P}_s$), on cooling below a transition temperature ($\boldsymbol{T}_C$; *Curie point*). Many ferroelectrics are low temperature modifications of a high temperature, higher symmetry structure (prototype) which has no spontaneous polarization. This prototypic structure is also called paraelectric. In the ferroelectric phase, modifications to cation and anion positions occur to give relative displacements of ions inside the unit cell, resulting in reversible spontaneous dipole moments. The moment which develops polarization (**P**) is equal to **qd/V**,

Table 1.1 A partial list of early ferroelectric crystals.[10,11,12]

Name and Chemical Formula	Curie Temperature, T_C (°C)	Spontaneous Polarization, P_S (μC/cm^2)	Year in which reported
Rochelle Salt $NaKC_4H_4O_6 \cdot 4H_2O$	23	0.25	1921
Potassium Dihydrogen Phosphate KH_2PO_4 (KDP)	-150	4	1935
Potassium Dihydrogen Arsenate KH_2AsO_4	-177	5	1938
Potassium Dideuterium Phosphate KD_2PO_4	-60	5.5	1942
Barium Titanate $BaTiO_3$	120	26	1945
Lead Titanate $PbTiO_3$	490	>50	1950
Potassium Niobate $KNbO_3$	415	30	1951
Lead Zirconate Titanate* $Pb(Zr_xTi_{1-x})O_3$	~350	>40	1952

*polycrystalline ceramic

where **q** is the electric charge on the displaced ion, **d** is the relative displacement, and **V** is the volume of the unit cell. This moment is related to the electric displacement as;

$$\overline{D} = \chi_0 \chi \overline{E} = \chi_0 \overline{E} + \overline{P} \tag{1.1}$$

where χ_0 and χ are the free space and relative susceptibilities or permittivities, respectively.[3,13]

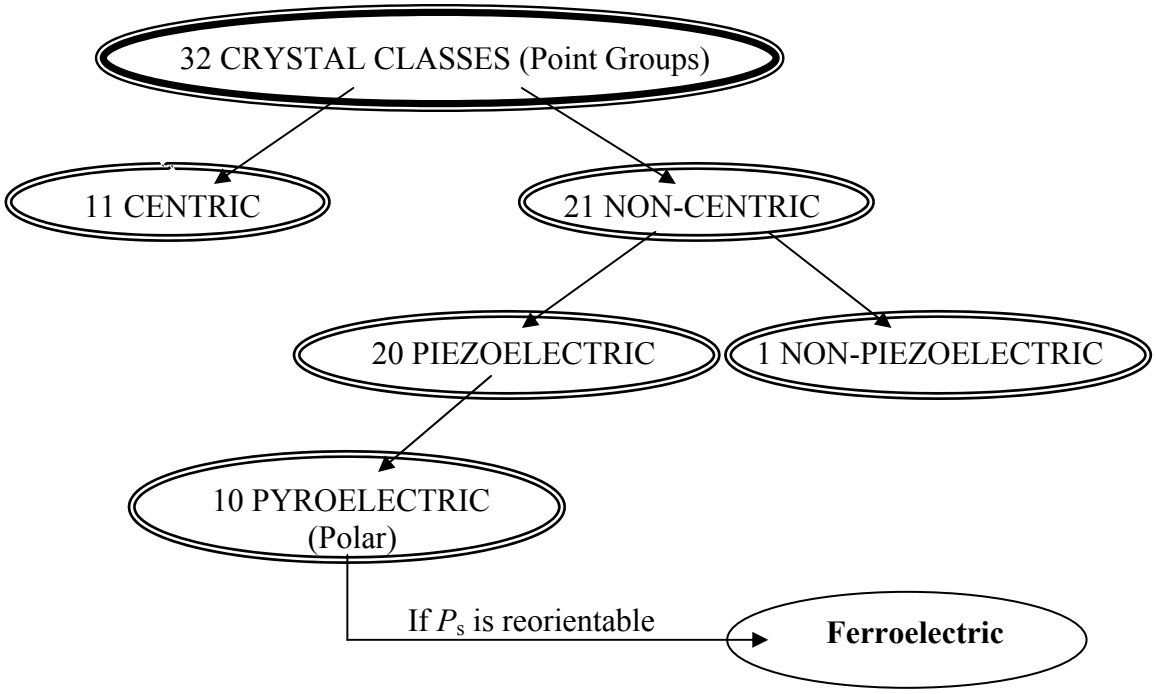

Figure 1.1 A classification scheme for the 32 crystallographic point groups.

1.1.2 Piezoelectricity

All ferroelectric materials are potentially piezoelectric (see Figure 1.1 for a crystal classification). Piezoelectricity is the ability of certain crystalline materials to develop an electrical charge proportional to an applied mechanical stress.[7] This is also called the direct piezoelectric effect. Piezoelectric materials also show a converse effect, where a geometric strain (deformation) is produced on the application of a voltage. The direct and converse piezoelectric effects can be expressed in tensor notation as,

$$P_i = d_{ijk}\sigma_{jk} \qquad \text{(direct piezoelectric effect)} \tag{1.2}$$

$$x_{ij} = d_{kij}E_k \qquad \text{(converse piezoelectric effect)} \tag{1.3}$$

where P_i is the polarization generated along the *i*-axis in response to the applied stress σ_{jk}, and d_{ijk} ($=d_{kij}$) is the piezoelectric coefficient. For the converse effect, x_{ij} is the strain generated in a particular orientation of the crystal on the application of electric field E_k along the *k*-axis.[3]

1.1.3 Perovskite Crystal Structure

Most of the useful ferroelectrics, such as barium titanate (BT), lead titanate ($PbTiO_3$), lead zirconate titanate (PZT), lead lanthanum zirconate titanate (PLZT), and potassium niobate ($KNbO_3$), have the perovskite structure. Perovskite is the mineral

name of calcium titanate ($CaTiO_3$). Its simplest structure is cubic, which is the high temperature form for many mixed oxides of the ABO_3 type. The simple cubic structure (space symmetry P*m3m*) consists of corner sharing oxygen octahedra (BO_6) arranged in three dimensions with smaller, highly charged cations (B: Ti^{4+}, Zr^{4+}, Sn^{4+}, Nb^{5+}, Ta^{5+}, W^{6+}, etc.) located in the middle of the octahedra, and lower charged, larger cations (A: Na^{+}, K^{+}, Ca^{2+}, Ba^{2+}, Pb^{2+}, etc.) in between the octahedra. The structure is shown in Figure 1.2. Most perovskite-type ferroelectrics are compounds with either $A^{2+}B^{4+}O_3^{2-}$ or $A^{1+}B^{5+}O_3^{2-}$ -type formula.[14]

The perovskite structure can be also regarded as a cubic close-packed arrangement of large A and O ions with smaller B ions filling the octahedral interstitial positions. The structure is also very tolerant to cation substitution to both A and B sites of lattice, and hence may lead to more complex compounds, such as $(K_{1/2}Bi_{1/2})TiO_3$, $Pb(Fe_{1/2}Ta_{1/2})O_3$, $Pb(Co_{1/4}Mn_{1/4}W_{1/2})O_3$, $Pb(Mg_{1/3}Nb_{2/3})O_3$, and $Pb(Zn_{1/3}Nb_{2/3})O_3$.[14, 15]

The most important member of the tetragonal phosphates is potassium dihydrogen phosphate (KH_2PO_4), commonly abbreviated as KDP.[11] Common characteristics of these early ferroelectrics are that they are colorless, water-soluble substances, and can be grown in large crystals from solution. As will be discussed later, ferroelectricity is mostly observed in certain temperature regions delimited by transition (or Curie) points ($\boldsymbol{T_c}$) above which the crystals are no longer ferroelectric. In Rochelle and KDP, ferroelectricity is present at low temperatures due to their T_c points, +23 and -150 °C, respectively.[11,12] For study of the ferroelectric effect, these crystals served their purpose. However, from the device application point of view, water solubility, low T_C points, and low polarization values are limiting factors.

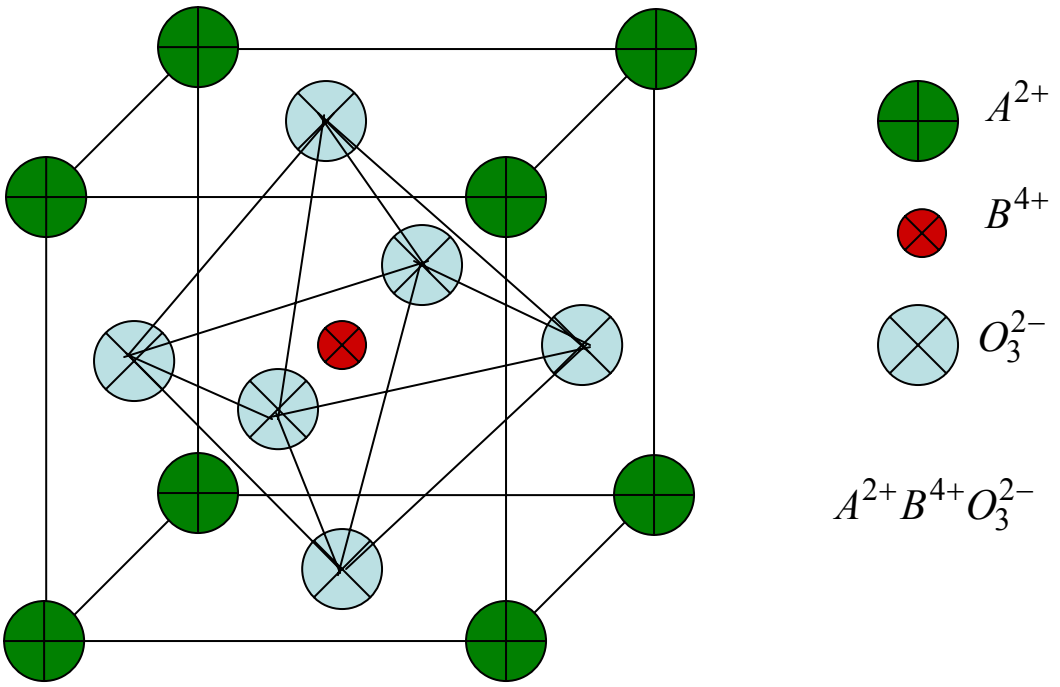

Figure 1.2 A cubic ABO_3 perovskite-type unit cell.

In 1945, barium titanate ($BaTiO_3$), the first ceramic material in which ferroelectric behavior was observed, was reported.[16] With its much simpler structure (perovskite), better ferroelectric properties, chemical and mechanical stability, barium titanate (BT) became one of the most extensively studied ferroelectric materials.[10] $BaTiO_3$ was considered not only as a model system for ferroelectricity, but also for practical applications. Added to the chemical and mechanical stability, it exhibits ferroelectric properties at and above room temperature and can be easily prepared and used in the form of polycrystalline samples.[12]

By the 1950's the solid solution system $Pb(Ti,Zr)O_3$ (PZT), which also has the perovskite structure, was found to be ferroelectric. PZT compositions are now the most widely exploited of all piezoelectric ceramics both in research and industry. An up to date brief description of BT and PZT systems can be found in ref.[17]

As an example of complex perovskites, a relaxor type ferroelectric system will be discussed separately in a later section.

1.1.4 Ferroelectric Phases and Domains

Ferroelectrics may exhibit one or more ferroelectric (polar) phases (Figure 1.3) that show a *domain structure* in which the individual domain states can be reoriented by an applied field. In a ferroelectric crystal usually there are many domains (regions with uniform polarization). Within each individual domain, all the electric dipoles are aligned in the same direction. These domains in a crystal are separated by interfaces called *domain walls*.[14] Since these walls differ from the perfect crystal, there is a certain amount

of energy (W_{dw}; domain wall energy) associated with them, in addition to the elastic energy, W_e. From energy considerations, in real materials, domain patterns depend on many factors, including the existing defect structure and concentration, stress and electric history, boundary conditions, temperature relative to T_c, and even the history of crystal preparation.[10,18]

The ferroelectric domains were first demonstrated in astudy of spontaneous birefringence.[19,20] The explanation for the origin of a ferroelectric domain, from a phenomenological point of view, is that the polydomain system is in a state of minimum free energy. From a microscopic viewpoint, domains were attributed to the change in the electrostatic forces acting on the crystal's faces owing to the spontaneous polarization that occurs as the crystal goes through the paraelectric-ferroelectric phase transition. Figure 1.4 depicts 180° domain formation which minimizes the electrostatic energy of the system. Defects and internal stresses must be also considered for a crystal that exhibits piezoelectricity in the paraelectric state.[14] The presence of mechanical stress in a crystal results in the development of non-180° domain walls configured to minimize the strain. An example is presented in Figure 1.5.[17]

The structure of a ferroelectric domain depends on the structure of the crystal. In a ferroelectric crystal, the variety of domain patterns and the number of types of domain walls depend on the number of orientations of the dipole moment when the spontaneous polarization occurs from the prototype phase.

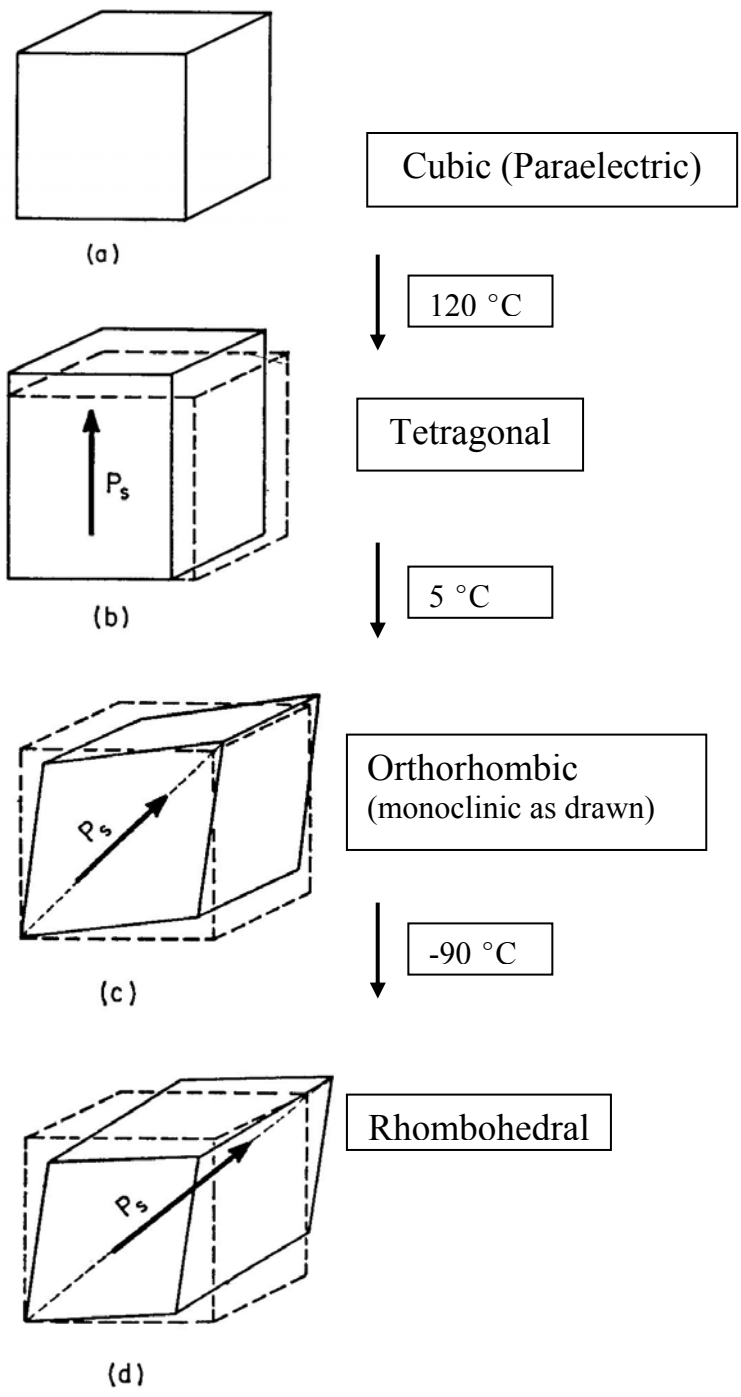

Figure 1.3 Unit cells of the four phases of $BaTiO_3$: a) Cubic, stable above 120 °C (T_C), b) Tetragonal, stable between 120 °C and 5 °C, c) Orthorhombic, stable between 5 °C and -90 °C, (monoclinic as drawn) d) Rhombohedral, stable below -90 °C. (The dotted lines in (b), (c), and (d) delineate the original cubic cell. Arrows indicate the direction of the spontaneous polarization, P_s, in each phase.[12]

Ferroelectric domain structures can be observed by various methods:

a) *Optical birefringence*: In optically anisotropic crystals (where the refractive index for light polarized along the polar axis is different from at least one other axis in a crystal) domains can be observed due to the presence of birefringence by using a polarized light microscope.

b) *Second-harmonic generation*: This technique can be used for any crystal which can be phase matched for second harmonic generation with light depends on the optical interaction length with a single domain of either sign.[10] This technique can be also used to measure the width of extremely small domains with periodic geometry.[21]

c) *Etching and Scanning Electron Microscopy*: For the ferroelectric crystals with sub-micrometer size domain structures, electron microscopy is utilized. Since the information is limited to the surface, very thin crystals are needed. Chemical etching is also commonly used to reveal the domain structures by selective etching of positive and negative ends of domains. Etched samples can be observed by scanning electron microscopes. HCl was commonly used for the early studies in $BaTiO_3$.[4,12]

d) *Powder pattern method*: This technique involves use of a colloidal suspension of charged particles that can preferentially deposit on either positive or negative ends of domains.[22]

e) *Liquid crystal method*: This technique can be used to reveal 180° domain walls.[23] This simple technique is fast and the liquid crystal can respond rapidly to changes of the domain configuration.

f) *X-ray topography*: This technique utilizes anomalous dispersion of X-rays causing a difference between the positive and negative ends of domains.[24]

g) *Transmission Electron Microscopy*: A technique using diffraction contrast methods and can be applied to both 180° and non-180° domains.

Certainly domain observation techniques are not limited to these techniques mentioned here. The usefulness of each technique varies from one material to another, with the shape, size, transparency of the crystal, and the expected outcome of the observations.[10] Sometimes depending on these criteria, these techniques can be combined for the maximum efficiency.

Domain structures are strongly dependent on the symmetry of the ferroelectric phase. As the changes occur in symmetry resulting in different domain configurations, the other material properties will also be influenced. Discussion of the thermodynamics of ferroelectricity is beyond the scope of this thesis but a brief description is given in the following section.

1.1.5 Ferroelectric Phase Transitions and Curie-Weiss Behavior

In most cases, ferroelectrics have a transition temperature called the Curie point, T_c. Exceptions involve melting or decomposition before a T_c is obtained. At a temperature $T>T_c$ the crystal does not exhibit ferroelectricity, while for $T<T_c$ it is ferroelectric.[10,11,12] On decreasing the temperature through the Curie point, a ferroelectric

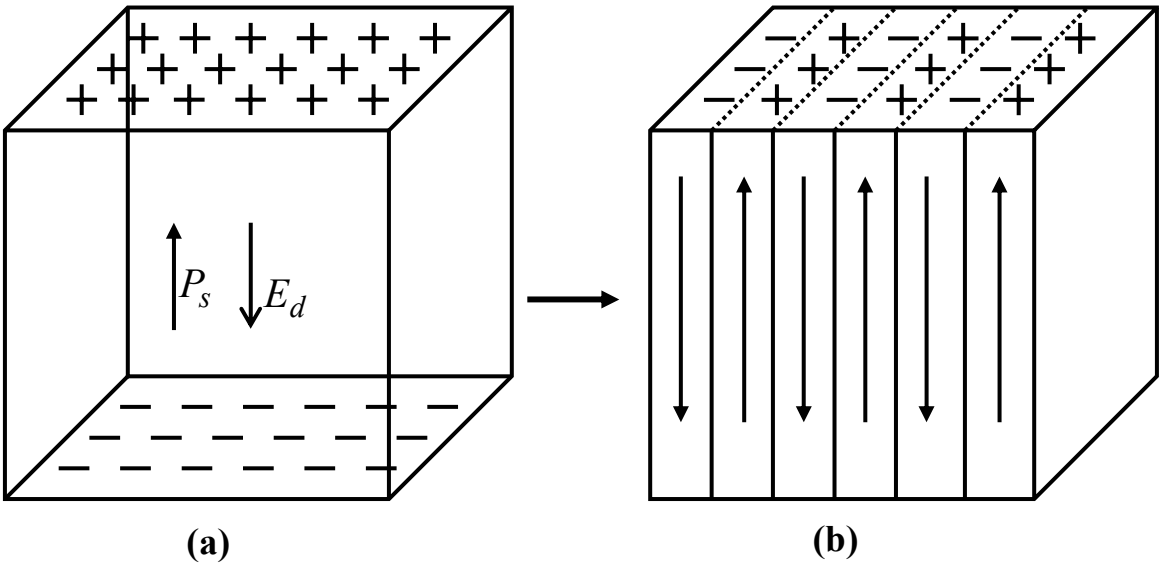

Figure 1.4 a) Surface charge and depolarizing field (E_d) associated with spontaneous polarization (P_s); b) formation of 180° domains to minimize electrostatic energy.[17]

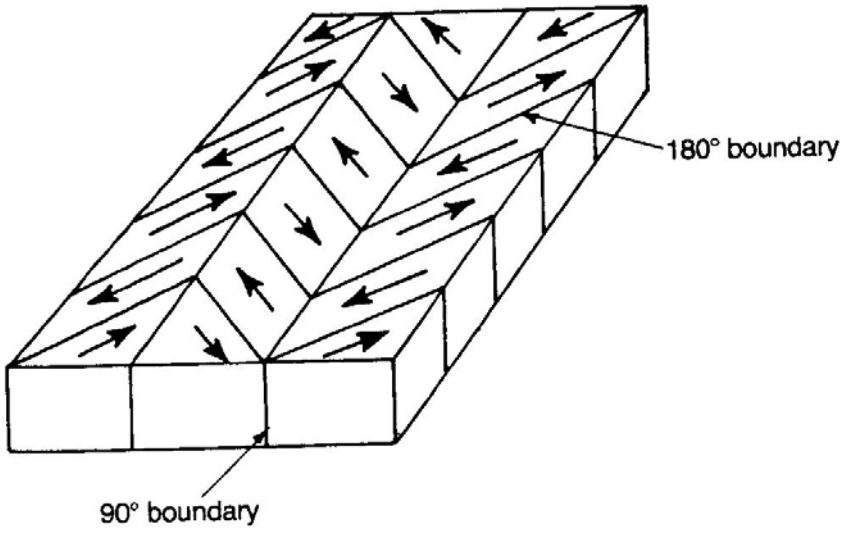

Figure 1.5 Schematic illustration of 180° and 90° domain walls.[17]

crystal undergoes a phase transition from a non-ferroelectric phase to a ferroelectric phase. If there are more than one ferroelectric phases as shown in Figure 1.3, the temperature at which the crystal transforms from one ferroelectric phase to another is called the transition temperature. Early research studies on ferroelectric transitions has been summarized by Nettleton.[25,26] Figure 1.6 shows the variation of the relative permittivity (ε_r) (or dielectric constant) with temperature as a $BaTiO_3$ ferroelectric crystal is cooled from its non-ferroelectric (or paraelectric) cubic phase to the ferroelectric tetragonal, orthorhombic, and rhombohedral phases. Near the Curie point or phase transition temperatures, thermodynamic properties including dielectric, elastic, optical, and thermal constants show an anomalous behavior. This is due to a distortion in the crystal as the phase changes. The temperature dependence of the dielectric constant above the Curie point ($T>T_c$) in most ferroelectric crystals is governed by the Curie-Weiss law:[27]

$$\varepsilon = \varepsilon_0 + \frac{C}{(T - T_0)} \tag{1.4}$$

where ε is the permittivity of the material, ε_0 is the permittivity of the vacuum, C is the Curie constant and T_0 is the Curie-Weiss temperature. The Curie-Weiss temperature T_0 is, in general, different from the Curie point T_c. For first order transitions $T_0 < T_c$ while for second order phase transitions $T_0 = T_c$.[7,27] Transition into a ferroelectric

phase occurs differently in different type of ferroelectric materials. These transitions may be of first order or second order in classical proper ferroelectrics.[10] The order of the phase transition is defined by the discontinuity in the partial derivatives of the Gibbs free energy (***G***) of the ferroelectric at the phase transition temperature.[28] For an n^{th}-order phase transition, the n^{th}-order derivative of G is a discontinuous function at the transition temperature. Thus, spontaneous polarization and strain change continuously at the phase transition for a ferroelectric with the second order phase transition, and are discontinuous at the phase transition temperature for first-order ferroelectrics. Other ferroelectrics show diffuse phase transition behavior. An additional subset in the diffuse ferroelectrics, called "relaxors", will be discussed separately in later section. General property changes with ferroelectric phase transitions are summarized in Figure 1.7, schematically.[28]

By definition, an applied electric field can reorient the direction of polarization in any ferroelectric crystal, regardless of what type of ferroelectric behavior is exhibited. A general description of polarization reversal process is provided in the following section.

1.1.6 Polarization Switching and Hysteresis Loop

A ferroelectric crystal, as grown, has multiple domains. A single domain can be obtained by domain wall motion made possible by the application of an appropriate electric field. A very strong field could lead to the reversal of the polarization in the domain, known as *polarization (or domain) switching*.[14]

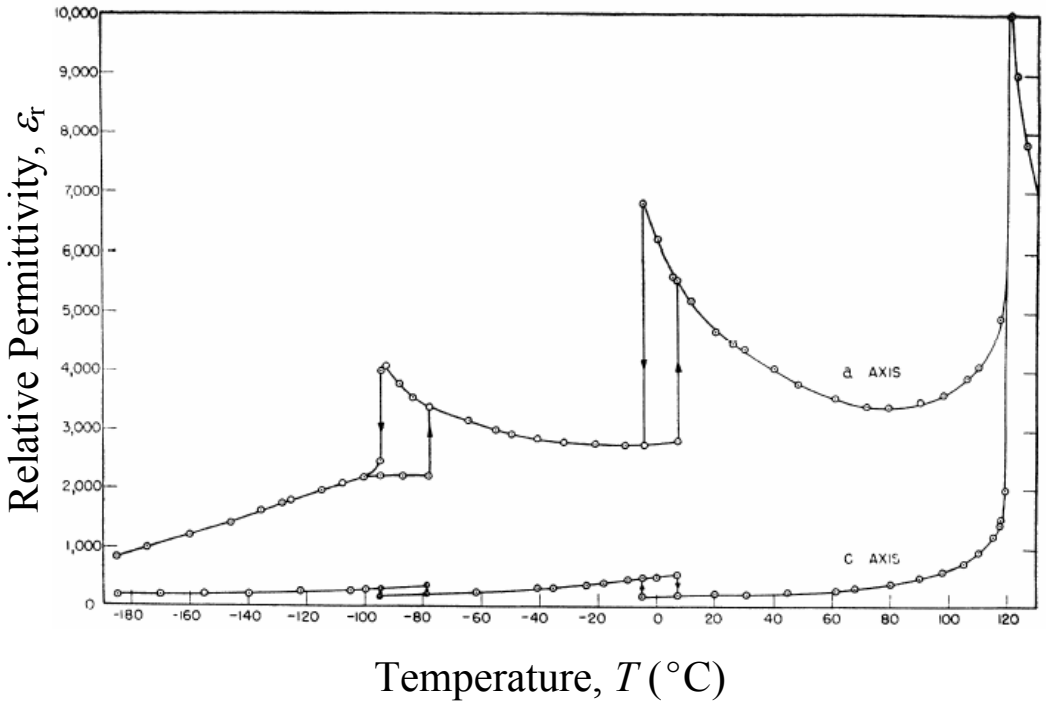

Figure 1.6 Relative permittivities measured along the a and c directions of a poled tetragonal $BaTiO_3$ crystal versus temperature in a ferroelectric.[32] Note that the samples were not repoled at lower temperatures. It is a residual poling that yields the apparent anisotropy in the rhombohedral phase.

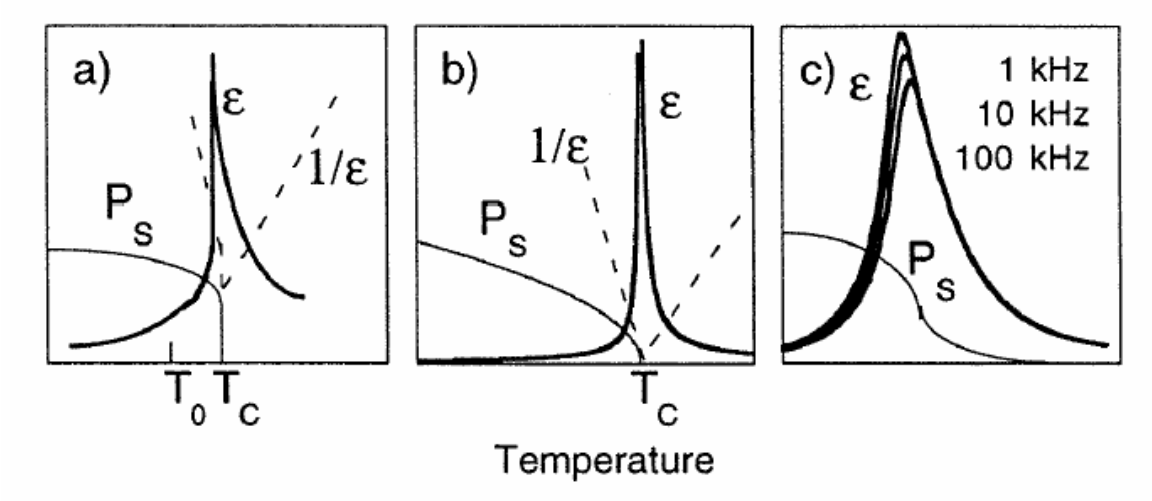

Figure 1.7 Schematic temperature dependence of the dielectric permittivity (ε) and spontaneous polarization (P_s) for a) a first- and b) a second-order ferroelectric and c) for a relaxor ferroelectric.[28]

This dynamic characteristic of a ferroelectric domain is anisotropic and depends on temperature and on the applied electric field.[29,30] When an external field is applied opposite to the direction of polarization of a domain, a new domain may occur in the old domain by means of *nucleation* and *growth*.[14]

Polarization reversal (switching) is a characteristic of ferroelectricity which can be observed by measuring the hysteretic polarization versus electric field (*P*-*E*) relationship below T_C.[10,14] The observation of hysteresis loops (e.g., with a modification of the Sawyer-Tower circuit[31] of Figure 1.8) is still frequently used for the identification of ferroelectrics. An alternating voltage $\boldsymbol{V}$ is applied across the electrodes on the ferroelectric material $\boldsymbol{C_x}$ placed on the horizontal plates of an oscilloscope; hence the quantity plotted on the horizontal axis is proportional to the field across the ferroelectric material. $\boldsymbol{C_0}$ is a linear capacitor (with large capacitance) that is connected in series with the ferroelectric material $\boldsymbol{C_x}$. The voltage across the linear capacitor $\boldsymbol{C_0}$ is therefore proportional to the polarization of the ferroelectric material. A typical loop is shown in Figure 1.9. Application of a low electric field generates a linear relationship between *P* and *E*, because the field is not large enough to switch any domains and the crystal will behave as a normal dielectric material (paraelectric) which can be described as;

$$P_i = \varepsilon_0 \chi_{ij} E_i \tag{1.5}$$

This behavior corresponds to the segment OA of *P*-*E* loop in Figure 1.9. As the electric field strength increases, a number of the domains with opposite polarization direction will switch towards the field direction, producing a rapid increase in polarization (segment AB). When all the domains are aligned as well as possible in the field direction a

saturation state is reached (BC). At this saturation state, appropriately oriented crystals will be composed of a single domain.

As the field strength decreases, the polarization will decrease (BD) but does not go back to zero. When the field is reduced to zero, some of the domains will remain aligned and the crystal will exhibit a *remanent polarization* (P_r). The extrapolation of the linear segment BC of the hysteresis loop back to the polarization axis (CBE) represents the value of the spontaneous polarization (P_s), in the case of an appropriately oriented, fully poled crystal.

The remanent polarization in a crystal can not be removed until the applied field in the opposite direction reaches a certain value (at the point F in the Figure 1.9). The strength of the field required to reduce the polarization back to zero is called the *coercive field strength* (E_c). Further, increase of the field in the negative direction will cause an alignment of the dipoles in this direction and the cycle can be completed by reversing the field direction once again. Thus the relation between P and E is represented by a hysteresis loop (CDFGHC) as shown in Figure 1.9.[12,14]

In addition to the polarization-electric field (*P*-*E*) hyteresis loop, polarization switching by an external electric field leads to strain-electric field (x-*E*) hysteresis in ferroelectric materials, as shown in Figure 1.10.(b). The x-*E* hysteresis loop, which resembles the shape of a butterfly, is due to three types of effects in ferroelectrics. One is the normal converse piezoelectric effect of the lattice, and the other two are due to switching and domain wall movement.

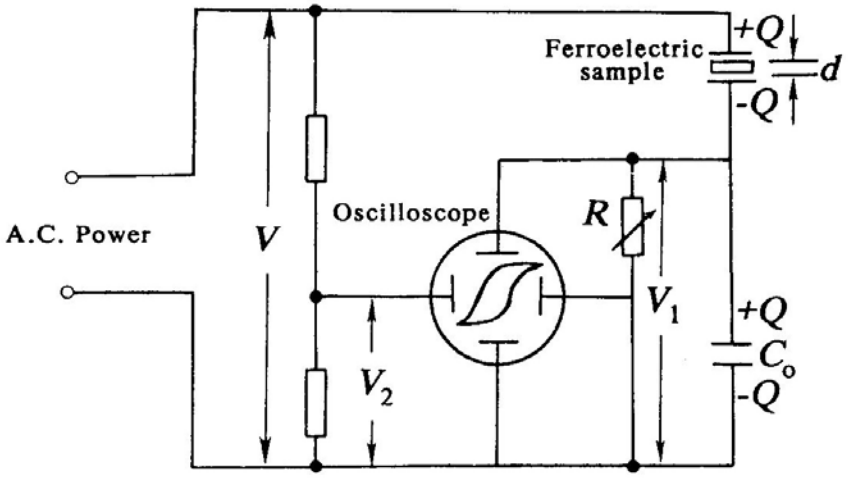

Figure 1.8 Schematic circuit of Sawyer-Tower bridge for the observation of *P*-*E* characteristics of ferroelectrics.[14](Variables are defines in the text).

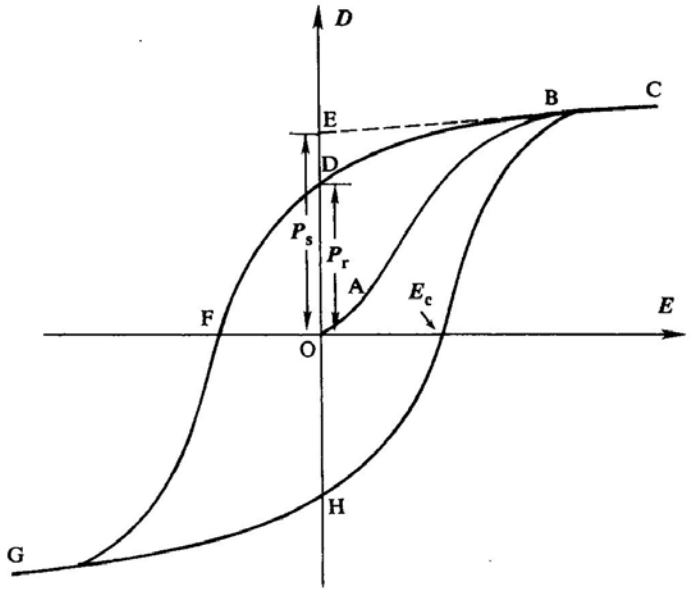

Figure 1.9 A typical *P*-*E* hysteresis loop in ferroelectrics.[14]

The quadratic *x*-*E* hysteresis loop can be best understood in relation to the *P*-*E* hysteresis loop, reproduced, for convenience, in Figure 1.10.(a).[12] The straight portions 1-3 and 5-6 represent the true piezoelectric component of the strain. The slope of these lines, in Figure 1.10.(b), represents the piezoelectric modulus, d_{33}. Between 0 and 3, and 0 and 6, the field opposes the spontaneous polarization, but is not large enough to switch it. At 3 and 6, the coercive field is reached, the spontaneous polarization is reversed and the piezoelectric effect changes sign. In actual crystals, different portions of the sample alter orientation at different parts of the cycle and a smooth curve results, as depicted in Figure 1.10.(c).[12]

As already stated, polarization reversal is a dynamic process. That is, the form of the alternating field (defining the frequency (time) and strength) is important. The first quantitative experiments to determine the time and field dependence of polarization reversal were carried out by Merz on $BaTiO_3$.[32] The experimental procedure involves application of a step-function field to the crystal and measurement of the displacement current density as a function of time.[10] Figure 1.11 shows a typical applied voltage wave form and switching current, $i \propto dP/dt$, for a ferroelectric.

The field applied antiparallel to the polarization switches the polarization from state $-P_r$ to $+P_r$. The total current consists of two parts. The first spike is due to the fast linear response of the dielectric and the bell-shaped curve is the current due to polarization switching. The total area under the curve is equal to

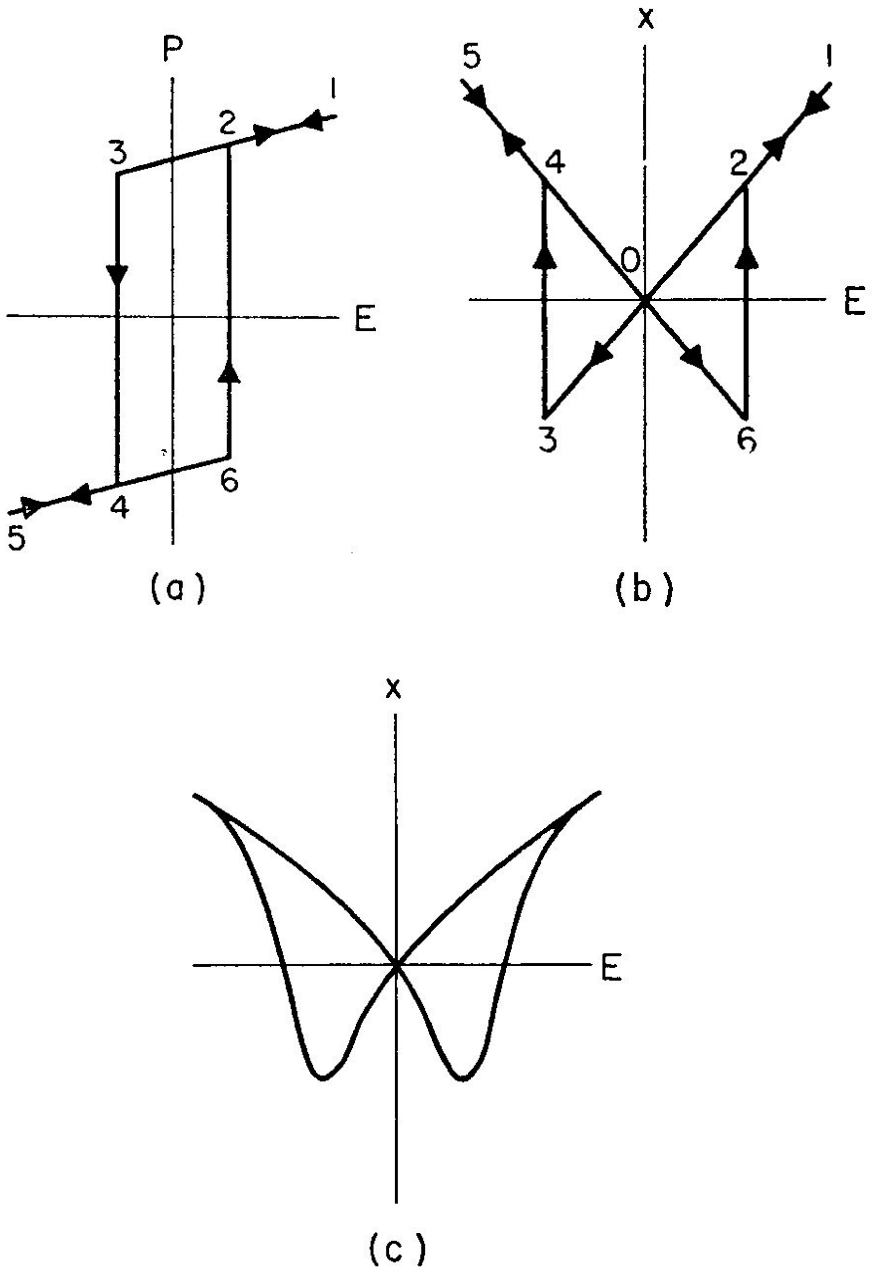

Figure 1.10 Switching and hysteresis effects in a ferroelectric crystal: a) Polarization (*P*)-Electric field (*E*), and b) Strain (*x*)-Electric field (*E*) hysteresis loops in an ideal single crystal ferroelectric. c) Actual *x*-*E* "butterfly" loop.[12]

$$\int_0^{t_s} i(t)dt = \varepsilon_0 \varepsilon EA + 2P_r A \qquad (1.6)$$

where A is the area of electrodes. Once the ferroelectric is switched, the same pulse may be applied again, this time parallel to the polarization to obtain only the transition from the fast response of the dielectric, assuming no back-switching. The area under the fast transient pike is then $\varepsilon_0 \varepsilon EA$ and from Equation 1.6 the remanent polarization may be calculated.[10,28,33,34,35]

It was recognized that the polarization reversal does not occur simultaneously in the whole volume of the ferroelectric crystal.[4,10,12] When a field is applied to a crystal opposite to the direction of the spontaneous polarization, polarization reversal begins by formation of domain nuclei at random on the surface of the crystal according to a statistical process. The switching of polarization begins in these local regions and spreads out from there. Formation of nuclei has been explained to be due to crystal inhomogeneities, weak spots, lattice defects, surface layers etc.[36] Then only those domain nuclei which have dimensions larger than the critical value will continue to grow in the direction of the field until they become domains and reach the opposite side of the crystal. More nuclei will be formed as a flat step on the existing domain wall, with a thickness equal to one unit cell. These typically have an elongated triangular shape as illustrated in Figure 1.12. The nuclei will grow very fast to the whole area of the existing domain wall. Thus the domain expands by one unit cell via sideways motion. During this expansion, a new domain may form from a new nucleus and also starts growing sideways; and this process will be continuously repeated with newer nucleation and

growth events. As these domains grow large enough and join each other through successive nucleation, sideways growth, and coalescence, eventually the polarization is completely reversed in the whole sample. The nucleation and growth process is illustrated in Figure 1.12.[37]

The probability of nucleation of a new domain, P_n, is given by[14]

$$P_n = P_0 \exp(-\alpha / E) \tag{1.7}$$

where α is the activation field of nucleation and is a function of temperature; $\boldsymbol{E}$ is the external field strength.

When an electric field E is applied, the velocity of domain-wall motion, ν, can be expressed as,[14]

$$\nu = \mu E \tag{1.8}$$

where μ is the mobility of the domain wall. In fact, the motion of the domain wall is related to the stress distribution, space charges, and defects in the crystal.

The energy required for the polarization reversal was calculated by Miller and Weinreich[37] based on the experimental results. The energy for the formation of a new nucleus of volume $\boldsymbol{V}$ and domain-wall area $\boldsymbol{A}$ is given as

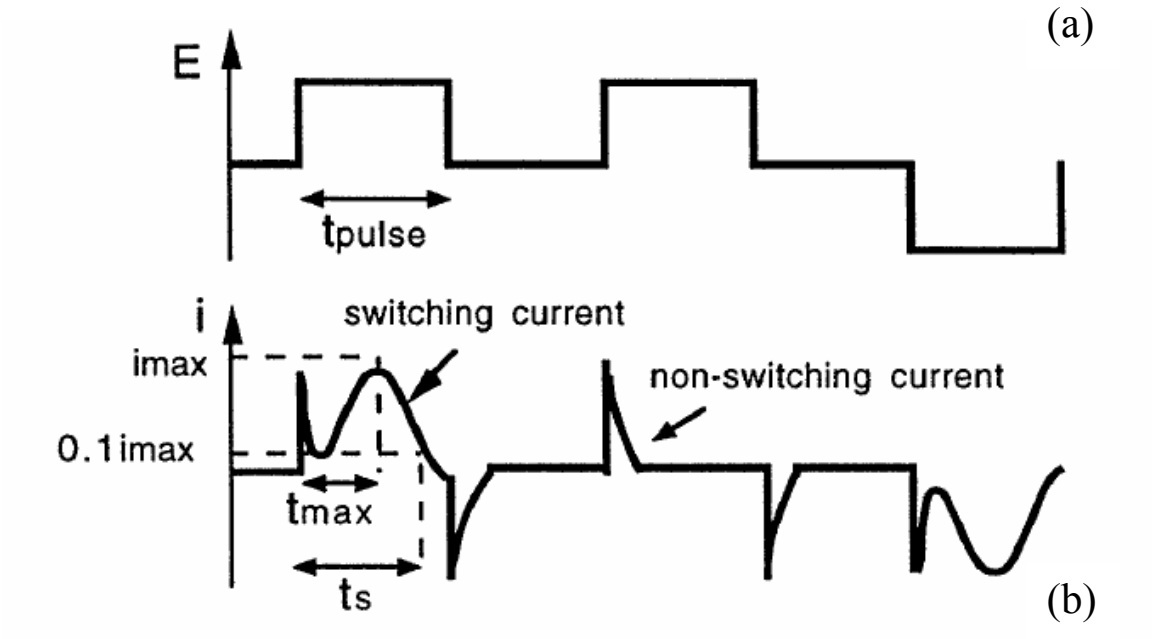

Figure 1.11 Switching and transient current during polarization switching; a) applied electric field and b) current as a function of time.[28]

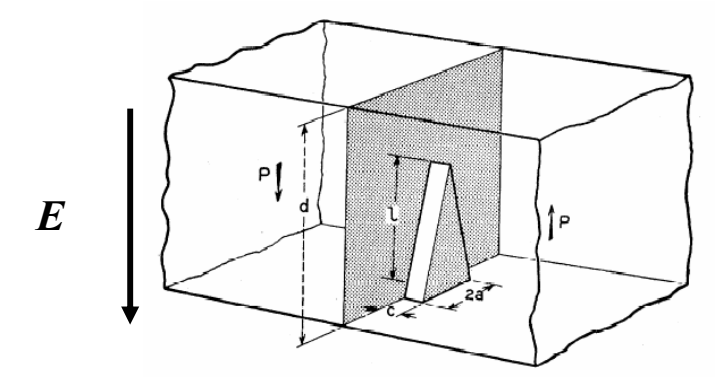

(a)

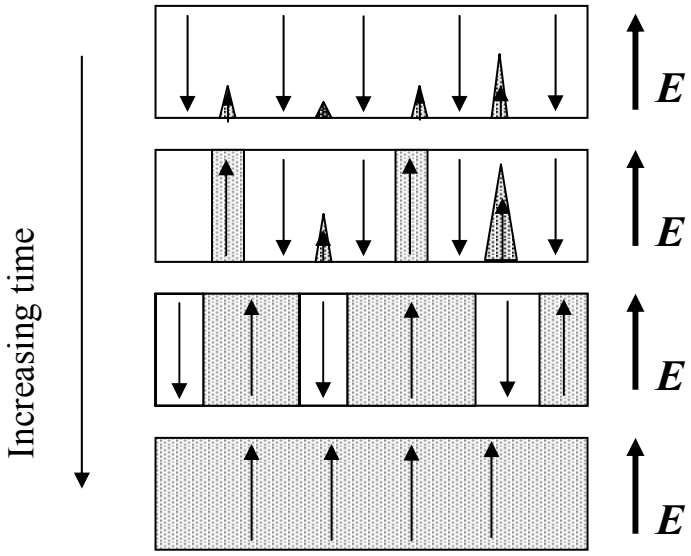

(b)

Figure 1.12 Schematic drawing of a) a triangular step on a 180° domain-wall.[37] and b) growth of domain by forward and sideways motion under an external electric field.

$$\Delta U = -2P_s EV + \sigma_w A + U_d \tag{1.9}$$

in which $\boldsymbol{\sigma_w}$ is the wall energy per unit area, $\boldsymbol{P_s}$ the spontaneous polarization and $\boldsymbol{U_d}$ the depolarizing energy. The first term represents the electrostatic energy gained by the formation of a nucleus, the second term represents the surface energy.

The kinetics of polarization reversal may be described by measuring the switching time, t_s, for different amplitudes of the electric field pulse as given in Figure 1.11. A detailed study of polarization switching kinetics was performed by Merz[32] in barium titanate single crystals. Switching current (i_{max}) flows during switching and current spikes occur when polarization is reversed by alternating applied electric fields. This is to compensate the change of surface charge resulting from the polarization reversal process.

Both switching current (i) and time (t) are dependent on the magnitude of the external field. The exponential relationship can be expressed as[4]

$$i_{\max} = i_\infty \exp(-\alpha / E) \tag{1.10}$$

$$t_s = t_\infty \exp(\alpha / E) \tag{1.11}$$

where i_∞ and t_∞ are the current and switching time for an infinite field strength E and α is the constant activation field dependent on the crystal thickness and temperature. Drougard[38] determined how the instantaneous, rather than the maximum, value of the

switching current depends on the state of net polarization of the crystal. According to Drougard's results, the switching process can be described fairly accurately by the law

$$i_s = Q_s \beta [1 - (\frac{P}{P_s})^2] \exp(-\alpha / E) \tag{1.12}$$

where i_s is the actual switching current at any instant of time, P is the net polarization of the sample ($-P_s \leq P \leq +P_s$) and Q_s the total charge switched during a complete reversal of polarization. The coefficient β was found to vary from 0.4 to 2.3×10^{-7} sec^{-1} in different crystals. α is again a temperature dependent constant (for a given crystal) which is independent of the state of polarization of the sample.[12]

It has recently been suggested that detailed information on nucleation, growth, and coalescence of domains may be obtained from the switching current data.[34] The theoretical model of this approach is partly based on the classical Kolmogorov-Avrami theory of crystallization that was subsequently adapted to domain switching in ferroelectrics by Ishibashi and Takagi.[39] A description of the model and detailed discussion of polarization reversal may be found in a recent review paper by Shur.[34]

Direct microscopic domain observation techniques were combined with macroscopic electrical property measurements and especially switching current data to understand the different aspects of polarization switching. It should be mentioned though, that the problem is very complex and there does not seem to be a universal mechanism which would be valid for polarization reversal in all ferroelectrics.

1.2 Ferroelectrics for Electronic Applications and Polarization (Switching) Fatigue

1.2.1 Introduction

Especially after the discovery of barium titanate, ferroelectric crystals and ceramics have been studied for a variety of electronic devices, including actuators, filters, sensors and capacitors, due to their piezoelectric, pyroelectric, ferroelectric, and dielectric properties.[7,10,14 ,17,32] As discussed in the previous section, extensive research has been done on the study of polarization switching from one state to another under the application of an external field in various ferroelectric materials.[34,40] The concept of utilizing the reversible spontaneous polarization as a memory state was one of the motivations for this extensive work from the early days of ferroelectric research.[32] In this regard, many researchers have studied electric field cycling in various ferroelectrics, mostly in single crystals.[41,42,43,44,45,46] These fundamental studies established the ground work for electronic devices which utilize the repeated reversal of spontaneous polarization.

With the advances in thin film technology, high quality ferroelectric films with better material properties have been receiving renewed attention for electronic applications since the 1980's.[47] The major device type under investigation is the ferroelectric non-volatile memory, which utilizes the spontaneous, reorientable polarization of a ferroelectric film as a memory state. A key feature is that the devices are typically read destructively, which leads to the requirement that the ferroelectric materials

endure large numbers of switching cycles.[48] In the following two sections, a brief description of ferroelectric non-volatile memories will be provided, followed by a discussion on polarization fatigue as one of the major reliability issues limiting the applicability of ferroelectrics in memory devices.

1.2.2 Non-Volatile Ferroelectric Random Access Memories (NVFRAM)

The hysteretic behavior of ferroelectrics relating polarization and applied field, is utilized for nonvolatile memory applications. In these materials, there is a nominal threshold (or coercive field), above which the polarization changes sign. The two zero-field values $\pm P_r$ are equally stable. Either of the two states of polarization could be encoded as a "1" or a "0" in the memory device and since no external field is required to maintain these states, the memory is nonvolatile.[49] This bistable operation may be contrasted with the operation of memories such as nematic liquid crystal display devices, which relax back to a single favored state if the applied voltage is interrupted, or with Si-DRAMs, which require a "refresh" voltage many times per second to maintain their stored information.[47] Besides allowing unique applications, NVFRAMs are ideal replacements for standard random access memory, erasable programmable read-only memory and Flash memories due to their fast access speed, low power consumption, extended read/write endurance, and ability to store data without the need for battery backup power. NVRAMs have been mass produced since 1992, following the first NVFRAM demonstration in 1989.[50] Current applications include smart cards, data collection and storage (e.g., power meters), configuration storage, and buffers.

Figure 1.13 shows two currently used types of NVFRAM cells consisting of a number of capacitor (C) and transistor (T) pairs.[50]

Current trends for the improvement of NVFRAMs are size reduction and density (bits) increase. A chronological profile of progress is presented in Figure 1.14. For the performance and reliability of the memory elements, certain specifications are given in Table 1.2.

Further details of the non-volatile ferroelectric memories can be found in several publications.[47,48,50,51] For the scope of the thesis, more emphasis will be put on the discussion of polarization switching fatigue. The next section presents a summary of generally agreed upon polarization fatigue mechanisms, as well as strategies to control fatigue and improve fatigue resistance.

1.2.3 Polarization (Switching) Fatigue

Ferroelectric (polarization) fatigue is defined as the loss of the switchable remanent polarization in a ferroelectric material undergoing bipolar drive. Figure 1.15 shows a schematic of the polarization decay in a ferroelectric material as a function of the number of cycles, and also the corresponding evolution of the hysteresis loops. This phenomenon has received a great deal of investigation over the past ten years to aid the development of thin film ferroelectric random access memories. Fatigue is generally agreed to be the result of charge injection and the accumulation of space charge that pins switching.[41,42,43,44,45,46,47,49] The mechanisms of polarization fatigue are presently not well understood. Both bulk and thin film ferroelectric materials are susceptible to polarization fatigue.

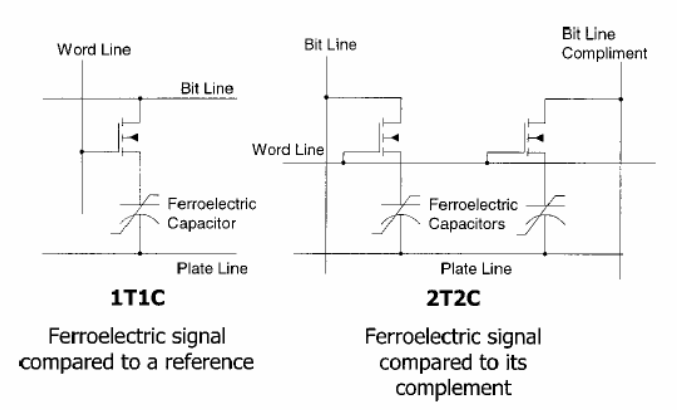

Figure 1.13 Schematics of two types of NVFRAM cells.[50]

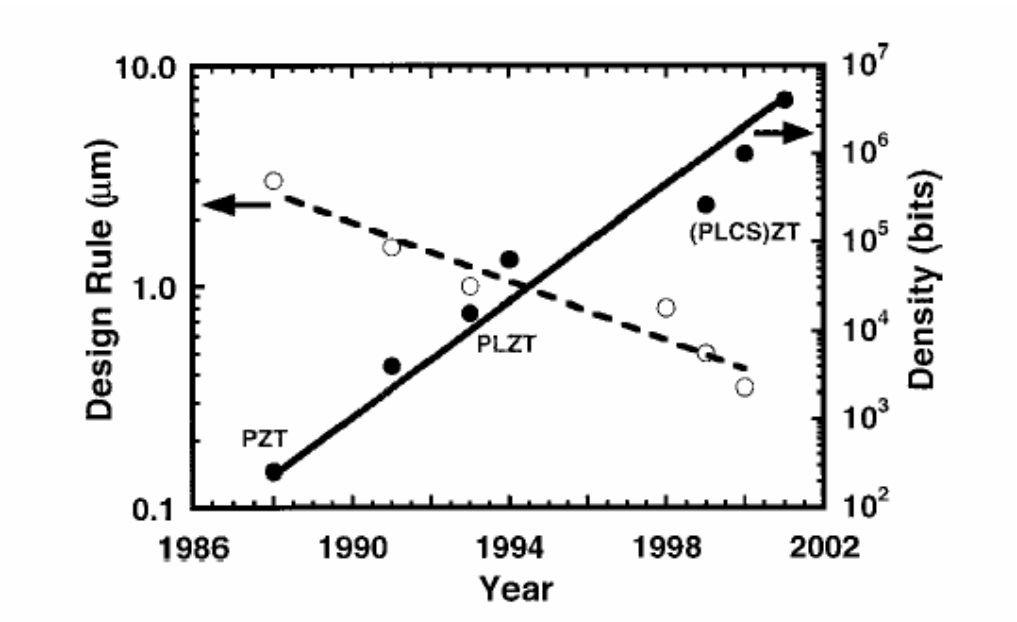

Figure 1.14 Progression of NVFRAM density and design rule in mass production.[50]

Table 1.2 Specifications for NVFRAM memories.[50]

Memory cell type	2T2C
Density	4-256 kbit
Read/Write time	70-150 ns
Read/Write endurance	$>10^{10}$ cycles
Data retention	10 yr. (@-40 to 85 °C)

Since the early studies (mostly confined to single crystals), extensive research on ferroelectric fatigue has produced a large body of experimental data. The influence of various conditions (i.e., ambient atmosphere, temperature, composition of the ferroelectric material, choice of electrode, and the characteristics of the external electric field) on fatigue has been studied. These parameters are sometimes varied to improve the fatigue resistance, as shown below.

1.2.3.1 Strategies to Control Polarization Fatigue

Extensive research on polarization switching produced a number of strategies to improve fatigue resistance in ferroelectrics. These can be summarized in three major categories, which will be very briefly discussed below.

Compositional Changes and Doping

Most material properties are dependent upon the composition. Currently studied ferroelectrics are generally solid solutions of two compounds of different characteristics.

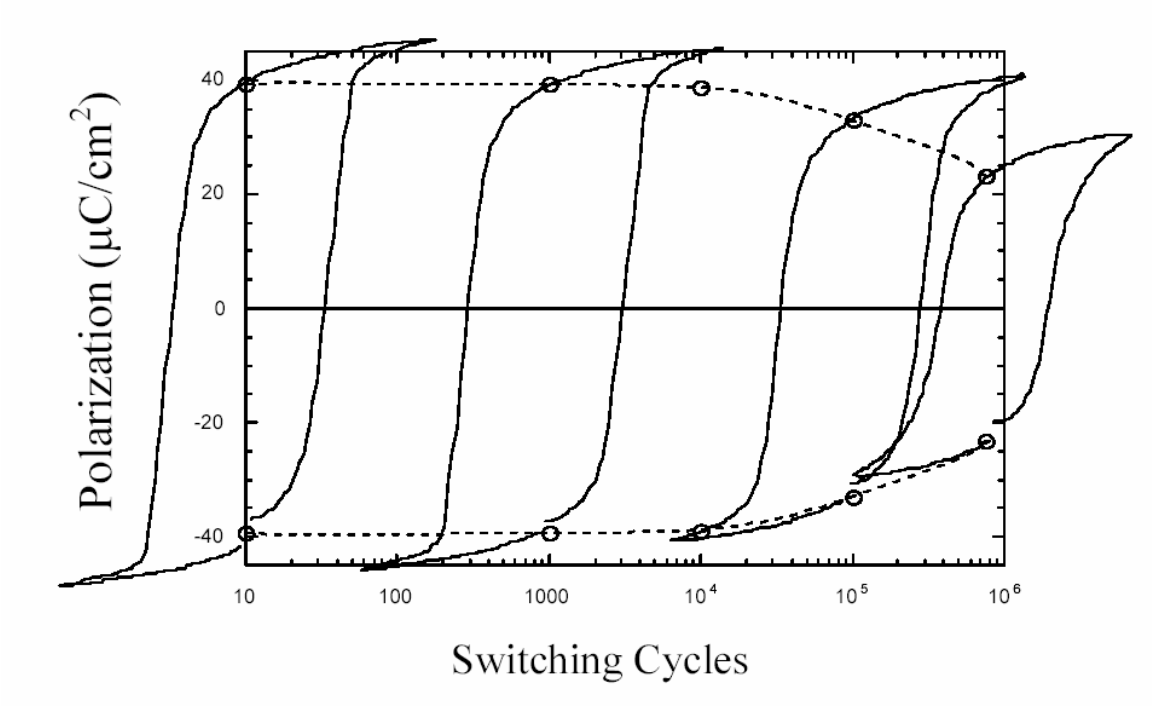

Figure 1.15 A schematic illustration of polarization decay as a function of the number of the switching cycles.

Often there exists a phase boundary at a defined composition. Depending on the composition, ferroelectrics possess different symmetry.

Several studies were done on the influence of composition on the electric fatigue.[52,53] In an early study, Taylor[52] investigated the fatigue behavior in $Pb_{0.99}[(Zr_xSn_y)_{1-z}Ti_z]_{0.98}Nb_{0.02}O_3$ ceramics, and found minimum fatigue at compositions giving minimum strain under the applied electric field. Jiang et al[53] studied the effect of composition on electric fatigue in La-doped lead zirconate titanate (PLZT) ceramics. Ceramic samples with pure rhombohedral compositions were noticed to exhibit better fatigue performance compared to compositions near phase boundaries. Improved fatigue resistance in pure rhombohedral PLZT was attributed to the crystal structure and/or domain structure. Microcracking was reported in fatigued samples of non-rhombohedral compositions. The ease of switching by electric field and smaller internal stress in rhombohedral ferroelectrics (which possess lower E_c values than tetragonal materials) were considered to be possible sources for the absence of fatigue and microcracking.[53,54]

It is well known that the electrical properties of bulk PZT ceramics can be modified by ion substitution: this is termed doping. Depending on their location in the crystalline structure, the dopants may be classified as donors, acceptors, or isovalents substituents. Lanthanum (La^{3+}) and niobium (Nb^{5+}) are commonly used dopants in PZT ceramics as A-site and B-site donors, respectively. Some of the effects of donor doping important for polarization switching processes and fatigue can be summarized as follows:[7,17]

-reduced oxygen vacancy concentration,

-high remanent polarization and low coercive field

-relatively square loops

-easy poling

-increased domain wall mobility

-low aging effects

Reduced oxygen vacancy concentration and easier domain reorientation have been presented as the key for the largely improved electrical properties in donor doped ferroelectric bulk ceramics[7,55,56] and thin films.[57,5859,60,61] Improvement of ferroelectric fatigue properties is observed in PZT thin films.[62,63] Haccart at al.[63] also reported that there is an optimum dopant concentration (2 at.%) for the maximum improvement as shown in Figure 1.16. A similar observation was made in bulk PZT ceramics donor doped with 0, 2, 4, and 6 at.% Nb, 4 at.% giving the best results. Compositional studies for the improvement of fatigue, especially in PZT thin films, also include changing Zr/Ti ratio.[64,65,66,67] In general, tetragonal compositions are preferred for NVFRAM applications due to the squarer hysteresis loops obtained on silicon substrates.

It is generally believed that oxygen vacancies, which are the most mobile species in perovskite PZT, contribute to fatigue of ferroelectric capacitors. Despite all the attempts to control oxygen vacancy by doping or changing processing conditions, compositional studies have provided only marginal improvement in fatigue behavior.

Use of Oxide Electrodes

As the positive effect of donor doping on ferroelectric properties and fatigue was attributed to the reduced oxygen vacancy concentration, another idea was use of oxide

electrodes to suppress the detrimental effects of oxygen vacancies. These conducting oxides included RuO_2,[68,69] IrO_2,[70,71,72] $SrRuO_3$,[73,74] $YBa_2CuO_{7-\delta}$,[75,76] and $(La,Sr)CoO_3$.[77, 78, 79] When these oxide electrodes were used in place of metal (mainly platinum) electrodes, polarization fatigue could be reduced or eliminated as shown in Figure 1.17.[80]

There is clearly an advantage to using oxide electrodes in terms of improving ferroelectric fatigue behavior. The reason why ferroelectric films with oxide electrodes have improved fatigue is generally explained in terms of oxygen vacancies migrating towards the electrode/film interface (under ac drive), where resulting internal fields may prevent subsequent switching. It is speculated in fatigue models based on the role of oxygen vacancies that the oxide electrodes may act as sinks for the oxygen vacancies, thereby reducing or eliminating fatigue.

Overall, the selection of electrodes requires particular attention depending on the application and also processing conditions. There have been reports on a variety of issues associated with the electrode/ferroelectric interactions critical both for the short term and the long term properties. Compared to oxide electrodes, metals still have the advantage of their much lower resistivity. The resistivity of the electrode material should be as low as possible for the optimum device speed. However, even with Pt electrodes there are several issues such as Pt-Ti interactions and Ti oxidation during processing involving high temperatures.[80]

With their much simpler processing and superior conductivity, the use of metal electrodes is still attractive if fatigue issues can be solved.

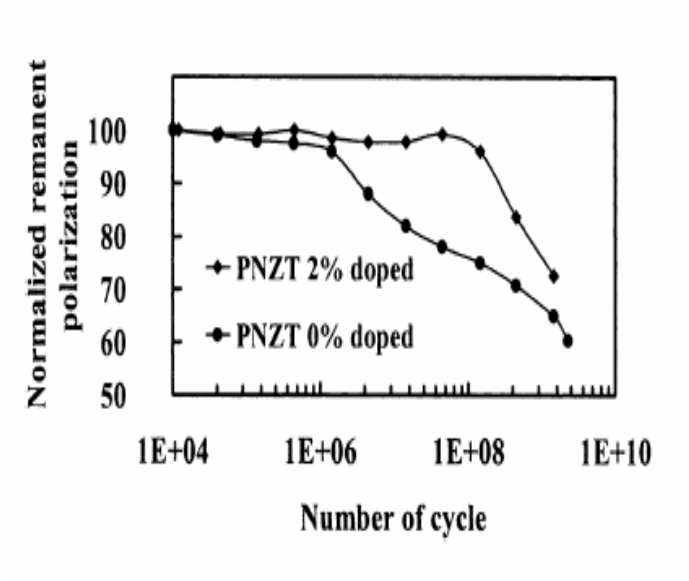

Figure 1.16 Fatigue characteristics of undoped (0%) and Nb-doped PZT (2%).[63]

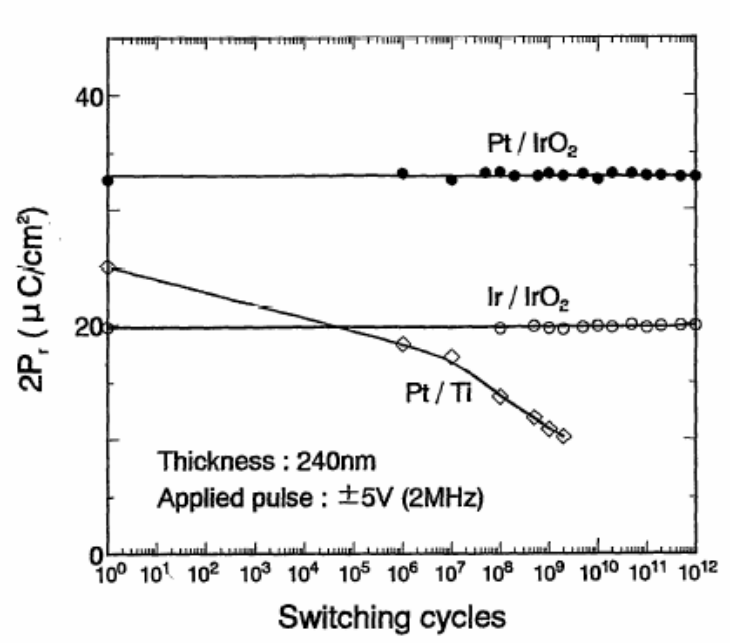

Figure 1.17 Polarization fatigue properties of PZT (52/48) thin films using oxide electrodes.[70]

Alternative Ferroelectric Systems

Early in 1992, certain layered type perovskite ferroelectrics ($SrBi_2Ta_2O_9$ and similar compounds) were reported to show negligible polarization fatigue (up to 10^{12} switching cycles) with Pt electrodes.[81,82] Figure 1.18 shows polarization fatigue behavior in a $SrBi_2Ta_2O_9$ ferroelectric thin film capacitor. From the application point of view, this was a most interesting achievement and has been studied in several layered perovskite ferroelectrics with Pt electrodes, e.g., $SrBi_2Ta_2O_9$ or $SrBi_2Nb_2O_9$.[83,84]

The absence of fatigue by field cycling in layered perovskite ferroelectrics compared to simple perovskite PZT with metal electrodes is explained by;

i) a relatively small magnitude of ferroelectric polarization (and therefore weaker trapping or smaller concentration of trapped charges in the domain wall region),

ii) shallow electronic charge trapping centres (holes and electrons associated with Bi^{4+} and Ta^{4+}, respectively) which may be easily detrapped by the field,

iii) and possibly lower accumulation of oxygen vacancies at the electrode/film interface due to layer structure of this material.[28]

Reversibility of Fatigue Process

In most cases and for most reported experimental conditions, the fatigue appears to be reversible. Application of an electric field usually at higher magnitude than the fatigue field and sometimes for a number of cycles, illumination with UV light, a high temperature (above T_c) anneal or the combined effects of the three can nearly fully restore many films to their initial state of the polarization.[28,85] This does not mean that

fatigue mechanisms by which ferroelectrics become permanently damaged or changed are absent or impossible; it simply indicates that in most reported studies in which fatigue is performed under usual experimental conditions the fatigue process is, at least partially, reversible. However, it was also reported that rejuvenated ferroelectrics fatigue faster on subsequent cycling, which indicates that some sort of permanent change, which nevertheless allows partial reversibility of the fatiguing process, may have occurred in the ferroelectric material fatigued by electric field cycling.[28,86]

1.2.3.2 Polarization Fatigue Mechanisms

All of the experimental results briefly discussed above led to the development of many theoretical models for the fatigue phenomenon. An up-to-date review is presented by Tagantsev et al.[87] The presently considered fatigue mechanisms in ferroelectrics include:[28,87]

i) surface layer formation,

ii) damage of electrode and/or electrode/ferroelectric interface

iii) pinning of the domain walls by defects segregated in the wall region,

iv) clamping of polarization reversal by volume defects,

v) suppression of nucleation of oppositely oriented domains at the surface

These mechanisms will modify either the applied electric field or the switching process itself.

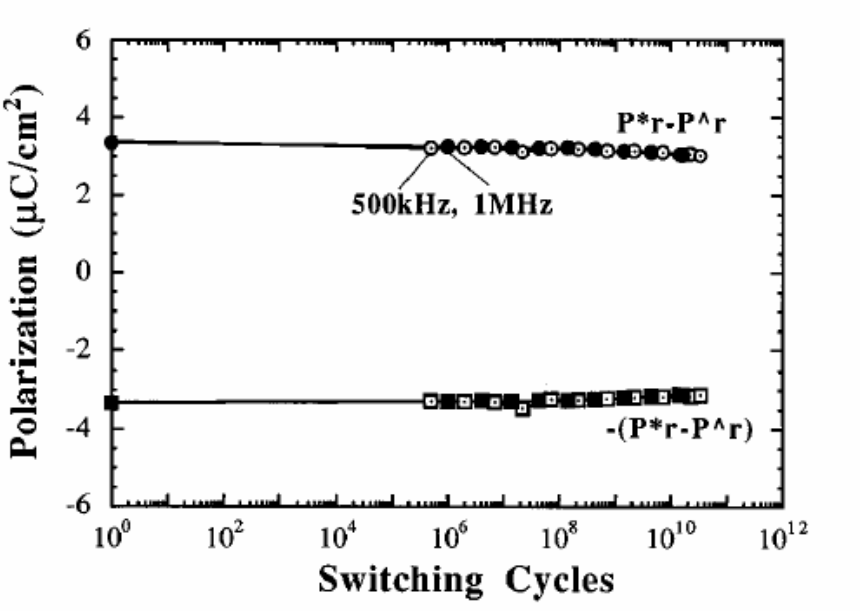

Figure 1.18 Polarization fatigue behavior of $Pt/SrBi_2Ta_2O_9/Pt$ thin film capacitors at 500 kHz and 1 MHz switching frequencies with no difference observed after 10^{11} cycles.[83]

1.2.3.2.1 Modification of the Applied Electric Field

Burning or delamination of electrodes provoked by cycling can reduce the contribution to the total switching via the reduction of the effective applied field. This mechanism is generally identified by the strong correlation between several properties as the same amount of degradation is expected. A manifestation of this kind of mechanism via electrode delamination or burning has been reported in PZT films.[88,89] Though this mechanism can be a reason for fatigue degradation, for high quality processed ferroelectric capacitors, it can be considered rather as an exception.

The formation of a nearby-electrode low-dielectric constant or nonswitching layer ("passive layer") as a result of cycling is another possible reason for fatigue. Cycling-driven appearance of passive layer as a fatigue mechanism has been forwarded by Larsen et al.[90] Modeling of this mechanism shows that the fatigue should be accompanied by a strong tilt of the polarization hysteresis loop, whereas the coercive field is either not influenced or slightly decreases (not increases as often assumed), on cycling.[91] This mechanism is consistent with some features of the polarization fatigue in PZT thin films but can be considered only as one of the mechanisms contributing to fatigue due to lack of strong arguments in support of this possibility.[87]

1.2.3.2.2 Modification of the Switching Process

Another possibility for the reduction of switching polarization in ferroelectrics exposed to electric field cycling may be related to the changes in the switching process itself. As discussed in more detail in early sections, polarization switching involves two

main steps: i) nucleation of new domains and ii) growth of existing domains. In real materials, imperfections serve as the nucleation sites or seeds.

Two major mechanisms have been proposed to explain the difficulty in the switching process as a ferroelectric material experiences fatigue:

i) Domain wall pinning

ii) Seed inhibition

These are summarized in Figure 1.19. When the ferroelectric is exposed to the cycling field, first, a seed gives a macroscopic domain whose boundaries are pinned (somehow immobilized) (Figure 1.19.b) so that it is available to act as a nuclei. If a domain does not contain seeds with inverted polarization, the area occupied by the domain does not contribute to switching anymore. This is the so called "wall-pinning" mechanism. Second, all the seeds of domains with inverted polarization are inhibited (somehow made unable to produce macroscopic domains) (Figure 1.19.c). As a result, this area ceases to contribute to switching. This is the scenario of so-called "seed inhibition" mechanism.

All the fatigue mechanisms involve a variation in the density of the defects. For the "passive layer" and "seed inhibition" mechanisms, fatigue should result in an increase of the defect concentration near the surface whereas, for the wall pinning mechanism, there is defect segregation near the domain walls. Variations in the defect density may occur mainly in two ways: i) redistribution of existing defects,[92,93,] and ii) creation of new defects due to electron injection from the electrodes.[94,95]

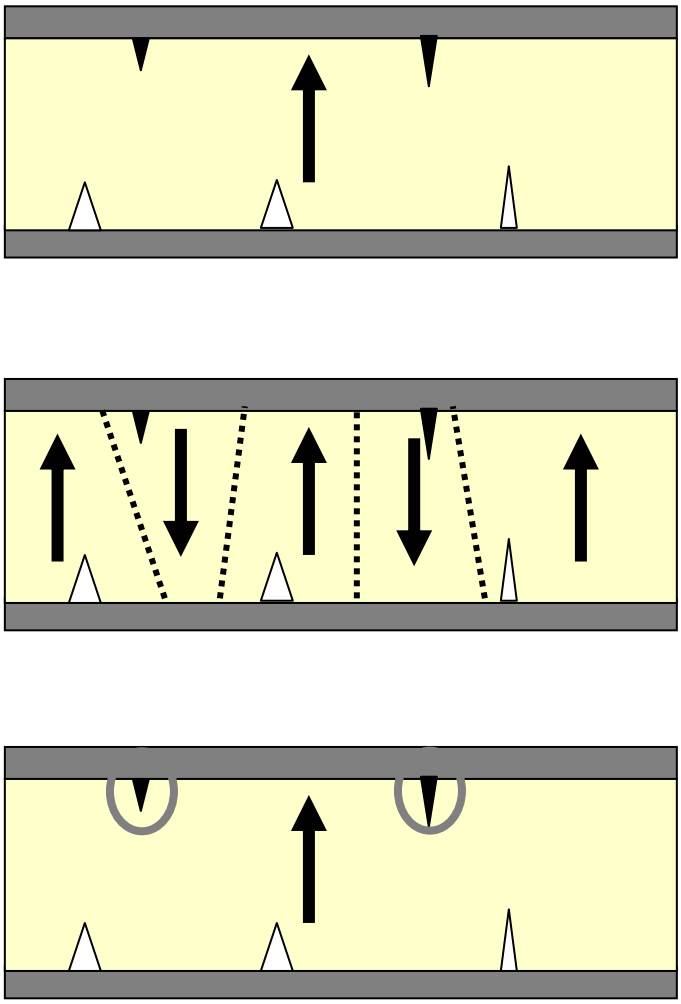

Figure 1.19 Two scenarios of fatigue via modification of the switching process: (a) Schematic drawing of a section of a ferroelectric capacitor in the virgin state. The electrodes are shown in gray. The active seeds of nucleation of new domains with the upward and downward direction of the polarization are shown with opened and filled triangles, respectively. The arrows show the direction of the spontaneous polarization. b) Schematic drawing of the same section in the fatigued state according the ‘‘wall pinning’’ scenario. Dashed lines stand for pinned domain walls. c) Schematic drawing of the same section in the fatigued state according the ‘‘seed inhibition’’ scenario. The circled triangles stand for the nucleation seeds which have become inactive.[87]

The data available on the understanding of fatigue in ferroelectrics present different trends sometime contradicting each other. The overall picture of polarization switching and fatigue phenomenon in ferroelectrics suggests that it is controlled by more than one mechanism.

1.3 Relaxor Ferroelectric Single Crystals and Anisotropic Properties

In recent years, complex perovskite type relaxor ferroelectric single crystals have emerged as a group of promising materials for various applications. So-called "domain engineered" crystals exhibit extraordinarily large properties in one direction compared to the others. With the new explorations in these relaxor based single crystals, understanding the nature of polarization switching may be helpful to the study of fatigue. In this section, some basic properties of relaxor based single crystals, i.e., $Pb(Zn_{1/3}Nb_{2/3})O_3$-$PbTiO_3$, will be presented in comparison to the normal ferroelectrics such as $BaTiO_3$ (which was discussed in the early sections).

1.3.1 Introduction

Complex perovskites with a formula $A(B'_{1-x}B''_x)O_3$ as illustrated in Figure 1.20 (oxygen ions are not drawn) were first reported in the 1950's.[96] The discussion will be limited to the Pb-based complex perovskite relaxor ferroelectrics, such as $Pb(B'_{1-x}B''_x)O_3$. The A-site is occupied by Pb^{2+} ions with twelve-fold coordination. On the B-site, a mixture of cations is found with an overall valence equal to [4+]. Generally

B' is a lower valence cation (like Mg^{2+}, Zn^{2+}, Ni^{2+}, Fe^{3+}) and B" is a higher valence cation (like Nb^{5+}, Ta^{5+}, W^{5+}). The B-site cations are centered in oxygen octahedra. The B-site cations are dispersed randomly in the structure on a global scale; however, on a local scale their ordering varies from totally disordered to long-range order. The details of B-site ordering has been studied in detail by several researchers.[97,98,99]

1.3.2 Characteristics of Relaxor Ferroelectrics

A special family of substituted perovskites which have extraordinarily high dielectric constants have been called "relaxors". The major characteristics of relaxors are discussed here, mostly concentrated in the polarization switching aspects.

Relaxor ferroelectrics like $Pb(Zn_{1/3}Nb_{2/3})O_3$ (PZN) or $Pb(Mg_{1/3}Nb_{2/3})O_3$ (PMN) can be distinguished from normal ferroelectrics such as $BaTiO_3$ (BT) and PZT, by the presence of a broad, diffused, and dispersive phase transition on cooling over the so-called Curie maxima, $\boldsymbol{T_{max}}$. The Curie maxima is the temperature of the maximum dielectric permittivity. The ferroelectric properties of relaxors are dependent on the measurement frequency. The Curie maxima shifts to higher temperatures with increasing frequency.[100] Also, the maximum in the dielectric constant and dielectric loss do not coincide at the same temperature (Figure 1.21). The dielectric constant maximum does not characterize the exact paraelectric to ferroelectric phase transition as in normal ferroelectrics. For relaxors which have a diffuse phase transition, the remanent polarization, P_r, gradually decreases to zero on increasing the temperature towards T_{max}.[98,101,102]

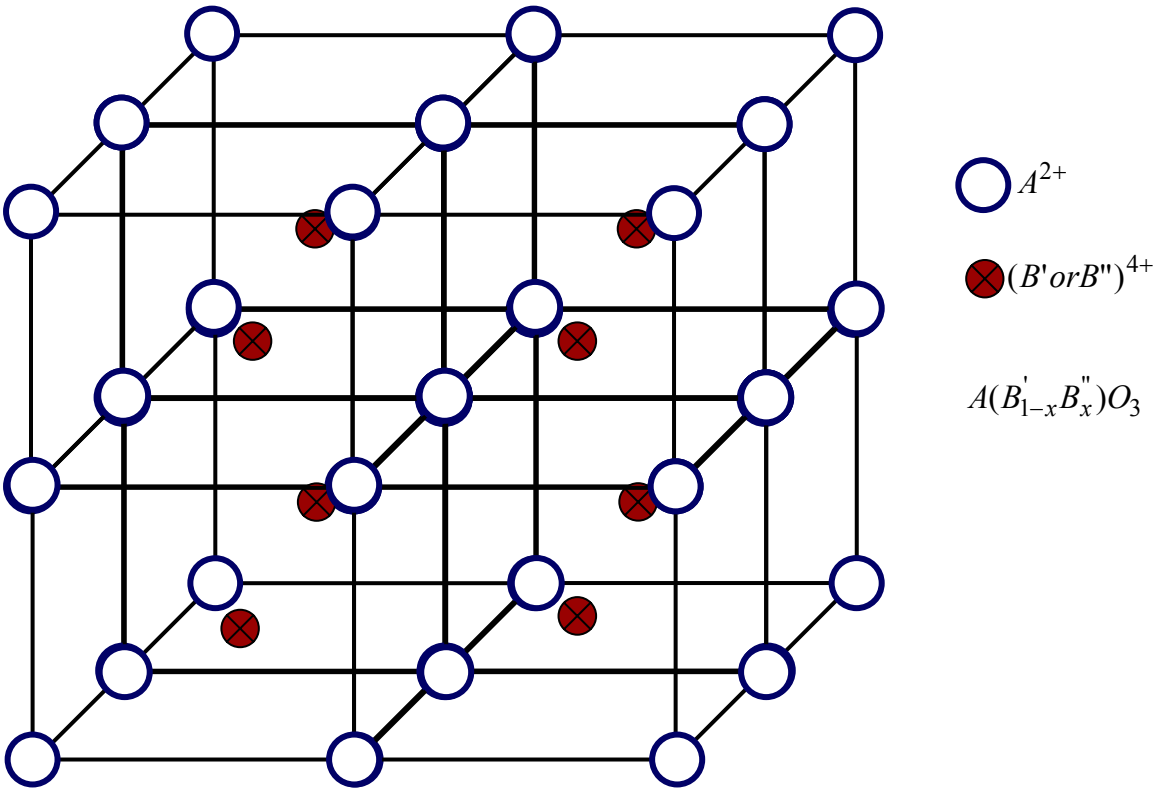

Figure 1.20 An illustration of the complex perovskite structure $A^{2+}(B'_{1-x}B''_x)^{4+}O_3^{2-}$ (oxygen ions are not drawn).

With decreasing temperature, the number of polar regions increases, so that the regions are in contact and grow; however, since these regions are randomly oriented along different polarization directions, the crystal still appears isotropic. Larger and more stable and slower macropolar regions will be formed at still lower temperatures.

The development of hysteresis evolves as a function of cooling through the Curie range. At high temperatures, slim loop behavior occurs with very weak remanent polarization. At lower temperatures the loop develops with high remanent polarization and more squared shape. There have been numerous theories proposed to explain the properties of relaxor ferroelectrics, such as Skanavi model,[103] compositional fluctuations model,[100] superparaelectricity model,[98] dipolar glass model,[104] and random local field model.[105] The details of these models can be found in these references.[98,100,103,104,105]

1.3.3 Polarization Switching in Relaxor Ferroelectrics

Micro- to Macro-domain transition occurs in relaxor ferroelectrics.[106,107] This is schematically described in Figure 1.22. In the absence of any external field, the domain structure of relaxor ferroelectrics contains randomly oriented micropolar regions as depicted in Figure 1.22.(a). When an electric field is applied, microdomains orient along the field direction and macrodomains occur. Cold-stage TEM studies revealed the existence of microdomains by freezing in of such polar regions. The phase transition of microdomains to macrodomains was also confirmed by ‘in-situ’ switching by means of an electron beam inducing local stresses to align the domains.[106,107]

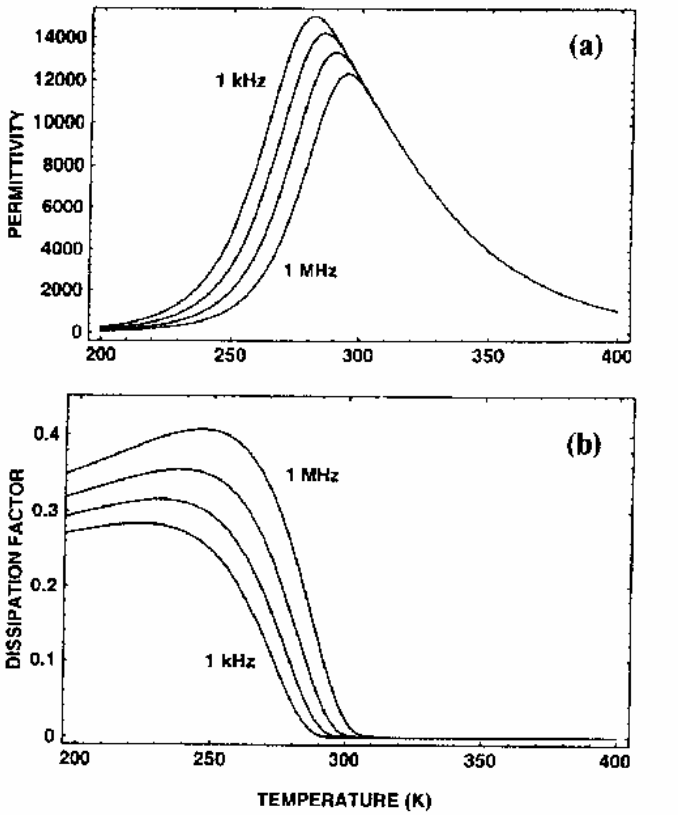

Figure 1.21 Variation of the dielectric properties of a relaxor ferroelectric PMN with temperature at frequencies of 1, 10, 100 kHz and 1 MHz: (a) dielectric permittivity, and (b) dissipation factor.[108]

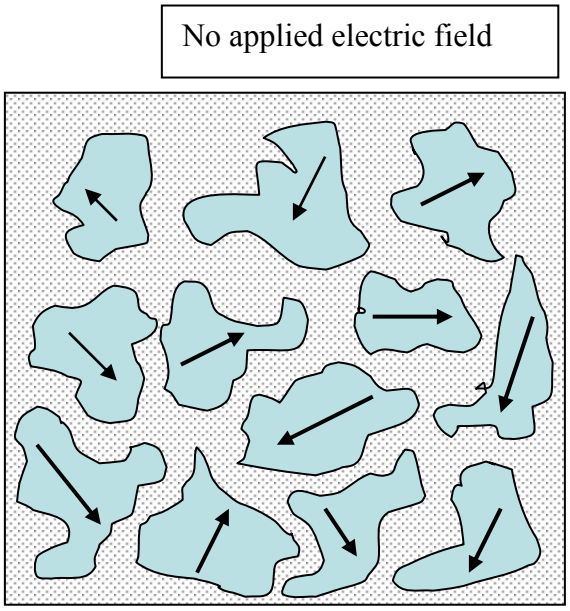

(a)

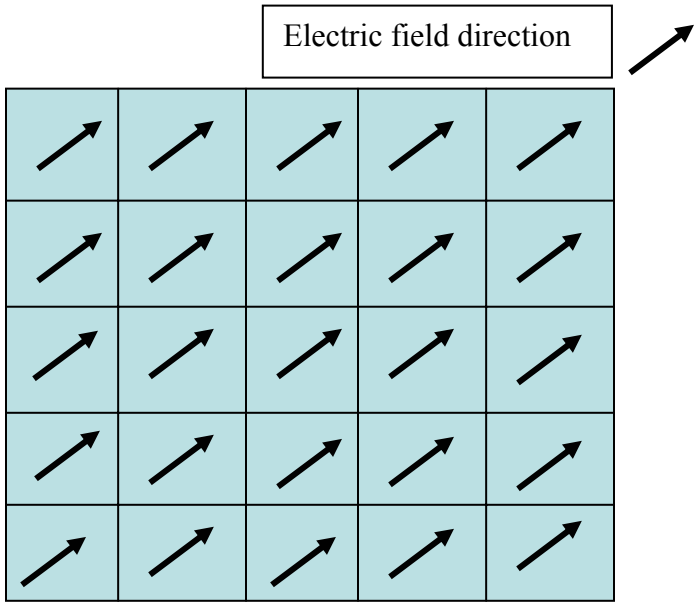

(b)

Figure 1.22 Illustration of the electric field induced microdomain to macrodomain transition in a relaxor ferroelectric: (a) no applied field and $T<T_f$;freezing temperature, (b) applied electric field in a given direction.

Application of an electric field to a relaxor material results in several other developments associated with the long range dipole ordering, such as a hysteresis loop, and an increase in the elastic and dielectric compliances and dielectric losses. Birefringence is also exhibited due to macrodomain formation. This anisotropic behavior is present even after the field is removed but disappears when T_{max} is reached. It was suggested that the paraelectric to ferroelectric phase transition could occur in either of two steps. The first is the polar-phase growth over a wide range of temperatures. A second step would involve the orientation of these regions by an applied electric field.[109] As already mentioned, PZN is an example of lead based complex perovskite relaxor ferroelectric. It has short and intermediate range chemical ordering on the B-site sublattice.[110] The size of ordered regions (or microdomains) were reported as ~100 Å.[99] Once macrodomains are formed at a critical electric field level (E_{th}), or at the percolation threshold, the macrodomains align with the field and can be switched.

Polarization switches through island formation in the structure. The islands exhibit sideways growth, perpendicular to the switching field. This is illustrated in Figure 1.23. The domain walls expand in the direction of the applied field and contract with a reversed polarity (negative) voltage. At the last step, the expanded islands merge with the adjacent one, forming uniform domain modulations. However, at low temperatures, near $\boldsymbol{T_f}$ (domain freeze-in temperature), domain islands may not have enough energy to merge completely. If this is the case, switching may occur within each island independently.[111] The size of the islands depends on the temperature. Mulvihill reported that the island region widths in PZN are about 200 μm in size at high temperatures (>100 C), and 40 μm near room temperature.[111]

1.3.4 Lead Zinc Niobate – Lead Titanate ($Pb(Zn_{1/3}Nb_{2/3})O_3 – PbTiO_3$) Single Crystals

Relaxor ferroelectric lead zinc niobate, $Pb(Zn_{1/3}Nb_{2/3})O_3$ (PZN) crystals possess a maximum dielectric constant (~70,000 at 120 Hz) near 140°C where the paraelectric to ferroelectric phase transition occurs.[112] As illustrated in the phase diagram in Figure 1.24, the pseudocubic symmetry is rhombohedral at room temperature.[100] Lead titanate, $PbTiO_3$ (PT) is a simple perovskite normal ferroelectric with tetragonal symmetry below its Curie point of 490 °C. The addition of PT shifts the T_c of PZN towards higher temperatures. Single crystals of the solid solution system can relatively easily be grown by a flux method over the whole range of the composition.[113,114,115,116]

Large piezoelectric (d_{33} ~1100 pC/N), dielectric (K_{RT} ~3600), and electromechanical coupling parameters (k_{33} ~85%) have been reported in PZN single crystals.[114,117,118] For the known perovskite ferroelectrics, the largest k_{33} of 94% was reported in PZN-8%PT along the <001> orientation. The d_{33} value was also large and measured as >2500 pC/N. The measured k_{33} and d_{33} values along the <111> direction were 68% and 625 pC/N, respectively, for the same composition.[115] This indicates a large anisotropy in the measured properties of PZN-PT based single crystals.

Later, Park et al. explored the strain vs. electric field dependence upon crystallographic orientation.[118] For $[001]_C$- poled crystals, large piezoelectric coefficients and very high strain levels up to 0.7 % with reduced hysteresis were observed. The large strain with minimized hysteresis behavior was attributed to the stable engineered domain configuration. For the $[111]_C$- poled crystals, much smaller values were reported both for

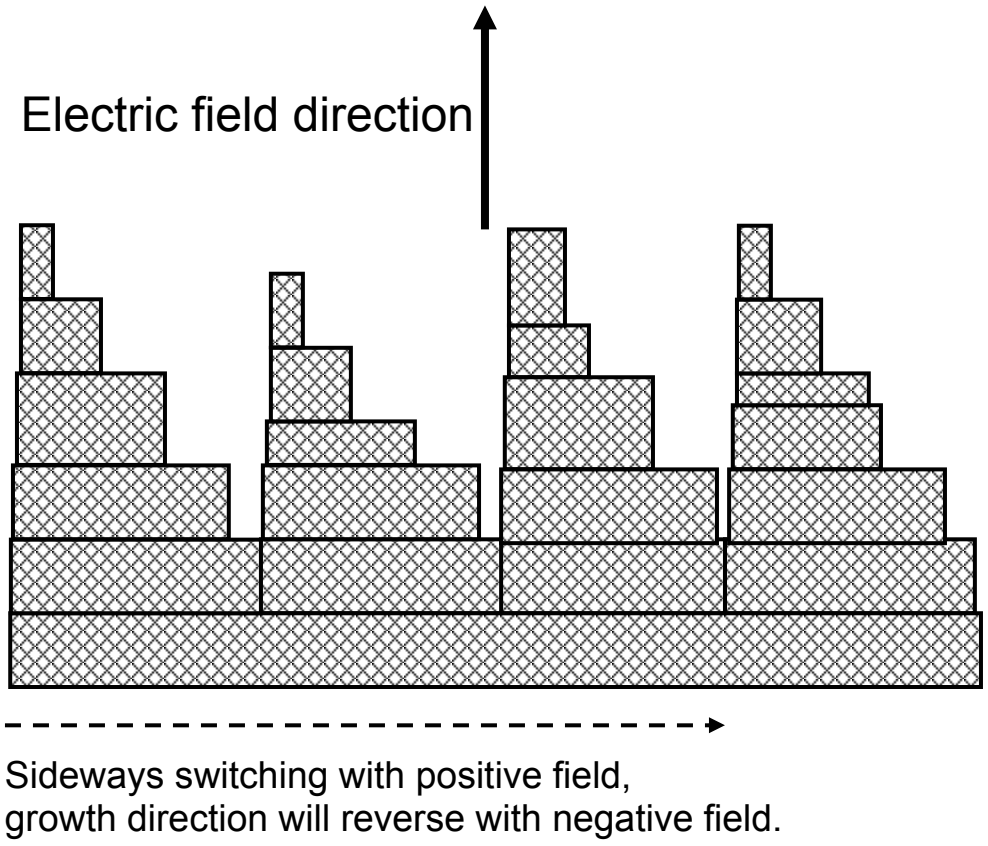

Figure 1.23 The macrodomain switching sequence of nucleation and merging under applied electric field along the <111> directions in PZN.[111]

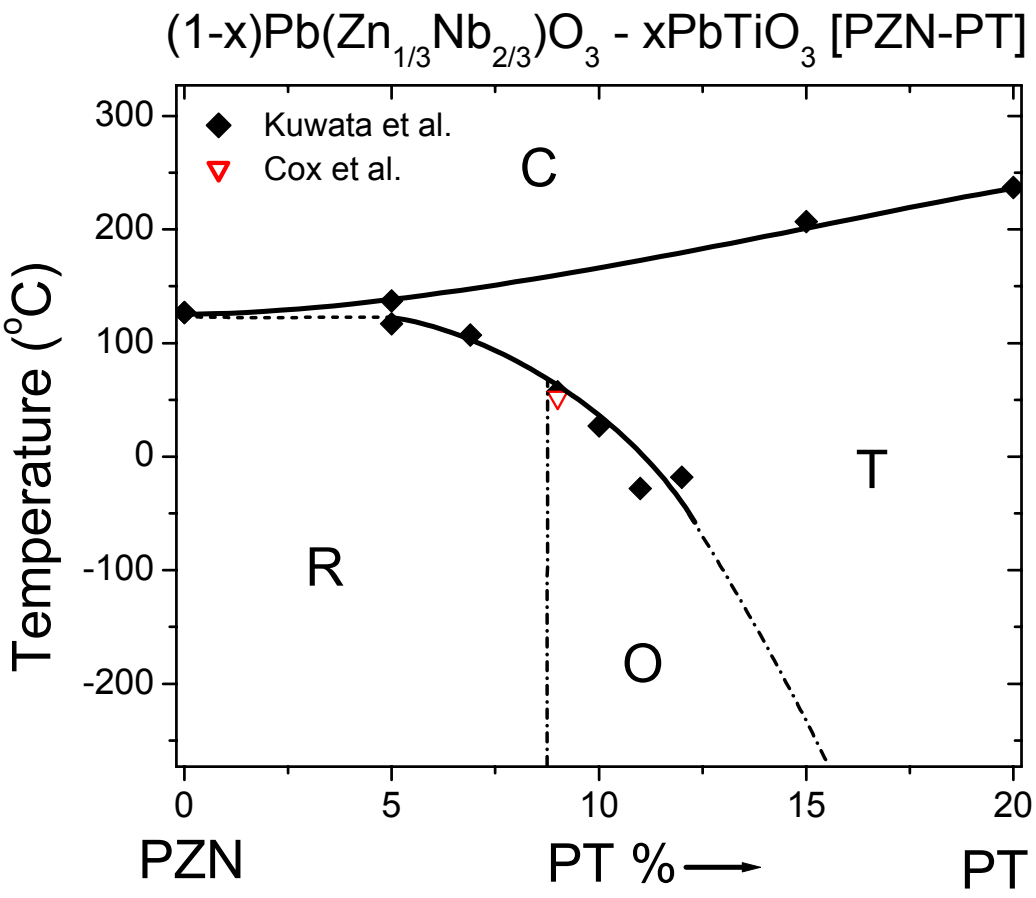

Figure 1.24 Phase diagram for PZN-PT solid solution.[119,114] (R: Rhombohedral, O: Orthorhombic, T: Tetragonal, C: Cubic).

d_{33} and strain. This was explained by a combination of domain reorientation (or depoling) upon the removal of the poling field. A recent study also reported the orientation dependent piezoelectric response in PZT thin films.[120]

1.4 Summary

Perovskite type ferroelectric materials are promising candidates for many applications. For the improvement of properties, it is critical to understand the total response of these materials when exposed to external conditions. When used in certain device applications and exposed to certain environmental conditions (i.e., stress, electric field) the interactions will be influenced by the micro scale features such as defects and disorder, as well as the macro scale factors like geometry or contact properties. For applications utilizing the reorientable polarization characteristic of ferroelectrics, domain formation and reversal processes will be involved under the applied operating electric fields. Given the complexity of these processes, it would be very helpful to use single crystal ferroelectrics as model systems to simplify the characterization, facilitating sound conclusions.

In this chapter, basic concepts of normal and relaxor ferroelectricity were discussed with actively studied examples. In particular, domain formation and polarization switching processes were described as it is relevant for the scope of the thesis. In the following chapter, the motivation, major goals, and outline of the study will be presented.

1.5 References

[1] J. Valasek, Phys. Rev. **17**, 475 (1921).
[2] W. Kanzig, Ferroelectrics and Antiferroelectrics, Academic Press, New York 1957.
[3] J. F. Nye, Physical Properties of Crystals, Oxford University Press, Oxford 1957.
[4] E. Fatuzzo and W. J. Merz, Ferroelectricity, North-Holland 1967.
[5] J. C. Burfoot, Ferroelectrics, Van Nostrand, New York 1967.
[6] J. B. Grindlay, An Introduction to Phenomenological Theory of Ferroelectricity, Pergamon Press, Oxford 1970.
[7] B. Jaffe, W. R. Cook, H. Jaffe, Piezoelectric Ceramics, London and New York 1971.
[8] T. Mitsui, I. Tatsuzaki, and E. Nakamura, An Introduction to the Physics of Ferroelectrics, Gordon and Breach, London 1976.
[9] W. G. Cady, Piezoelectricity, McGraw – Hill, New York 1946.
[10] M. E. Lines and A. M. Glass, Principles and Applications of Ferroelectrics and Related Materials, Clarendon Press, Oxford 1977.
[11] H. D. Megaw, Ferroelectricity in Crystals, Methuen and Co., London 1957.
[12] F. Jona and G. Shirane, Ferroelectric Crystals, Pergamon Press, Oxford 1962.
[13] D. D. Viehland, "The Glassy Behavior of Relaxor Ferroelectrics", Ph.D. Thesis, The Pennsylvania State University, University Park, PA (1991).
[14] Y. Xu, Ferroelectric Materials and Their Applications, North-Holland Elsevier Sci. Publ., Amsterdam 1991.
[15] L. E. Cross, Ferroelectrics, **151**, 305 (1994).
[16] B. Wul and I. M. Goldman, C. R. Acad. Sci. U. R. S. S. **46**, 177 (1945).
[17] A. J. Moulson and J. M. Herbert, Electroceramics, Chapman and Hall Press, New York 1996.
[18] R. Landauer, J. Appl. Phys. **28**, 227 (1957).
[19] H. Blattner, W. Kanzig, W. J. Merz, and H. Sutter, Helv. Phys. Acta **21**, 207 (1948).
[20] B. T. Batthias and A. von Hippel, Phys. Rev. **73**, 1378 (1948).
[21] R. C. Miller, Phys. Rev. **134**, A1313 (1964).
[22] G. L. Pearson and W. L. Feldmann, J. Phys. Chem. Solids **9**, 28 (1958).
[23] Y. Furuhata and K. Toriyama, Appl. Phys. Lett. **23**, 361 (1973).
[24] C. A. Wallace, J. Appl. Cryst. **3**, 546 (1970).
[25] R. E. Nettleton, Ferroelectrics **1**, 3, 87, 93, 111, 121, 127, 207, 221 (1970).
[26] R. E. Nettleton, Ferroelectrics **2**, 5, 77, 93 (1971).
[27] A.Safari, R. K. Panda, and V. F. Janas, Key Eng. Mater. **122-124**, 35 (1996).
[28] D. Damjanovic, Rep. Prog. Phys. **61**, 1267 (1998).
[29] B. T. Batthias and A. von Hippel, Phys. Rev. **73**, 1378 (1948).
[30] W. J. Merz, Phys. Rev. **95**, 690 (1954).
[31] C. B. Sawyer and C. H. Tower, Phys. Rev. **35**, 269 (1930).
[32] W. J. Merz, Phys. Rev. **95**, 690 (1954).
[33] J. C. Burfoot and G. W. Taylor, Polar Dielectrics and Their Applications, Macmillan, London 1979.

[34] V. Y. Shur, "Fast Polarization Reversal Process: Evolution of Ferroelectric Domain Structure in Thin Films" in Ferroelectric Thin Films: Synthesis and Basic Properties, pp. 153, ed. by C. P. de Araujo, J. F. Scott, and G. W. Taylor, Gordon and Breach, Amsterdam 1996.
[35] V. Shur and E. Rumyantsev, J. Korean Phys. Soc. **32**, S727 (1988).
[36] R. Landauer, J. Appl. Phys. **28**, 227 (1957).
[37] R. C. Miller and G. Weinreich, Phys. Rev. **117**, 1460 (1960).
[38] M. E. Drougard, J. Appl. Phys. **31**, 352 (1960).
[39] Y. Ishibashi and Y. Tagaki, J. Phys. Soc. Japan **31**, 506 (1971).
[40] Y. Ishibashi, Ferroelectric Thin Films: Synthesis and Basic Properties, vol.10, pp.135, ed. by C. P. de Araujo, J. F. Scott, and G. W. Taylor, Gordon and Breach, Amsterdam 1996.
[41] W. J. Merz, and J. R. Anderson, Bell Lab.Record **33,** 335 (1955).
[42] J. R. Anderson, G. W. Brady, W. J. Merz, and J. P. Remeika, J. Appl. Phys. **26,** 1387 (1955).
[43] H. L. Stadler, J. Appl. Phys. **29,** 743 (1958).
[44] R. Williams, J. Phys. Chem. Solids **26,** 399 (1965).
[45] W.C. Stewart, and L.S. Cosentino, Ferroelectrics **1,** 149 (1970).
[46] D. B. Fraser, and J. R. Maldonado, J. Appl. Phys. **41,** 2172 (1970).
[47] F. Scott, and C. A. Paz De Araujo, Science **246,** 1400 (1989).
[48] A. I. Kingon and S. K. Streiffer, Curr. Opin. Sol. St. M. **4**, 39 (1999).
[49] S. B. Desu, Phys. Stat. Sol.(A) **151,** 467 (1995).
[50] G. R. Fox, F. Chu, and T. Davenport, J. Vac. Sci. Technol. B **19**, 1967 (2001).
[51] S. Sinharoy, H. Buhay, D. R. Lampe, and M. H. Francombe, J. Vac. Sci. Techol. A **10,** 1554 (1992).
[52] G. W. Taylor, J. Appl. Phys. **38**, 4697 (1967).
[53] Q. Y. Jiang, E. C. Subbarao, and L. E. Cross, J. Appl. Phys. **75**, 7433 (1994).
[54] K. Okazaki, J. Am. Ceram. Soc. **63**, 1150 (1983).
[55] M. Pereira, A. G. Peixoto, M. J. M. Gomes, J. Europ. Ceram. Soc. **21**, 1353 (2001).
[56] C. K. Barlingay, S. K. Dey, Thin Solid Films **272**, 112 (1996).
[57] J. Chen, M. P. Harmer, and D. Smyth, ISAF 8 Proceedings, 111 (1992).
[58] H. Watanabe, T. Mihara, H. Yashimori, and C. A. Paz De Araujo, ISIF 4 Proceedings, 346 (1992).
[59] R. D. Klissurka, A. K. Tagantsev, K. G. Brooks, N. Setter, J. Am. Ceram. Soc. **80**, 336 (1997).
[60] B. Yang, T. K. Song, S. Aggarwal, and R. Ramesh, Appl. Phys. Lett. **71**, 3578 (1997).
[61] S-H. Kim, D-J. Kim, J. G. Hong, S. K. Streiffer, and A. I. Kingon, J. Mater. Res. **14**, 1371 (1999).
[62] E. M. Griswold, M. Sayer, D. T. Amm, and I. D. Calder, Can. J. Phys. **69**, 260 (1991).
[63] T. Haccart, D. Remiens, and E. Cattan, Thin Solid Films **423**, 235 (2003).
[64] H. Watanabe, T. Mihara, H. Yashimori, and C. A. Paz De Araujo, ISIF 3 Proceedings, 139 (1992).

[65] S. D. Bernstein, Y. Kister, J. M. Whal, S. E. Bernacki, and S. R. Collins, MRS Symp. Proc. **243**, 373 (1992).
[66] G. Toewee, J. M. Boulton, M. N. Orr, C. D. Baertlein, R. K. Wade, D. P. Birnie, and D. R. Uhlman, MRS Symp. Proc. **310**, 423 (1992).
[67] H. N. Al-Shareef, K. R. Bellur, O. Auciello, and A. I. Kingon, Thin Solid Films **252**, 38 (1994).
[68] D. P. Vijay and S. B. Desu, J. Electrochem. Soc. **140**, 2640 (1993).
[69] H. N. Al-Shareef, K. R. Bellur, A. I. Kingon, and O. Auciello, Appl. Phys. Lett. **66**, 239 (1995).
[70] T. Nakamura, Y. Nakano, A. Kanisawa, and H. Takasu, Jpn. J. Appl. Phys., Part 1 **33**, 5207 (1994).
[71] T. Nakamura, Y. Nakano, A. Kanisawa, and H. Takasu, Appl. Phys. Lett. **64**, 1522 (1994).
[72] K. Kushida-Abdelghafar, M. Hiratani, and Y. Fujisaki, J. Appl. Phys. **85**, 1069 (1999).
[73] J. T. Cheung, P. E. D. Morgan, and R. Neurgaonkar, Proceedings of the 4th International Symposium on Integrated Ferroelectrics, Colorado Springs, CO, 518 (1992).
[74] C. B. Eom, R. B. Van Dover, J. M. Phillips, D. J. Werder, C. H. Chen, R. J. Cava, R. M. Fleming, and D. K. Fork, Appl. Phys. Lett. **63**, 2570 (1993).
[75] D. J. Lichtenwalner, R. Dat, O. Auciello, and A. I. Kingon, Ferroelectrics **152**, 97 (1994).
[76] R. Ramesh, W. K. Chan, B. Wilkens, T. Sands, J. M. Tarascon, V. K. Keramidas, D. K. Fork, J. Lee, and A. Safari, Appl. Phys. Lett. **61**, 1537 (1992).
[77] R. Ramesh, H. Girchlist, T. Sands, V. G. Keramidas, R. Haakenaasen, and D. K. Fork, Appl. Phys. Lett. **63**, 3592 (1993).
[78] R. Dat, D. J. Lichtenwalner, O. Auciello, and A. I. Kingon, Appl. Phys. Lett. **64**, 2873 (1994).
[79] J. Yin, T. Zhu, Z. G. Liu, and T. Yu, Appl. Phys. Lett. **75**, 3698 (1999).
[80] H. N. Al-Shareef and A. I. Kingon, Ferroelectric Thin Films: Synthesis and Basic Properties, vol.10, pp.193, ed. by C. P. de Araujo, J. F. Scott, and G. W. Taylor, Gordon and Breach, Amsterdam 1996.
[81] C. A. Paz De Araujo, J. D. Cuchiaro, M. C. Scott, and L. D. McMillan, International Patent Application, International Publication No. WO 93/12542, 1993.
[82] C. A. Paz De Araujo, J. D. Cuchiaro, L. D. McMillan, M. C. Scott, and J. F. Scott, Nature **374**, 627(1995).
[83] R. Dat, J. K. Lee, O. Auciello, and A. I. Kingon, Appl. Phys. Lett. **67**, 572 (1995).
[84] S. Aggarwal, I. G. Jenkins, B. Nagaraj, C. J. Kerr, C. Canedy, R. Ramesh, G. Valasquez, L. Boyer, and J. T. Evans, Jr., Appl. Phys. Lett. **75**, 1787 (1999).
[85] L. F. Schloss and P. C. McIntyre, J. Appl. Phys. **93**, 1743 (2003).
[86] W. L. Warren, D. Dimos, B. A. Tuttle, G. E. Pike, R. W. Schwartz, P. J. Clews, and D. J. McIntyre, J. Appl. Phys. **77**, 6695 (1995).
[87] A. K. Tagantsev, I. Stolichnov, E. L. Colla, and N. Setter, J. Appl. Phys. **90**, 1387(2001).

[88] D. J. Johnson, D. T. Amm, E. Griswold, K. Sreenivas, G. Yi, and M. Sayer, Mater. Res. Soc. Symp. Proc. **200**, 289 (1990).
[89] E. L. Colla, A. K. Tagantsev, D. V. Taylor, and A. L. Kholkin, J. Korean Phys. Soc. **32**, S1353 (1998).
[90] P. K. Larsen, G. J. M. Dormans, D. J. Taylor, and P. J. V. Veldhoven, J. Appl. Phys. **76**, 2405 (1994).
[91] A. K. Tagantsev, M. Landivar, E. L. Colla, and N. Setter, J. Appl. Phys. **78**, 2623 (1995).
[92] I. Yoo and S. Desu, Phys. Status Solidi A **133**, 565 (1992).
[93] M. Dawber and J. F. Scott, Appl. Phys. Lett. **76**, 1060 (2000).
[94] T. Mihara, H. Watanabe, and C. A. Paz De Araujo, Jpn. J. Appl. Phys. Part 1 **33**, 3996 (1994).
[95] A. K. Tagantsev and I. A. Stolichnov, Appl. Phys. Lett. **74**, 1326 (1999).
[96] G. A. Smolenski and A. I. Agranovskya, Sov. Phys. Sol.-State. **1**, 1429 (1959).
[97] N. Setter, "The Role of Positional Disorder in Ferroelectric Relaxor", Ph.D. Thesis, The Pennsylvania State University, University Park, PA (1980).
[98] L. E. Cross, Ferroelectrics **76**, 241 (1987).
[99] C. A. Randall and A. S. Bhalla, Jpn. J. Appl. Phys. **29**, 327 (1990).
[100] V. A. Bokov and I. E. Myl'nikova, Sov. Phys.-Sol. State **3**, 613 (1961).
[101] T. R. Shrout and A. Halliyal, Am. Ceram. Soc. Bull., **66**, 704 (1987).
[102] G. Burns and F. Dacol, Sol. State Comm. **48**, 853 (1983).
[103] G. I. Skanavi, Y. M. Ksendzov, V. A. Trigubenko, and V. G. Prokhvatilov, Sov. Phys.-JETP **6**, 250 (1958).
[104] D. Viehland, J. F. Li, S. J. Jang, and L. E. Cross, Phys. Rev. B **43**, 8316 (1991).
[105] W. Kleemann and A. Clossner, Ferroelectrics **150**, 35 (1993).
[106] C. A. Randall, D. J. Barber, R. W. Whatmore, and P. Groves, Ferroelectrics **76**, 277 (1987).
[107] C. A. Randall, D. J. Barber, and R. W. Whatmore, J. Micro. **145**, 235 (1987).
[108] H. Qian, and L. A. Bursill, Int. J. Mod. Phys. B **10**, 2007 (1996).
[109] V. A. Isupov, Izvest Akad Nauk SSSR. Seri. Fiz. **47**, 559 (1983).
[110] H. Yu, "Dendritic Domain Studies in $Pb(Zn_{1/3}Nb_{2/3})O_3$-$PbTiO_3$ Single Crystals", M.S. Thesis, The Pennsylvania State University, University Park, PA (2001).
[111] M. L. Mulvihill, "In-Situ Observation of the Domain Behaviors in Normal and Relaxor Ferroelectric Single Crystals Under Applied Electric Field and Temperature", Ph.D. Thesis, The Pennsylvania State University, University Park, PA (1996).
[112] Y. Yokomizo, T. Takahashi, and S. Nomura, J. Phys. Soc. Jpn. **28**, 1278 (1970).
[113] S. Nomura, T. Takahashi, and Y. Yokomizo, J. Phys. Soc. Jpn. **27**, 262 (1969).
[114] J. Kuwata, K. Uchino, and S. Nomura, Ferroelectrics **37**, 579 (1981).
[115] J. Kuwata, K. Uchino, and S. Nomura, Jpn. J. Appl. Phys. **21**, 1298 (1982).
[116] M. L. Mulvihill, S.-E. Park, G. Risch, Z. Li, K. Uchino, and T. Shrout, Jpn. J. Appl. Phys., Part 1 **35**, 3984 (1996).
[117] Y. Yamashita, Jpn. J. Appl. Phys. **33**, 5328 (1994).
[118] S.-E. Park, T. R. Shrout, J. Appl. Phys. **82**, 1804 (1997).
[119] D.E. Cox, B. Noheda, G. Shirane, Y. Uesu, K. Fujishiro, and Y. Yamada, Appl. Phys. Lett. **79**, 400 (2001).

[120] D. V. Taylor and D. Damjanovic, Appl. Phys. Lett. **76**, 1615 (2000).

Chapter 2

STATEMENT OF THE PROBLEM AND THESIS OBJECTIVES

Chapter 1 introduced major characteristics of ferroelectrics which have been considered for a wide range of applications. Among the devices that utilize hysteretic polarization-electric field behavior are nonvolatile random access memories. The concept of utilizing the reversible spontaneous polarization as a memory state goes back to the early days of ferroelectric research. Consideration of ferroelectrics for memory applications led researchers to the study of electric field cycling in ferroelectric single crystals, especially in barium titanate compositions. Soon it was realized that repeated polarization reversals by the application of bipolar electric field cause a decay in the switching charge. This effect is known as ferroelectric (polarization) fatigue. Fatigue makes it difficult to distinguish between two states (i.e., $+P_r$: "1" and $-P_r$: "0"), and consequently limits the lifetime of the memories. Extensive research has been done on the understanding of polarization switching and resulting fatigue in ferroelectrics. Studies continued in the bulk polycrystalline ceramics and many aspects of fatigue phenomenon were uncovered. Establishment of theoretical understanding helped the materials scientists and electrical engineers to develop certain strategies to improve fatigue resistance in ferroelectrics. As summarized in chapter 1, most important of these included the use of oxide electrodes, and switching to alternative ferroelectrics that demonstrate fatigue resistance.

However, with the recent advances in thin film technology, integration possibilities of ferroelectrics into new electronic devices increased. As demand for smaller, lighter and portable devices increase, ferroelectric nonvolatile memories will continue to be attractive. Nonvolatile memory technology has been receiving a great deal of attention due to the richness of the subject matter offering interesting physics and opportunities for innovative device and circuit designs and applications, as well as the challenge of building reliability into the varied device structures. Not only developing strategies to control fatigue, but a broad understanding of fundamental issues associated with electric field response of ferroelectrics, is required for meeting the challenges for new applications.

Fatigue is closely related with the domain reorientation processes in ferroelectrics. When exposed to an external field, both the characteristics of the applied field (i.e., strength, orientation, exposure time etc.) and the structural nature of ferroelectrics (i.e., domain type, defect chemistry, chemical homogeneity etc.) are important. A number of factors (i.e., porosity, grain boundaries etc.) influence polarization switching and other material properties in polycrystalline ceramic ferroelectric materials. These will complicate the investigation of fatigue mechanisms and make it difficult to interpret the experimental results and reach conclusions. In this regard, single crystals are ideal for a fundamental study of fatigue through reducing the complexity of switching and possibly separating the influence of certain factors. Also, pure crystallographic orientations make it possible to interpret the domain structure-fatigue relationship.

Even though most of the early fatigue studies were confined to single crystals, quality and characterization issues associated with the single crystals have influenced the

obtained results, producing inconsistencies. The current status of single crystal growth and characterization technology provides opportunities to revisit the early work and build upon new approaches for the understanding of current issues.

In recent years, complex perovskite type relaxor ferroelectric single crystals have emerged as a group of promising materials for various applications. So-called “domain engineered” crystals exhibit extraordinarily large properties in one direction compared to the others. Large anisotropy and large electromechanical coefficients have been reported in these crystals. Fundamentally different piezoelectric behaviors in various crystallographic orientations were attributed to the different domain response when field is applied along certain directions. A recent study by Damjanovic et al suggested also the intrinsic lattice contributions. With the existence of these relaxor based single crystals, understanding the nature of polarization switching may be helpful to the study of fatigue. As shown in Figure 1.24, the relaxor-PT phase system offers a number of opportunities to study fatigue. Fatigue rates can be studied in correlation with orientation, temperature, composition, and ferroelectric phase. It is the aim of this study to create a clear dependence of these effects through systematic fatigue studies. Chapter 3 basically reports the results with a discussion toward the achievement of this goal.

It is also interesting to investigate polarization switching dynamics in different orientations as a function of fatigue history. Field and frequency dependence of switching would be informative for the understanding of orientation dependence and tracking changes with fatigue history. Chapter 4 presents the study of polarization reversal dynamics in PZN-4.5PT single crystals.

Another aspect of ferroelectrics is the complex interaction between domains and existing defects under dc field excitations. Probing the relaxation in a variety of orientations as a function of fatigue history in dc field excited single crystals upon the removal of the applied field will provide insight into the impact of existing disorder on the polarization behavior. Relaxation behavior of PZN-4.5PT single crystals along different orientations is discussed in chapter 5.

Observations on electrical characterization of polarization dynamics at the presence and absence of an applied field as presented in chapter 4 and chapter 5 can be verified by direct observation techniques. In chapter 6, an optical domain observation study is presented and demonstrates the complexity of domain structures in relaxor ferroelectrics. When combined together with the previous chapters, interpretation of the domain structures will be easier and fruitful.

Chapter 3

POLARIZATION SWITCHING AND FATIGUE ANISOTROPY IN LEAD ZINC NIOBATE – LEAD TITANATE SINGLE CRYSTAL FERROELECTRICS

This chapter introduces a new insight into polarization switching and fatigue phenomena based on a study in single crystals. Fatigue rates in the $Pb(Zn_{1/3}Nb_{2/3})O_3$–$PbTiO_3$ (PZN-PT) perovskite solid solution were investigated for different compositions in the rhombohedral and tetragonal phases in a variety of directions, and various field levels. It was found that the fatigue rates depend on both the ferroelectric phase and crystallographic orientation. In the rhombohedral phase when the field is applied along the $[001]_C$ direction (where the direction is given in terms of the cubic prototype), excellent fatigue resistance was obtained, contrary to normal fatigue in $[111]_C$ oriented rhombohedral PZN-PT.

The fatigue rates were then correlated more completely with respect to composition, orientation, temperature, and electric field strength. It is inferred that an engineered domain state in a relaxor based ferroelectric crystals with the spontaneous polarization inclined to the normal of the electrode is associated with negligible or no fatigue at room temperature. However, if thermal history, temperature, or field strength

induces a phase transition that produces a polarization parallel to the normal of electrode, these orientations fatigue.

The relative fatigue rates are also studied as a function of temperature in rhombohedral PZN-4.5PT. In directions, such as $[111]_C$ in the ferroelectric rhombohedral phase, the polarization fatigues at room temperature, but as temperature is increased the fatigue rate systematically decreases. This is explained in terms of a thermally activated process that limits the net fatigue rate of ferroelectrics.

Fatigue anisotropy was investigated also in several other ferroelectric systems including both relaxor based and normal ferroelectrics. Relaxor type $Pb(Yb_{1/2}Nb_{1/2})O_3$-$PbTiO_3$ with rhombohedral compositions exhibits fatigue anisotropy, as $[001]_C$-oriented crystals demonstrate fatigue resistance. However, $[001]_C$-oriented $BaTiO_3$ (BT) single crystals fatigue at rhombohedral phase stability temperatures. Possibilities for the absence of fatigue anisotropy in BT single crystals will be discussed.

In summary, this chapter gives information on the polarization states and orientation that control fatigue in ferroelectric crystals with a relaxor end member.

3.1 Introduction

Ferroelectric materials are widely investigated for applications in nonvolatile random access memories (NVFRAM). From the early days of research on NVFRAMs, major problems such as polarization fatigue and imprint by continuous polarization reversal have been encountered. A brief description of NVFRAMs and polarization fatigue was provided in chapter 1.

Ferroelectric (polarization) fatigue is the gradual decrease of switchable charge (or remanent polarization, $\boldsymbol{P}_r$) with polarization reversal in a ferroelectric material undergoing bipolar drive. Since the amount of charge that is stored in a ferroelectric capacitor is proportional to $\boldsymbol{P}_r$, fatigue is a serious issue. Early studies of fatigue[1,2,3,4,5,6,7] were mostly confined to single crystals, and fatigue was observed to be a general phenomenon in ferroelectrics. Fatigue is generally agreed to be the result of charge injection and the accumulation of space charge that pins domain walls or retards the nucleation of reversed domains to permit switching.[1,2,3,4,5,6,7,8,9]

There have been a number of strategies used to improve fatigue resistance in ferroelectrics; these include:

(i) Doping the dielectrics with donor dopants, e.g., La[10] or Nb[11] in $Pb(Zr,Ti)O_3$ (PZT).

(ii) Oxide electrodes, RuO_2,[12,13] IrO_2,[14,15,16] $SrRuO_3$,[17,18] and $(La,Sr)CoO_3$,[19,20,21] for PZT thin film ferroelectrics.

(iii) Nonfatiguing ferroelectrics with Pt electrodes, e.g., $SrBi_2Ta_2O_9$ or $SrBi_2Nb_2O_9$.[22,23]

The mechanism responsible for the improved fatigue resistance with oxide electrodes is not fully elucidated; one possibility is that such electrodes can act as oxygen sources, and so help limit pinning of the domain walls associated with point defects. Layered type perovskites (i.e., SBT and SBN) as alternative ferroelectrics have the spontaneous polarization lying in the a-b plane of the orthorhombic unit cell. There are only four possible polarization states with SBT or SBN.[24] In the polycrystalline case, the

remanent polarization is small, unless care is taken to control the crystallization orientation. The SBN family can be co-processed with Pt-electrodes and retains good fatigue resistance even in this case. There are, however, technological issues associated with the lower polarizations levels, the high crystallization temperatures and Bi-Pt reactions.[25]

Prior to this work, there has been a great focus on relaxor based single crystals such as PZN-PT, due to their superior electromechanical properties. The $Pb(Zn_{1/3}Nb_{2/3})O_3$-$PbTiO_3$ (PZN-PT) system is a complete solid solution, based on the perovskite crystal structure, of relaxor (PZN) and normal (PT) ferroelectric compounds. Figure 1.24 gives the ferroelectric phase diagram for PZN-PT. Composition-temperature diagrams play an important role in the understanding of the material properties. PZN-PT system encompasses a variety of ferroelectric phases which can be induced by variations in temperature, composition, and electric field application in certain orientations.[26,27] Another interesting feature of the PZN-PT is the curved MPB, which makes it possible to study the fatigue properties in a reasonable temperature range. In PZN-PT crystals, the dielectric and piezoelectric properties depend not only on the chemical composition (morphotropic phase boundary relationship) but more greatly on the crystallographic orientation and applied electricfield.[26,27] It is generally accepted that the key to the understanding of fatigue in ferroelectrics is the knowledge of the polarization switching process. Domain configuration, as in the case of other ferroelectrics, plays an important role in the polarization and strain behavior and the electromechanical performance of

rhombohedral PZN-PT crystals. Wada and coworkers proposed that the *E*-field direction affected domain stability in rhombohedral PZN-PT crystals.[28]

Since the discovery of the extraordinary piezoelectric properties (d_{33} ~2500 pC/N) with large, electric field induced strain (~1.7 %) in rhombohedral crystals oriented along $[001]_C$, numerous investigations have been made in this system.[26,28,29,30,31] It has been widely noticed that the measured properties of PZN-PT single crystals are strongly anisotropic. Park *et al.* explored the dependence of electric field–induced strains on crystallographic orientation in PZN-PT crystals. Large piezoelectric strains with extremely low hysteresis were observed in $[001]_C$ poled crystals, compared to lower strain with large hysteresis in the $[111]_C$ orientation. The very high strains, coupled with the low hysteresis of $[001]_C$ oriented crystals were attributed to the engineered-domain configuration in which the domain walls are not driven by applied fields in the poled state.[26] Wada et al.[32] studied domain engineering in barium titanate single crystals at room temperature. When an electric field is applied along $[111]_C$-orientation, high piezoelectric properties is achieved in tetragonal BT. Electric field induced domain configurations and domain switching under pulsed electric field conditions have been investigated by Yu *et al.* in PZN-PT crystals oriented at various crystallographic directions.[29,33] Both domain wall mobility and activation energies were reported to be higher in the $[001]_C$ direction than for $[111]_C$. The observed anisotropy in the switching under pulse conditions was believed to indicate that the engineered domain state along the $[001]_C$ direction is fundamentally different than that in the $[111]_C$ direction. Consequently, a higher activation field is needed in $[001]_C$ oriented crystals. However,

once the energy barrier is overcome during the switching process, domain walls move faster in $[001]_C$ oriented crystals.[29,33]

Yin and Cao[34] also explored the physical mechanisms of $[001]_C$ oriented rhombohedral PZN-PT crystals and reported that electric field application along the $[001]_C$ direction could cause the domain boundaries to be in a charged state, resulting in domain walls with a combination of L or T shapes. Some researchers hypothesize that charged walls are one of the reasons for the large dielectric and piezoelectric coefficients, but this is not universally accepted.

The objective of this study was to revisit fatigue in perovskite single crystals based on $Pb(Zn_{1/3}Nb_{2/3})O_3$–$PbTiO_3$, (PZN-PT) system. This fundamental study of fatigue is intended to determine how polarization fatigue correlates with the domain configuration and domain wall motion in relation with orientation, ferroelectric phase, temperature, and field strength in PZN-PT crystals. This clarification is expected to improve the understanding of polarization fatigue mechanisms controlling the long term reliability of the electronic devices which utilize the switching polarization of ferroelectrics.

3.2 Experimental Procedure

This section describes materials selection, and experimental procedure used to orient, cut, polish, and electrode the single crystals.

3.2.1 PZN-PT Single Crystal Compositions

Single crystals of (1-x)PZN-xPT (x=0.00, 0.045, 0.080, 0.10, and 0.12) were grown using the high temperature flux technique.[35] As shown in Figure 1.24, PZN and PZN-4.5PT crystals are rhombohedral (pseudocubic) at room temperature. For this composition, temperature dependence of dielectric properties at different frequencies (from 1 kHz to 1 MHz) is given in Figure 3.1. As the PT content increased beyond 8%, the orthorhombic phase becomes stable at room temperature. The morphotrophic phase boundary (MPB) separating orthorhombic and tetragonal ferroelectric phases is at ~10% PT. At compositions very close to the phase boundary small chemical inhomogeneities in the crystal will lead to mixed phases. PZN-12PT crystals are in a tetragonal ferroelectric phase field at room temperature.

3.2.2 Crystal Orientation

The crystal samples were oriented along the $[111]_C$, $[110]_C$, and $[001]_C$ crystallographic axes within ±2° by using the back reflection Laue x-ray technique[36] A computer controlled Laue Camera (Multiware Laboratories Ltd., real-time Laue machine) was used. The back reflection Laue technique uses white radiation emitted from an x-ray tube. The x-rays impinge on the stationary sample and reflect back only those planes which satisfy Bragg's law ($\lambda=2d\sin\theta$) for each wavelength. In this technique, the wavelength (λ) varies, θ (Bragg's angle) and d (interplanar spacing) are fixed. A schematic of the incident beam diffracting backward in the back reflection Laue method is shown in Figure 3.2. The incident beam impinges the crystal and diffracts backwards,

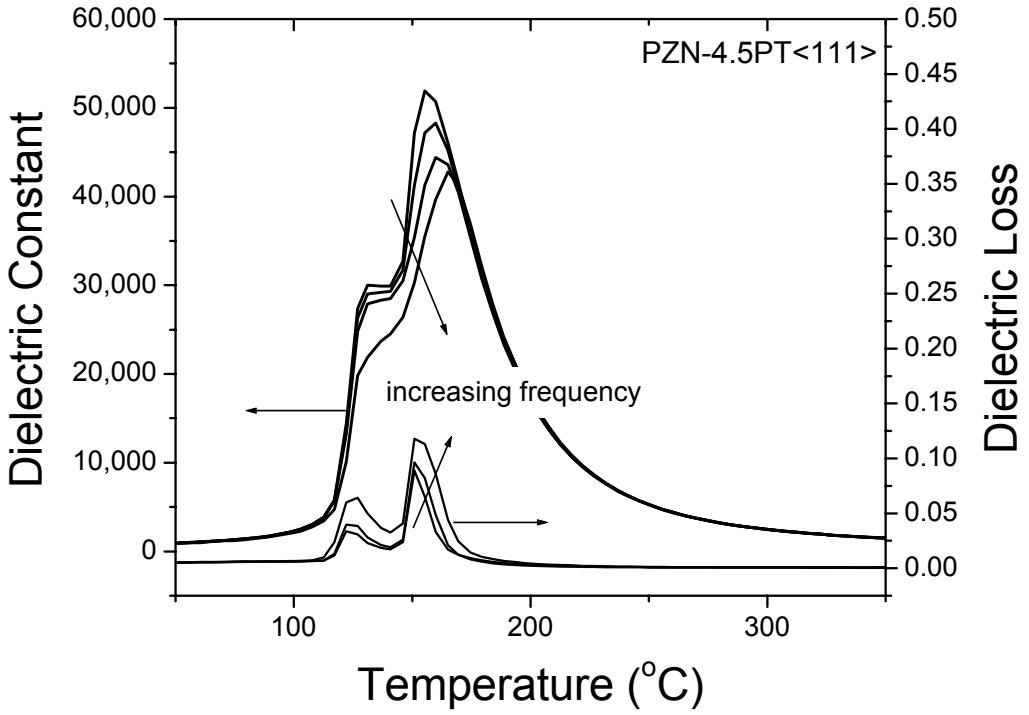

Figure 3.1 Temperature dependence of the dielectric constant and dielectric loss at different frequencies for PZN-4.5PT single crystals. As the frequency increases, dielectric constant decreases, dielectric loss increases, and T_{max} shifts to higher temperatures.

eventually giving an array of spots (see Figure 3.3). These spots represent reflections of planes along zones. The location of the spots depends on the orientation of the crystal relative to the incident beam. If the crystal quality is poor, the spots will be smeared. This technique gives information about the quality and orientation of the crystal. To obtain the desired plane orientation, the sample mounted to the goniometer-holder (sample holder) can be rotated. Once the zone axis is brought in parallel with the incident beam, the crystal orientation is achieved. After orientation is complete, the face was polished flat before removing it from the sample holder. This oriented and polished flat surface is the reference surface. The opposite side of the sample was polished to make it perfectly parallel to the reference side so that the desired orientation is achieved through the crystal.

3.2.3 Surface Preparation

Oriented crystals were then sliced to the desired thicknesses parallel to the oriented surfaces by using an Isomet low speed diamond saw (Buehler Inc.). Kerosene was used during cutting as a lubricant. Sliced crystal plates with a thickness about 400 μm to 1 mm, were then cut to obtain a square or rectangular shape. The final surface area of the samples before polishing varied from 4 mm^2 to 10 mm^2.

For polishing, plate-shaped samples were bonded onto the inner barrel of the sample holder sketched in Figure 3.4. The advantage of this sample holder is that the load on the crystal will be more homogeneous and constant compared to using finger. The outer barrel is used only to grip and move the sample holder freely. No force is applied to the inner holder especially during fine polishing steps. The following abrasives were used

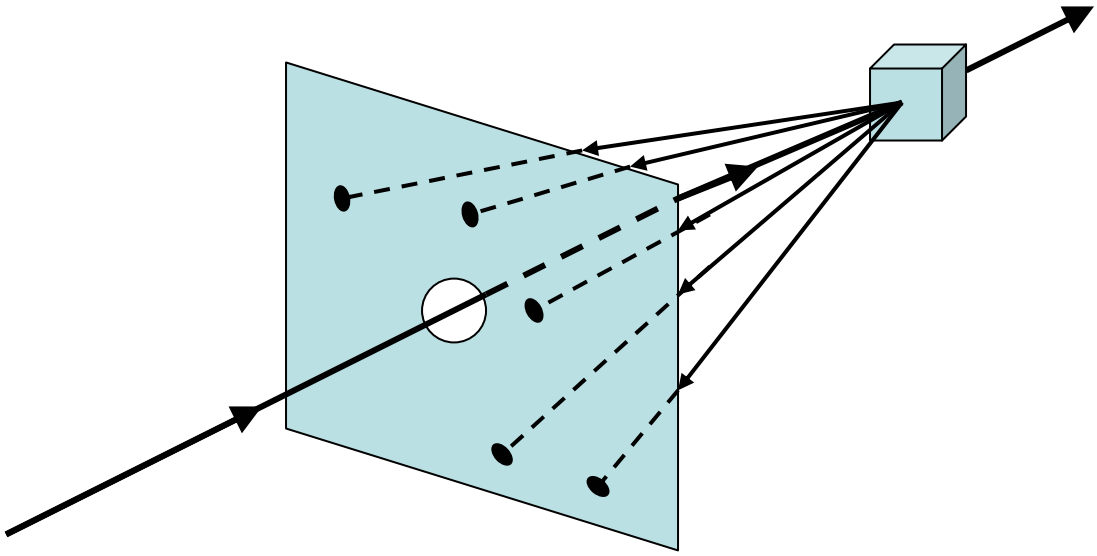

Figure 3.2 Schematic of incident beam diffracting backwards in the back reflection Laue method.[36]

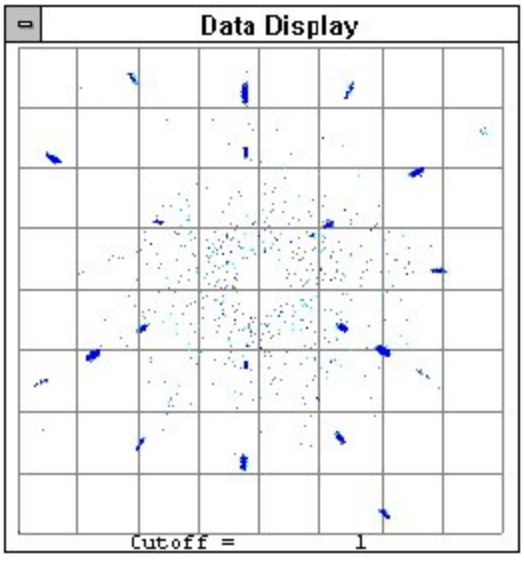

Figure 3.3 A back reflection Laue image by NorthStar commercial software.

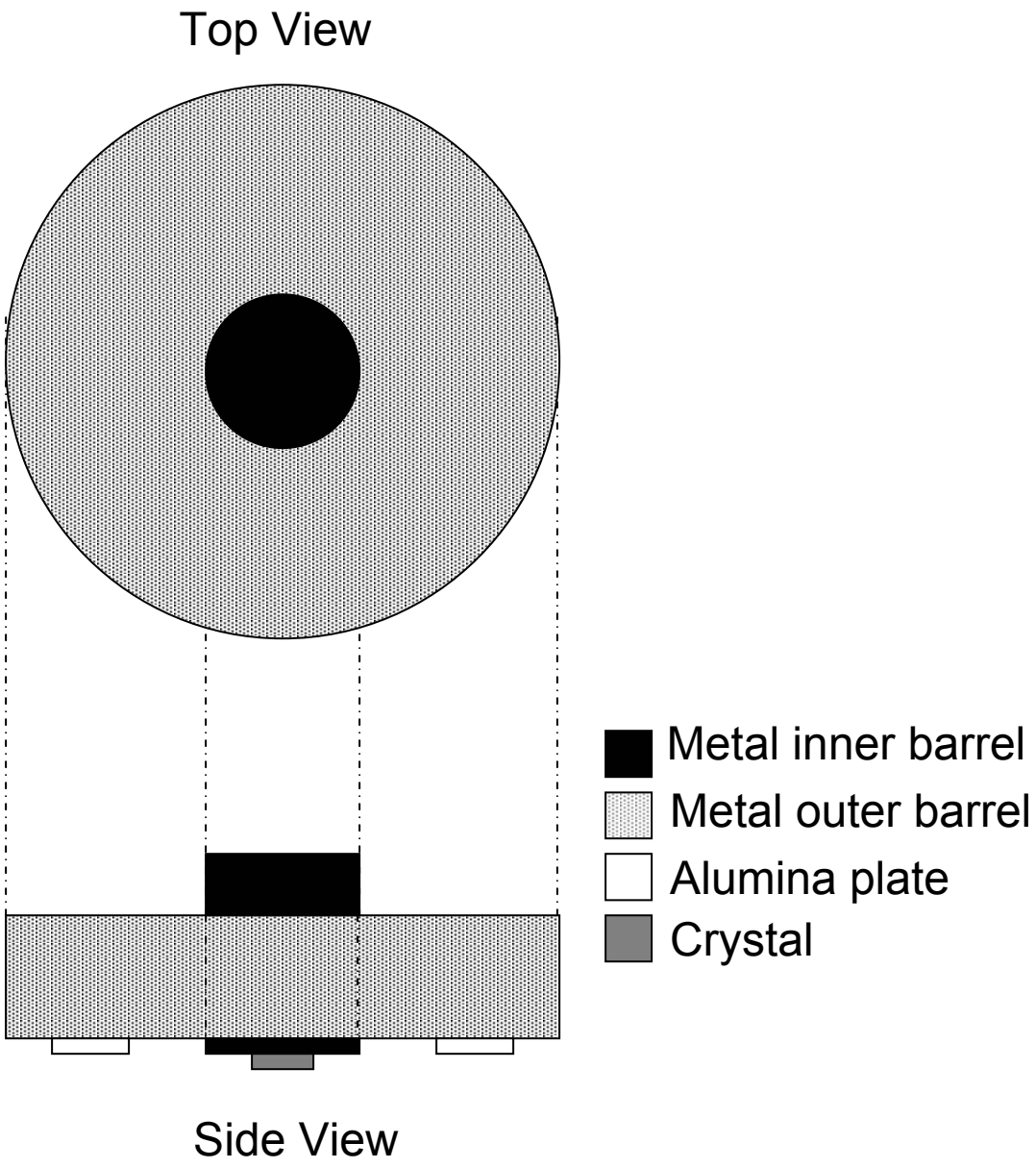

Figure 3.4 Schematic of the sample holder used for polishing.

used for polishing in the order of; a) silicon carbide paper (12 μm, 6 μm, and 3 μm), b) alumina powder (1 μm), c) diamond paste (0.3 μm), and d) silica gel (0.05 μm). Submicron polish was performed only when required by certain experiments, such as domain studies. The final thicknesses of the samples used in this study varied from 150 μm to 800 μm. Following the polishing steps, samples were cleaned by acetone in an ultrasonic cleaner, and dried in air. Prior to electroding for the electrical property measurements, samples were annealed at 300 °C for 5 hours to eliminate stresses during sample preparation steps.

3.2.4 Electroding and Electrical Property Measurements

For electrical property measurements silver paste (SPI conductive silver paint™, SPI#05001-AB) electrodes were applied on both surfaces of the samples. Silver paste electrodes were preferred because they can be removed easily by washing with acetone without changing the nature of the crystal/electrode interface after the electrode removal. A possible influence of the different electrodes or electroding methods were checked by using samples with sputtered Au or Pt and no remarkable difference was observed with different electrodes in this study.

Before high field electrical property measurements, room temperature capacitance (***C***) and dielectric loss (***tanδ***) were measured using an LCR meter (Model SR715, Stanford Research System) at 1 V and frequencies of 100 Hz, 1 kHz, and 10 kHz. This information is useful to verify the quality of the crystal and the electroding. Typically a tanδ< 0.02 is considered to indicate a good condition for the sample.

High field measurements including polarization and strain hysteresis utilized a modified Sawyer-Tower circuit (see Figure 1.8) and linear variable differential transducer driven by a lock-in amplifier (Stanford Research Systems, Model SR830). Electric fields (E) as high as ~85 kV/cm were applied in strain measurements using an amplified unipolar waveform at 0.1 Hz. In particular, the electric field was applied with a triangular bipolar waveform for the polarization switching and fatigue experiments. A high voltage dc amplifier (Trek Model 609C-6) was used in both strain and polarization fatigue property measurements. The magnitude and the frequency of the applied ac field were generally 20 kV/cm and 10 Hz, respectively, unless otherwise stated. The fatigue tests were interrupted after 10^1, 10^2,10^3, 10^4, and 10^5 switching cycles for P-E measurements at the fatiguing electric field but at a lower frequency (0.1 Hz) than the fatigue test. During measurements, the samples were submerged in Galden®, an insulating liquid, to prevent arcing. To study the influence of temperature on fatigue, the Galden® liquid was heated or cooled from room temperature using an oven and liquid nitrogen cryostat, respectively. The experiments were performed at temperatures ranging from –120 to 150 ˚C depending on the crystal composition.

The remanent polarizations (P_r) and the coercive fields (E_c) were computed from the recorded hysteresis loops. Fatigue rate is defined as the change in remanent polarization as a function of the number of switching cycles. All the changes are given as normalized values represented as percentages of both remanent polarization and coercive field. Additional experimental procedures will be described in subsequent chapters for specific experiments.

3.3 Results and Discussion

The crystallographic orientation dependence of polarization fatigue was studied in PZN-PT single crystals at varying composition, temperature, and applied electric field strength. First, the basic observation of fatigue anisotropy in rhombohedral PZN-PT will be introduced. Second, the influence of various parameters on fatigue anisotropy will be discussed. In the third part, study of fatigue anisotropy in several other ferroelectric systems will be briefly described.

3.3.1 Polarization Fatigue Anisotropy

3.3.1.1 Crystallographic Orientation Dependence of Fatigue in PZN-PT

Figure 3.5 and Figure 3.6 show P_r, E_c, and hysteresis loops for $[111]_C$- and $[001]_C$- oriented PZN - 4.5 PT crystals as a function of the number of switching cycles. The amplitude of the alternating triangular electric field (E_{max}) was 20 kV/cm, and the frequency of the field was 10 Hz. The initial P_r value for the $[001]_C$-oriented crystal ($P_{r,[001]}$) is approximately equal to $1/\sqrt{3}$ of $P_{r,[111]}$. In $[111]_C$-oriented crystals, the remanent polarization during cycling is along $[111]_C$ for $\boldsymbol{E}$ // [111], or $\left[\bar{1}\bar{1}\bar{1}\right]_C$ for $\boldsymbol{E}$ // $\left[\bar{1}\bar{1}\bar{1}\right]$. Thus, the domains switch between [111] and $\left[\bar{1}\bar{1}\bar{1}\right]$ states. In $[001]_C$-oriented crystals, the spontaneous polarization lies along one of four possible polar directions, for example $[111]_C$, $\left[\bar{1}11\right]_C$, $\left[1\bar{1}1\right]_C$, or $\left[11\bar{1}\right]_C$ for $\boldsymbol{E}$ // [001]. With a reverse electric field, these domains

switch to $[\bar{1}\bar{1}1]_C$, $[\bar{1}\bar{1}\bar{1}]_C$, $[\bar{1}1\bar{1}]_C$, or $[1\bar{1}\bar{1}]_C$, and this can be done via 180˚, 71˚, or 109˚ switching processes, assuming rhombohedral symmetry.

As shown in Figure 3.5(a), the P_r values for $[111]_C$-oriented crystals are almost constant up to 10^3 cycles and then decrease rapidly with further switching cycles. $[111]_C$-oriented crystals obviously fatigue. The E_c values increase after the onset of fatigue. In contrast, the P_r and E_c values for $[001]_C$-oriented crystals are almost constant up to 10^5 switching cycles as shown in Figure 3.6(a). The shape of the hysteresis loop does not change even after 10^5 cycles as shown in Figure 3.6(b). The E_c value slightly decreases with switching cycles. As will be discussed below, this decrease in E_c as a function of cycling was observed for $[001]_C$-oriented crystals measured with a wide variation in field amplitudes. We infer that some domain walls are weakly pinned in the initial state, causing some resistance to switching, but during cycling these domain walls are detached from the original pinning sites. Possible origins for the pinning include impurities, oxygen or lead vacancies, or damage produced during crystal growth, polishing, or electroding.

3.3.1.2 Optimum Orientation and Domain Configuration of the Crystals

Figure 3.7 (a) shows the fatigue behavior for PZN - 4.5 PT single crystals oriented along $[001]_C + \alpha$, where α is the degree of deviation from $[001]_C$ ($\alpha = 0°$) toward $[111]_C$ ($\alpha = 54.7°$), as shown in Figure 3.7(b). The initial P_r and E_c values increase with α, and the initial P_r magnitude is consistent with projection of the $P_{r,[111]}$, *i.e.* $P_{r,[111]} \cos (54.7° - \alpha)$. The fatigue rate is enhanced when crystals are oriented with $\alpha \geq 15°$. The induction

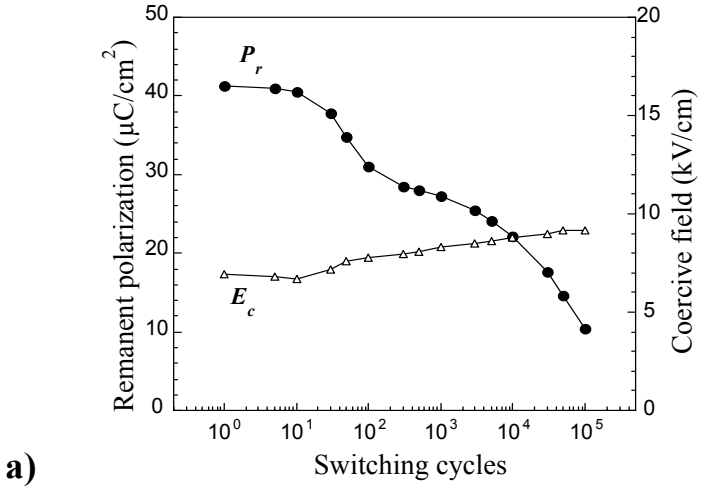

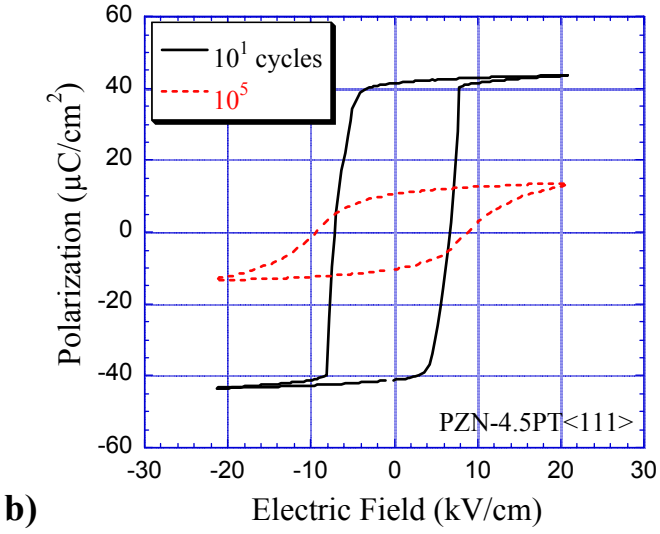

Figure 3.5 Switching cycle dependence of a) remanent polarization, P_r (solid circles), and coercive field, E_c (open triangles), b) hysteresis loops for $[111]_C$-oriented PZN - 4.5 PT single crystals. In Fig. 1(b), the solid line is the hysteresis loop after 10 cycles, and the broken line is that after 1 x 10^5 cycles.

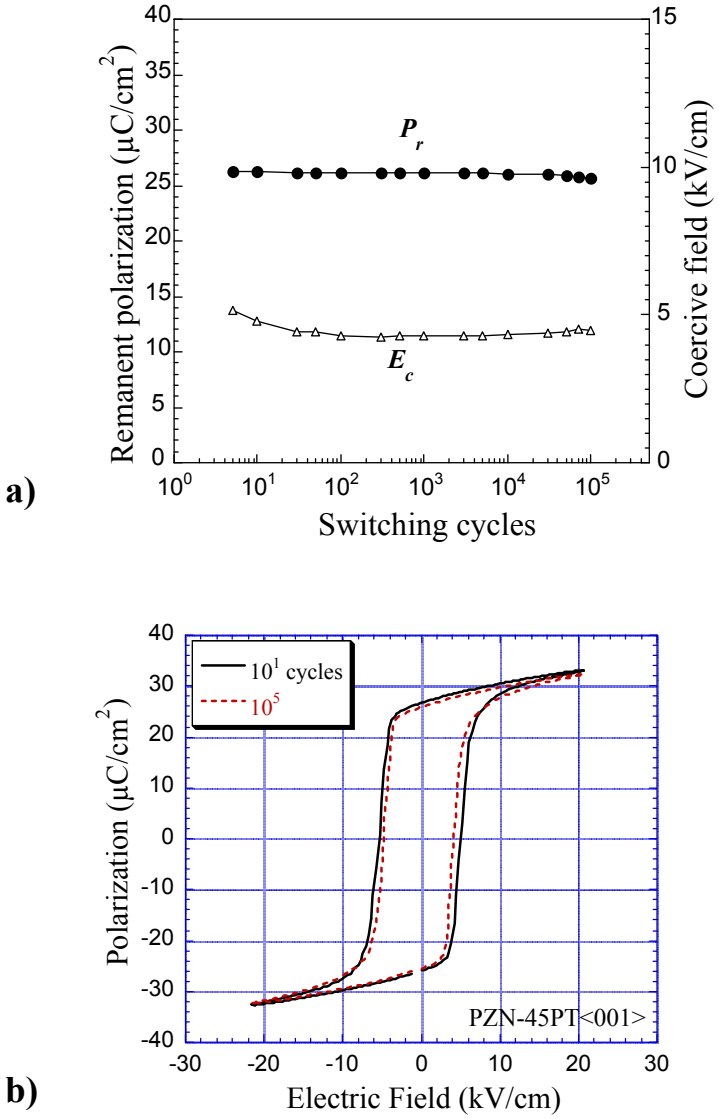

Figure 3.6 Switching cycle dependence of a) remanent polarization, P_r (solid circles), and coercive field, E_c (open triangles), b) hysteresis loops for $[001]_C$-oriented PZN - 4.5 PT single crystals. In Fig. 2(b), the solid line is the hysteresis loop after 10 cycles, and the broken line is that after 1 x 10^5 cycles.

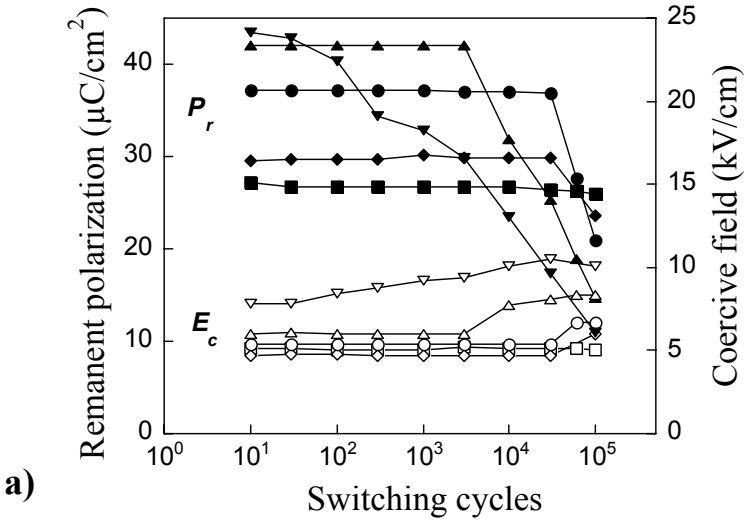

a)

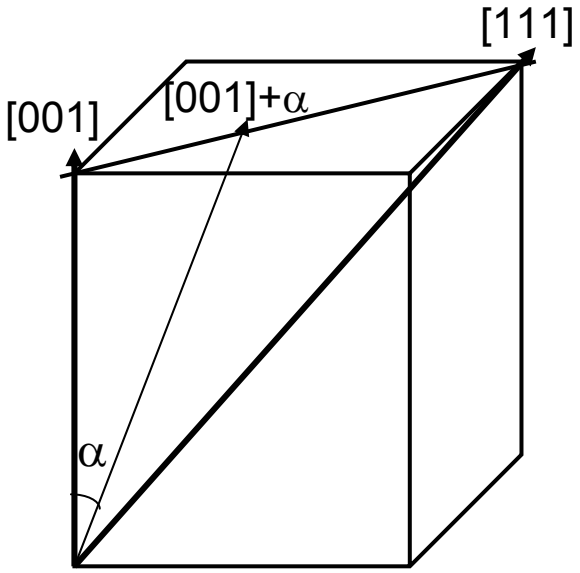

b)

Figure 3.7 Effect of deviation from $[001]_C$ direction on fatigue for PZN–4.5PT single crystals. The deviation angle from $[001]_C$ toward $[111]_C$ (α) is defined in Fig. 12 (b). Solid markers show P_r, and open markers show E_c (■,□; α = 0° [001], ♦,◊; α = 15°, ●,○; α = 30°, ▲, Δ; α = 45°, ▼,∇; α = 54.7° [111]). The switching frequency was 10 Hz. and E_{max} = 20 kV/cm.

period before fatigue onset gradually decreases with increasing α. Fatigue in the rhombohedral PZN-PT single crystals is systematically dependent on crystallographic orientation, with $[001]_C$-oriented rhombohedral ferroelectric single crystals believed to have the lowest fatigue rate.

3.3.2 Stability Conditions for Polarization Fatigue Anisotropy

3.3.2.1 Compositional Changes

The same orientation dependence of fatigue is also observed in pure PZN single crystals, as shown in Figure 3.8. Fatigue is studied also in crystals with higher PT content. Figure 3.9 shows that PZN-8PT single crystals still exhibit high fatigue resistance along $[001]_C$ orientation, while the $[111]_C$ orientation fatigues. When the PT content is higher than 10%, which is about the MPB composition, PZN-PT crystals are expected to be tetragonal. Fatigue is observed in $[001]_C$-oriented PZN-12 PT tetragonal crystals as shown in Figure 3.10(a). In tetragonal PZN-12 PT, the polar direction is along $[001]_C$. Thus, domain switching involves polarization directions normal to the electrode-crystal interface, and presumably is accomplished predominantly through 180˚ domain wall motion. However, fatigue occurs also along $[111]_C$ orientation in the tetragonal region as shown in Figure 3.10(b). The origin of fatigue in tetragonal PZN-PT crystals is believed to be similar to that found in tetragonal $BaTiO_3$ single crystals. Fatigue anisotropy may be related with the relaxor nature of ferroelectricity.

Nevertheless, the above results indicate again that rate of fatigue is strongly dependent on both the ferroelectric phase and the crystal orientation in relaxor-PT single

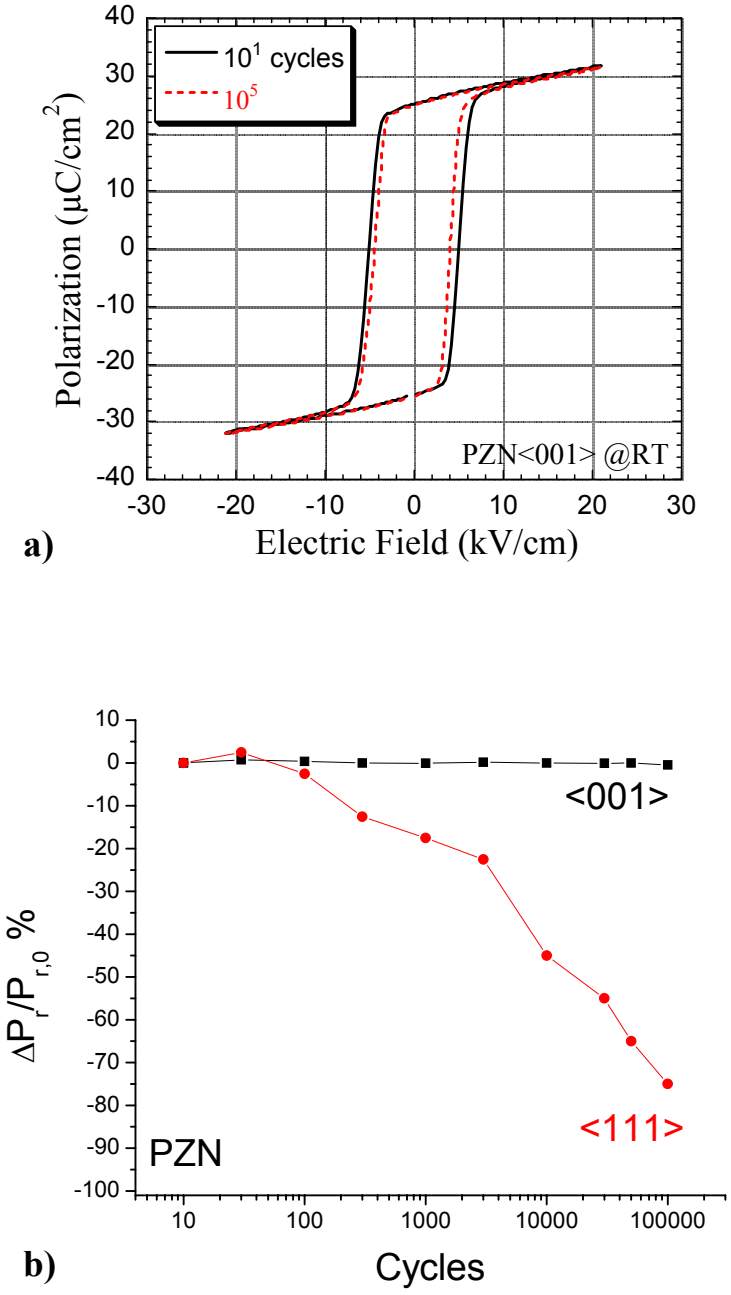

Figure 3.8 Polarization fatigue anisotropy in PZN single crystals. a) *P-E* loops after 10 and 10^5 cycles in PZN<001>$_C$, b) Switching cycles dependence of remanent polarization along $[001]_C$ and $[111]_C$ orientations.

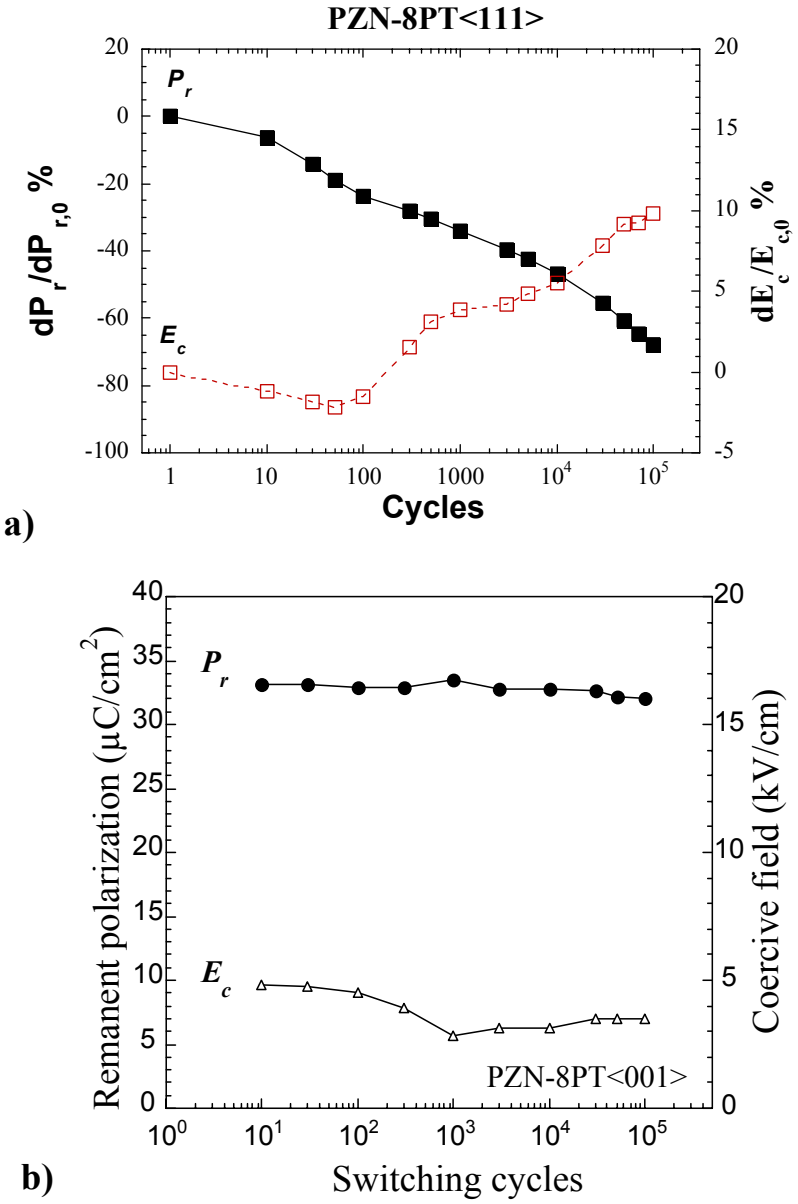

Figure 3.9 Switching cycle dependence of remanent polarization (P_r) and coercive field (E_c) in PZN-8PT along a) $[111]_C$, and b) $[001]_C$ orientation. In Fig.b), change in P_r is given relative to the initial value ($P_{r,0}$) as $dP_r/dP_{r,0}$.

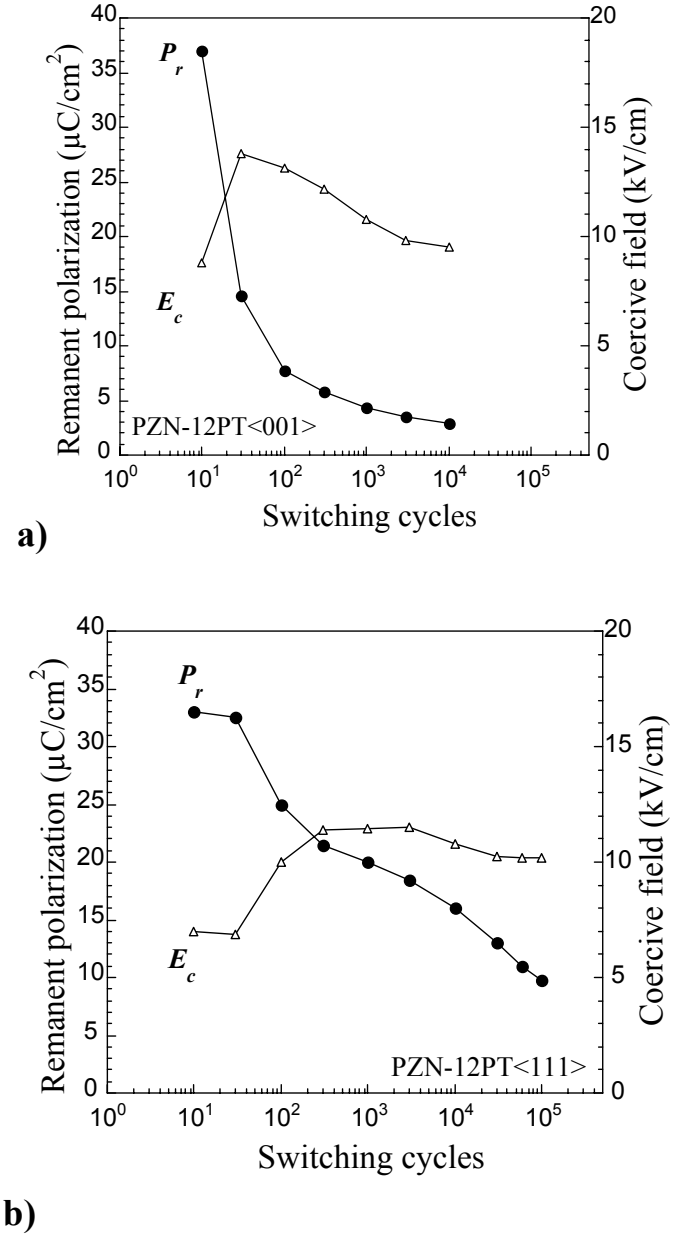

Figure 3.10 Fatigue occurs in tetragonal PZN-12PT crystals both a) along $[001]_C$, and b) $[111]_C$ orientations.

crystals. The $[001]_C$- oriented rhombohedral phase showing no notable fatigue up to 10^5 cycles for the slow alternating field required to switch the polarization in the crystal capacitors.

3.3.2.2 Switching Electric Field Strength and Frequency

In ferroelectric thin films, the magnitude of the applied fields can influence the fatigue rates.[37,38] Figure 3.11(a) shows that the $[111]_C$-oriented PZN-4.5 PT single crystals fatigue for a wider range of E_{max} values. For field strengths above the coercive fields and providing full saturation in switching, no systematic influence of electric field magnitude was observed. $[001]_C$-oriented PZN-4.5 PT crystals, in contrast, do not fatigue under various E_{max} levels, as shown in Fig. 3.7(b). We therefore can infer that the crystal orientation, rather than E_{max}, governs the fatigue resistance for these PZN-PT crystals, provided the E_{max} does not induce ferroelectric phase transitions.[39] Figure 3.12 shows the switching cycle dependence of P_r and E_c values for $[111]_C$- and $[001]_C$-oriented PZN-4.5 PT single crystals measured at various switching frequencies between 0.1 Hz and 10 Hz. In the present study, fatigue lifetime does not depend on the switching frequency (when saturation is obtained in switching) for $[111]_C$-oriented crystals.

Figure 1.24 recalls the phase diagram of the PZN-PT solid solution at low temperatures and for low electric field levels (< 1 kV/cm). In the rhombohedral phase region, the $[111]_C$ oriented crystals fatigue regardless of the applied electric field strength. In this case, the $[111]_C$ oriented crystals have a polarization vector parallel to the electric field. If an electric field is applied along the $[110]_C$ and $[001]_C$ directions, the

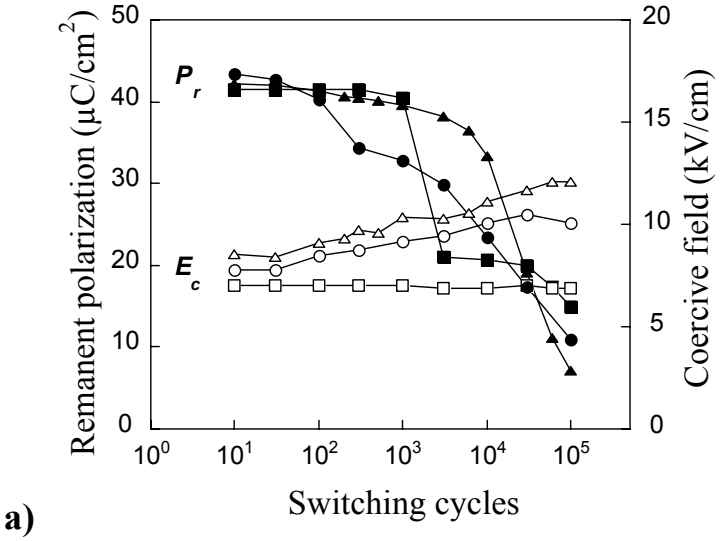

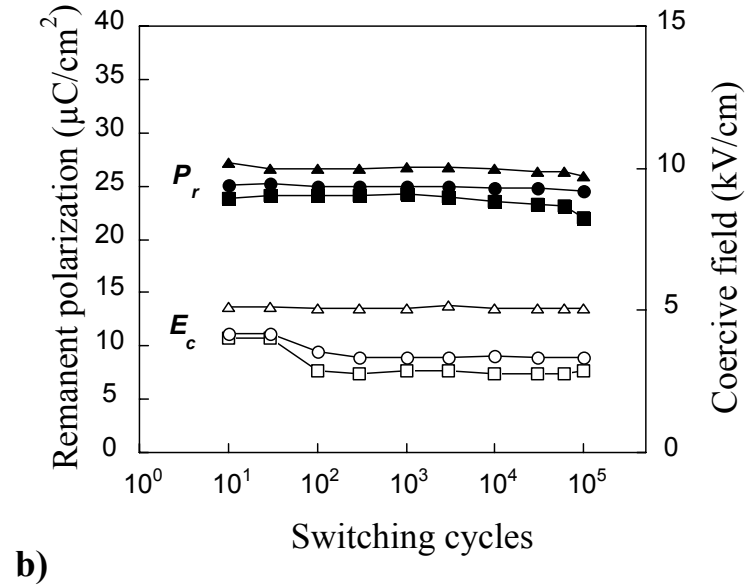

Figure 3.11 Switching cycle dependence of remanent polarization (P_r), and coercive field (E_c) for a) $[111]_C$-, b) $[001]_C$-oriented PZN-4.5PT single crystals under various switching field strengths (a) $[111]_C$:■,□; 10 kV/cm, ●,○; 20 kV/cm,▲Δ; 30 kV/cm, b) $[001]_C$:■,□; 5 kV/cm, ●,○; 10 kV/cm,▲Δ; 20 kV/cm). The switching frequency was 10 Hz.

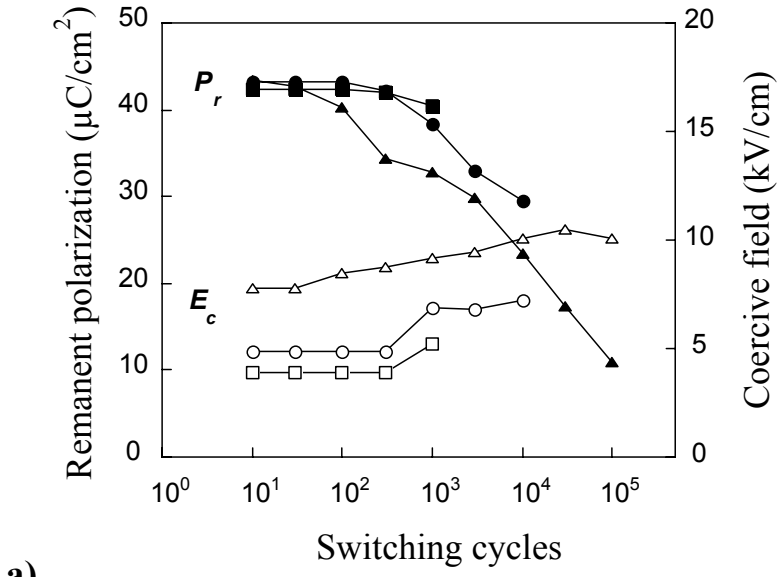

a)

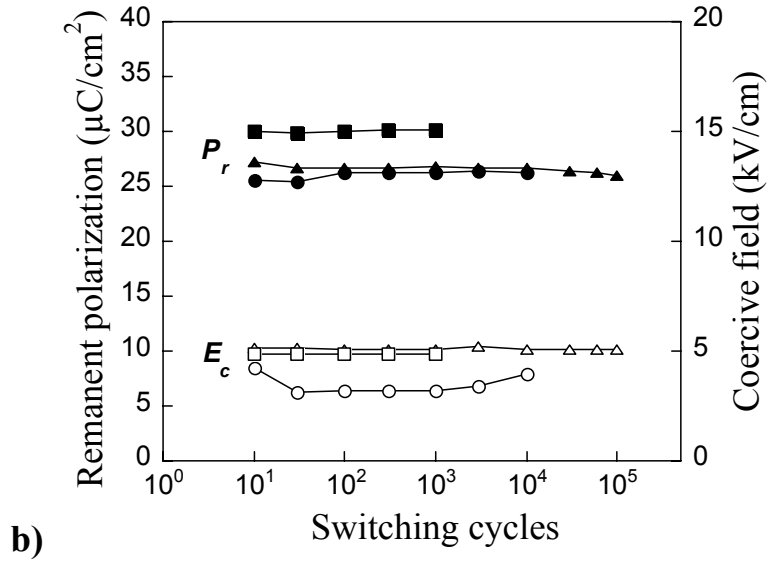

b)

Figure 3.12 Switching cycle dependence of remanent polarization (P_r), and coercive field (E_c) for a) $[111]_C$-, b) $[001]_C$-oriented PZN-4.5PT single crystals measured at various switching frequencies (■,□; 0.1 Hz, ●,○; 1 Hz, ▲Δ; 10 Hz. E_{max} was 20 kV/cm.

rhombohedral crystals do not show fatigue at low field strengths. In both of these cases the electric field develops an engineered domain structure with polarization vectors inclined with respect to the normal vector of the electrode plane.

However, it is known from the work of Park and co-workers[26,32,39] that under sufficiently high fields in specific directions, the rhombohedral ferroelectric phase can undergo field forced phase transitions. This can change the nature of the engineered domain state; for example in the $[110]_C$ direction it is possible to induce an orthorhombic phase and in the $[001]_C$ direction a tetragonal phase can be induced at room temperatures with unipolar electric field strengths of ~15 and 30 kV/cm, respectively. High field strain versus unipolar electric field behavior is given in Fig. 3.12 for PZN-4.5PT crystals with $[110]_C$ orientation, indicating the evidence for phase transformation. PZN-4.5PT crystals normally do not fatigue under small electric fields but show remarkable remanent polarization loss when driven at relatively higher fields as illustrated in Figure 3.13.b. Similar experiments were performed in $[001]_C$ oriented PZN-4.5PT crystals. Even though rhombohedral PZN-4.5PT crystals do not fatigue at room temperature, very pronounced fatigue occurred under electric field levels sufficiently high to induce another phase. The unipolar strain versus field curve, and the remanent polarization values as a function of the number of cycles in Figure 3.14 illustrate the important role of field induced phase transitions on fatigue. In the case of unipolar drive, different strain-field slopes are noted with a hysteretic transition between the rhombohedral and field induced phase. The field levels for the transformation under unipolar conditions is higher than under ac conditions. Hysteresis losses may locally heat the crystal to enable lower temperature transitions. The

transition from a ferroelectric rhombohedral to ferroelectric tetragonal (or orthorhombic) phase eventually creates a fatiguing of the crystals. The rate at which the tetragonal phase is induced from the rhombohedral phase depends on the compositions, temperature, and magnitude of the electric field. Evidence for electric field-induced phase transition was presented by x-ray diffraction. After poling by a high electric field in the $<001>_C$ direction crystals were shown to possess some remanent tetragonal phase mixed with the dominant phase.[40,41]

All of the above results suggest that in these crystals an engineered domain state with the polarization inclined to the electrode is necessary to minimize or eliminate fatigue. This now has been confirmed at a variety of temperatures, compositions, and in both single crystal and epitaxial thin film form.[42] The precise mechanism by which these engineered domain states limit fatigue is not understood. One possibility is that the inclined polarization states redistribute the space charge accumulation and thereby reduce the fatigue rate at a given temperature and composition. It still is under investigation, but it is also hypothesized that the engineered domain structures with the rhombohedral symmetry can have a higher percentage of charged domain walls. Charged walls could act as sinks to the injected charge in these systems. Another intriguing possibility is the multiple routes for domain switching that may exist in PZN-PT relaxor crystals; the complex dendritic domain wall structures observed under pulsed conditions indicate this great flexibility in switching paths, [29] and also indicate a switching process with a very high effective domain wall mobility.[33] This may also change the nature of the switching and thereby alter the fatigue mechanisms.

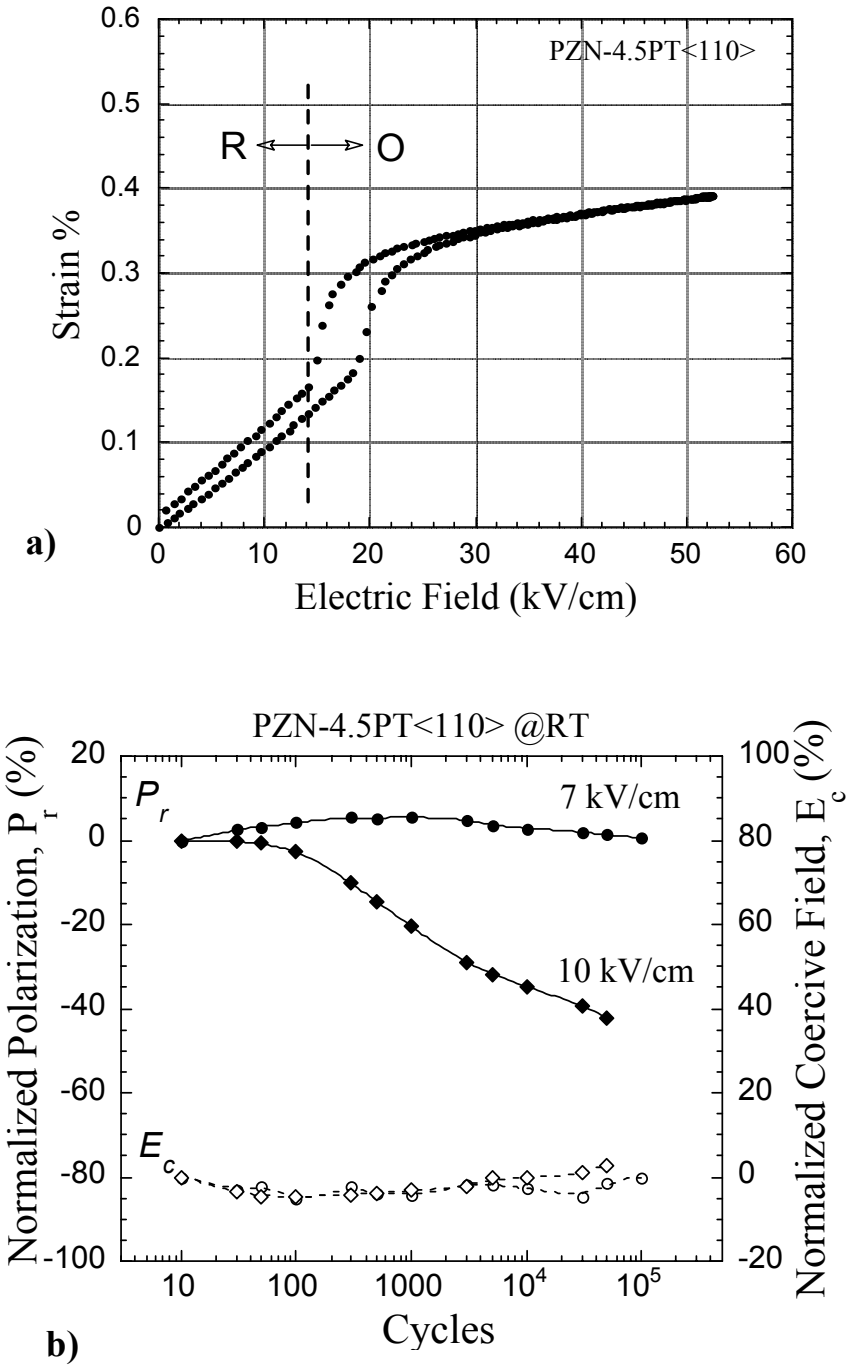

Figure 3.13 a) Electric field induced (rhombohedral -->orthorhombic) phase transition, and b) related fatigue behavior change in PZN-4.5PT single crystals with $[110]_C$ orientation.

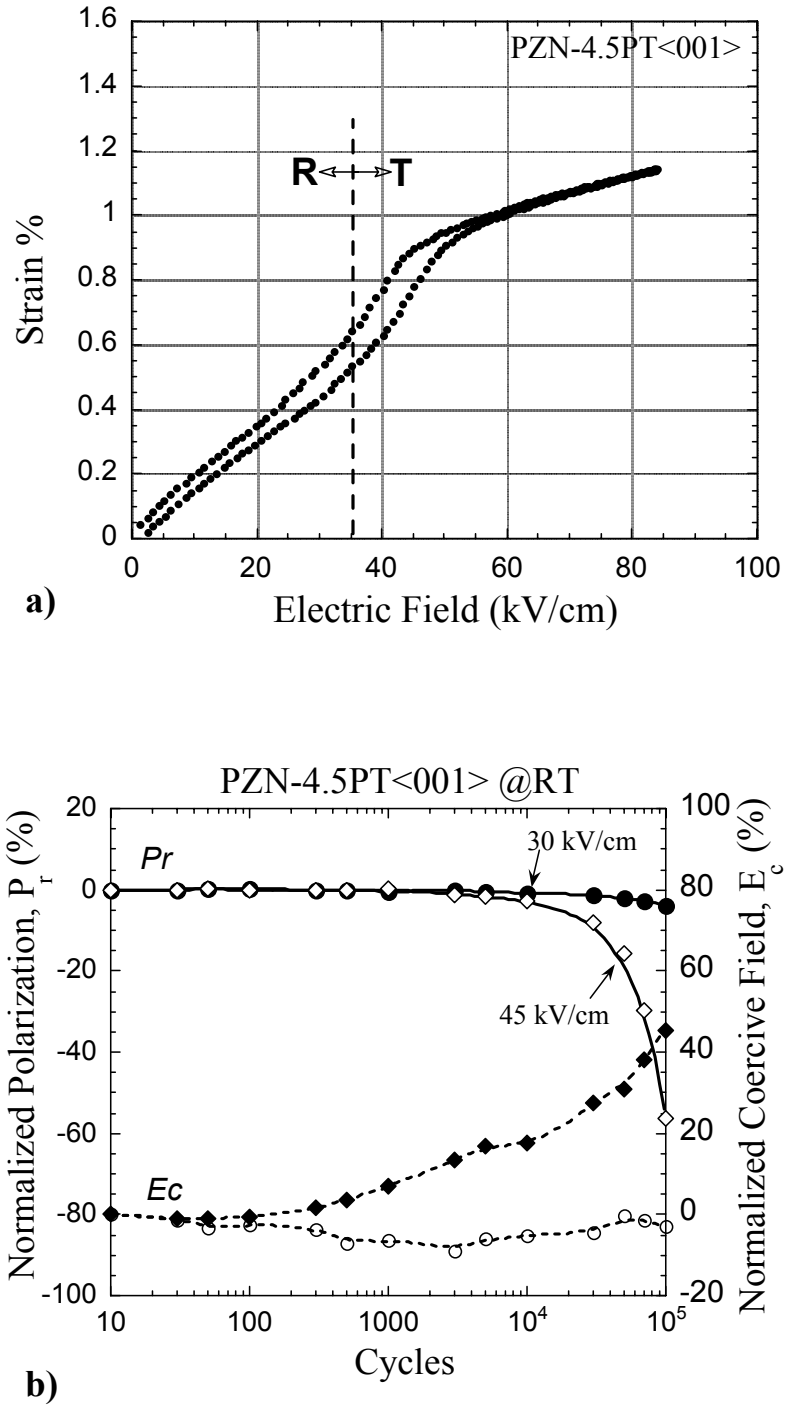

Figure 3.14 a) Electric field induced (rhombohedral -->tetragonal) phase transition, and b) related fatigue behavior change in PZN-4.5PT single crystals with $[001]_C$ orientation.

3.3.2.3 Influence of Fatigue History

As shown in Figure 3.9.b, PZN-8PT single crystals demonstrate a strong fatigue resistance up to 10^5 cycles at room temperature. PZN-8PT is rhombohedral at room temperature. The curved morphotropic phase boundary of the PZN-PT system permits fatigue to be studied in single crystals at different temperatures and ferroelectric phases. Crystals with the PZN-8PT composition and $[001]_C$ orientation were phase induced into the tetragonal phase at 125 ˚C under bipolar fields with amplitude 20 kV/cm at 10 Hz. As shown in Figure 3.15 (P_r; solid circles, E_c; open circles), the crystal was substantially (~35%, after 10^5 cycles) fatigued when cycled at high temperatures, where the tetragonal phase is induced. Then, these samples were cooled into the rhombohedral phase at room temperature and then driven under bipolar drive. The samples then continued to fatigue as shown in Figure 3.15 (P_r; solid squares, E_c;open squares). Even though $[001]_C$-oriented PZN-8PT (rhombohedral) crystals do not fatigue at room temperature, this changes when a tetragonal phase is induced by heating the crystals to higher temperatures (i.e., 125 °C). As PZN-8PT crystals are cycled at high temperatures and experience fatigue due to switching in tetragonal phase stability region, it is possible that the fatigued crystal may still have tetragonal regions. This could be clarified with controlling the cooling rate or annealing the crystal at a temperature below T_c, to see whether the transition to rhombohedral can occur in time. It is also noted that when pre-fatigued crystals are subsequently cycled at room temperature, the fatigue rate is even higher as seen in Figure 3.14. This is most probably due to the influence of higher temperatures, generally reducing the fatigue rates.

The above experiments demonstrate that when domain engineered crystals undergo a phase transition to produce polarization vectors parallel to the electric field, fatigue will occur. Further, the continuation of fatigue at room temperatures for PZN-8PT crystal indicates that the thermal history can also influence the fatigue. If a crystal can undergo a field that induces a domain state that fatigues, this ultimately controls the fatigue process, acting as a nucleation site for pinned domains in the whole crystal.

3.3.3 Study of Fatigue Anisotropy in Other Ferroelectric Systems

For the verification of fatigue anisotropy, polarization fatigue behavior was studied in several other ferroelectric systems. The measurements on the other systems are summarized and after discussion lead to the conclusion that both relaxor behavior and crystallographic anisotropy is required for fatigue free orientations.

3.3.3.1 $BaTiO_3$ and $Ba(Zr,Ti)O_3$ Single Crystals

Barium titanate is a normal ferroelectric which possesses several polar phases such as tetragonal, orthorhombic, and rhombohedral. Both undoped and 5% Zr-doped barium titanate single crystals grown by templated grain growth method[43] were tested for fatigue anisotropy. Zirconium addition increases the transition temperature so that rhombohedral or orthorhombic phases could be stabilized near room temperature. Based on the fatigue studies in PZN-PT relaxor based ferroelectric single crystals, only rhombohedral $[001]_C$- or tetragonal $[111]_C$-crystals were tested. Fatigue free behavior is observed only when an engineered domain state is induced by applying the electric field along the the directions other than the spontaneous polarization orientation. Figure 3.16

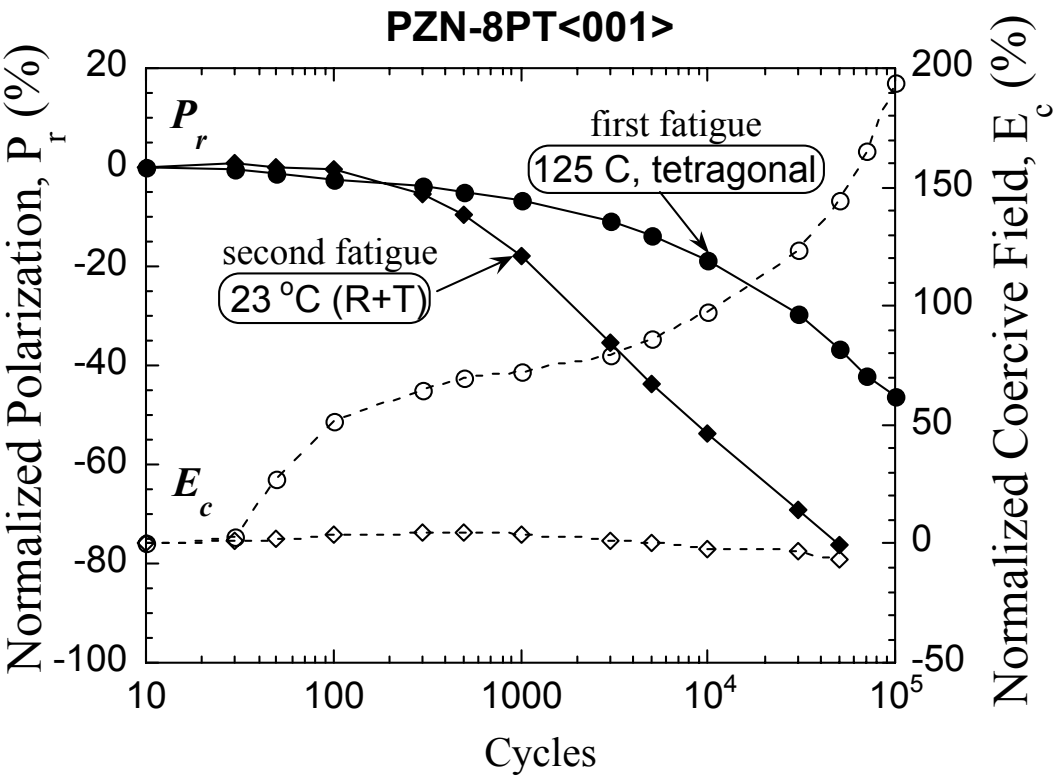

Figure 3.15 Influence of high temperature (inducing tetragonal phase) fatigue cycling on room temperature switching and fatigue behavior in PZN-8PT single crystals along $[001]_C$-orientation. a) Crystal first fatigued at tetragonal phase temperature (125 °C), and b) upon subsequent cycling at room temperature rhombohedral ("fatigue resistant" phase for $[001]_C$) region, fatigue continues, due to high temperature (tetragonal phase) fatigue cycling stabilized inclusions within the structure. R; rhombohedral, T; tetragonal in the figure.

shows polarization-electric field loops in undoped barium titanate before and after fatigue cycling. Fatigue occurs in both $[001]_C$-oriented rhombohedral and $[111]_C$-oriented tetragonal crystals.

$Ba(Zr_{0.05}Ti_{0.95})O_3$ (BZT) crystals experience ferroelectric phase transitions of cubic to tetragonal ~110 °C, tetragonal to orthorhombic ~50 °C, and orthorhombic to rhombohedral ~5 °C.[43] Rhombohedral BZT crystals with $[001]_C$ orientation were tested at -60 °C to check whether fatigue free behavior can be observed as demonstrated by PZN-PT. Figure 3.17 shows the remanent polarization change as a function of the number of switching cycles as well as the hysteresis loop evolution. BZT crystals fatigue similar to the undoped BT. Zr-addition did not improve the fatigue behavior as fatigue occurs in $[001]_C$-oriented rhombohedral BT single crystals at -60 °C and -120 °C. Stadler[44] had studied fatigue behavior of BT single crystals with silver electrodes at -195 °C, and reported stability of switching charge. However, he also studied switching at various temperatures (i.e., 0, -20, -80, and -100 °C) to check whether it is related to the rhombohedral phase. His results were inconclusive as fatigue occurred at -100 °C but not at -20 °C; all this work had many inconsistencies and plagued by crystal impurities.

One interesting observation made here is the great asymmetry in the *P*-*E* loops Figure 3.18). As reported in Table 3.1, negative values of the coercive fields are greater than the positive ones; this is reflected as a shift towards the negative side of the electric field axis. This type of shift is generally attributed to the existence of an internal bias in the material favoring one polarity to the other due to the orientation of the defect dipoles.[45] By simultaneous measurements of the internal bias and the dielectric constant in acceptor doped BT ceramics, a direct link was established between aging of the

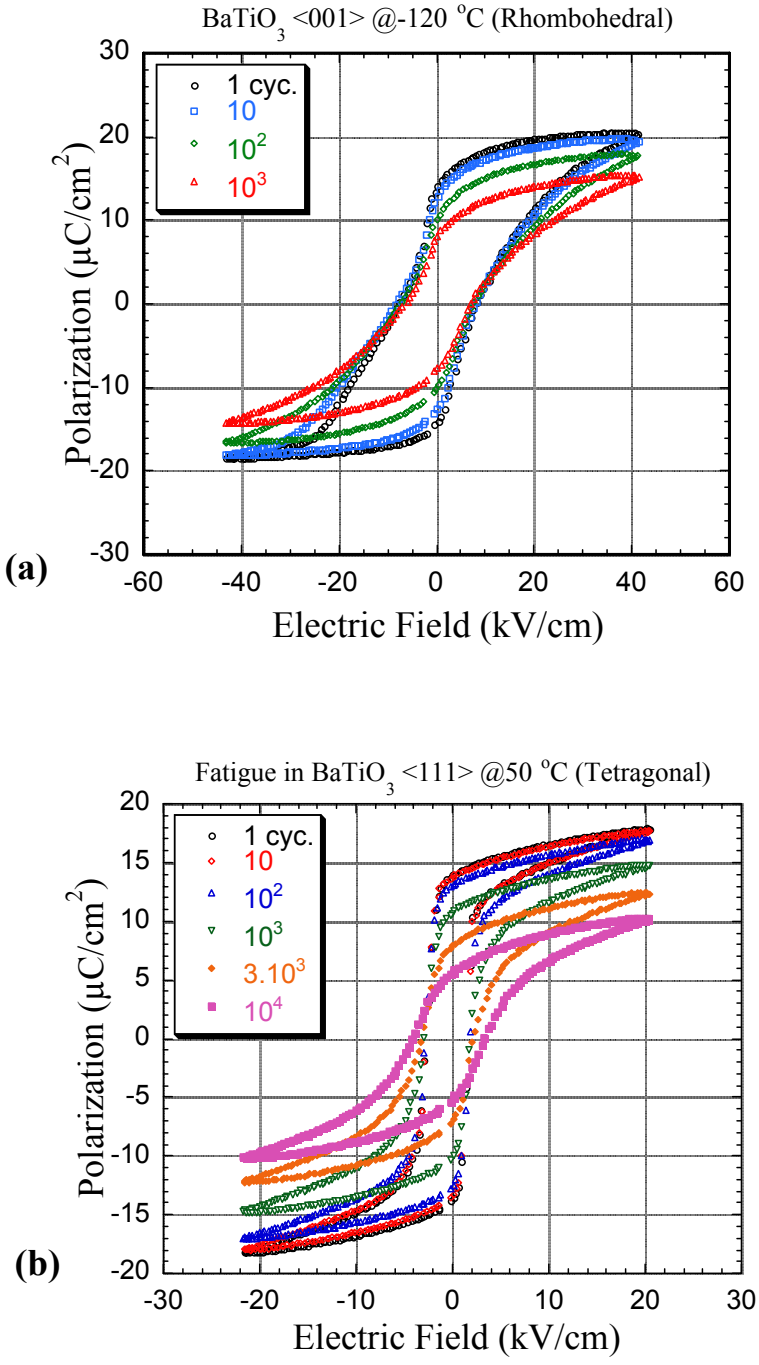

Figure 3.16 Polarization fatigue in a) rhombohedral $BaTiO_3$<001> at -120°C after 10^3 cycles, and b) tetragonal $BaTiO_3$ <111> at 50°C after 10^4 cycles.

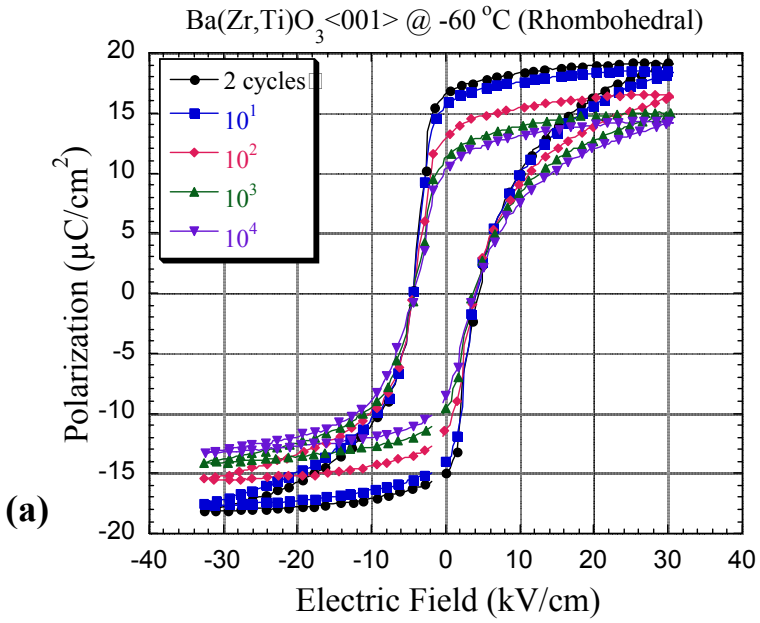

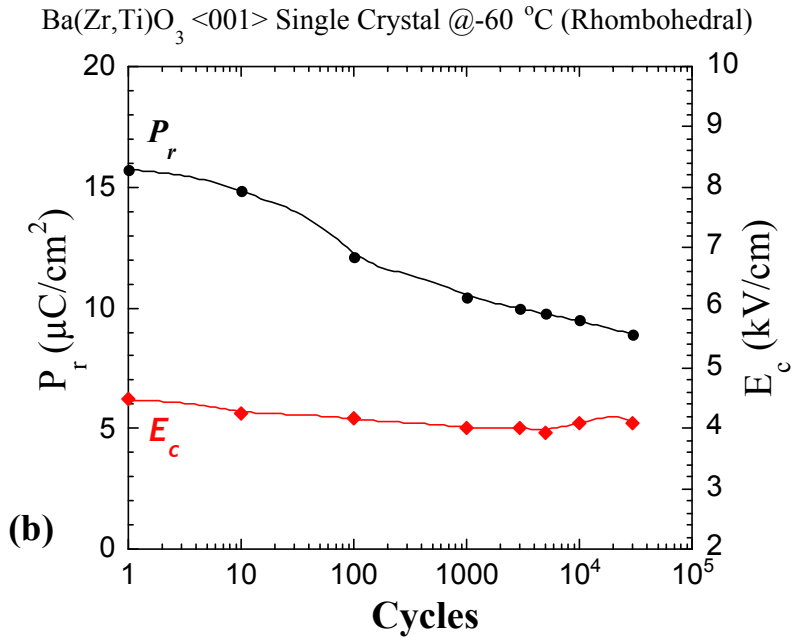

Figure 3.17 Polarization fatigue in a rhombohedral Ba(Zr,Ti)O_3<001> single crystal: a) Evolution of P-E loops with fatiguing cycles at -60°C up to 10^4 cycles, and b) change of remanent polarization, P_r, as a function of switching cycles.

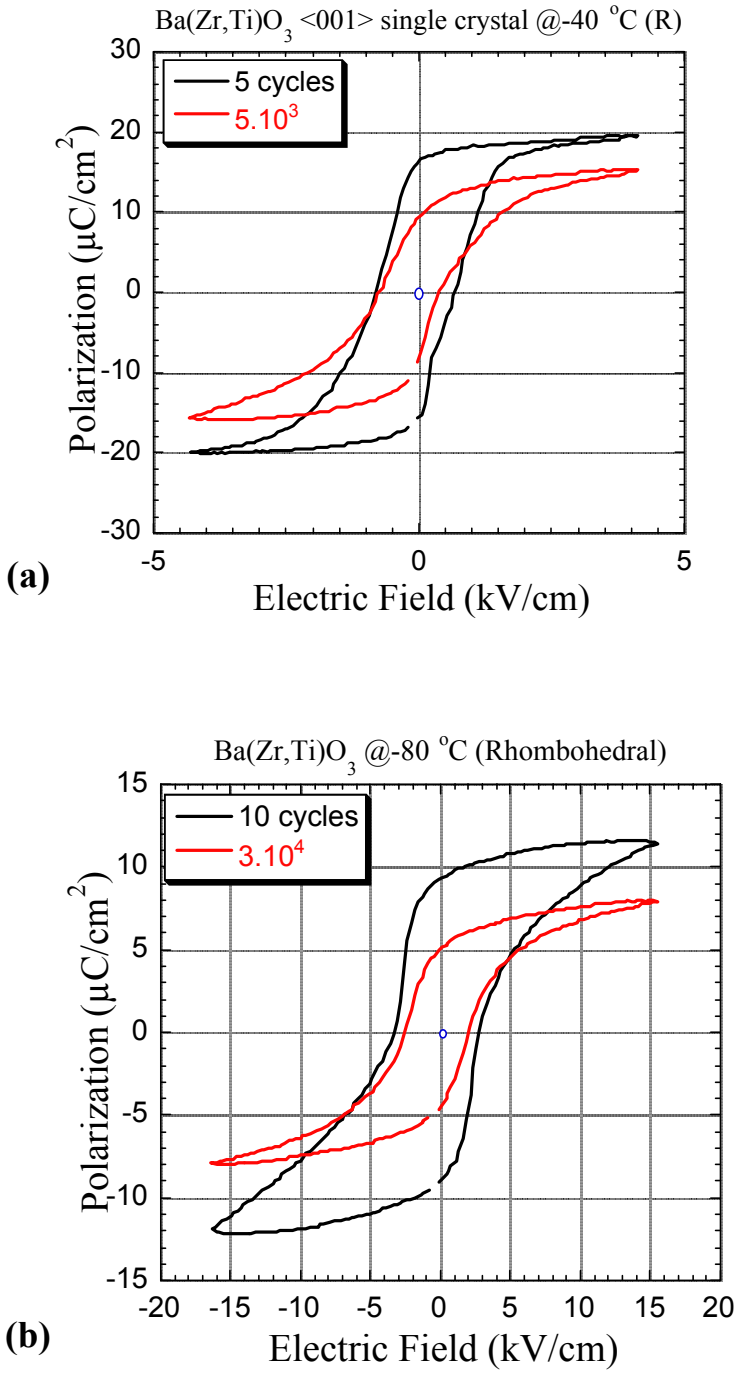

Figure 3.18 Existence of internal bias field in BZT single crystals at different temperatures.

Table 3.1 Internal bias fields in BZT single crystals.

	VIRGIN			FATIGUED		
T(°C)	$-E_c$ (kV/cm)	$+E_c$ (kV/cm)	**E_{int} (kV/cm)**	$-E_c$ (kV/cm)	$+E_c$ (kV/cm)	**E_{int} (kV/cm)**
-40	0.8	0.65	**0.075**	0.75	0.35	**0.2**
-80	3.2	2.8	**0.2**	2.6	2.0	**0.3**

material properties and the increase of the internal bias. Domain wall clamping due to the internal bias field was proposed to be a significant cause for the decrease of material properties.[46] A qualitative model was put forward to explain the aging behavior in acceptor doped ceramics as a result of the orientation of defects in time.[47] If aging in acceptor doped BT and PZT ferroelectric ceramics is due to the clamping of domain walls through an internal bias, this could also explain the origin of fatigue in BT and BZT, at least in $[001]_C$ orientation in this research. This may also explain the absence of fatigue anisotropy in barium titanate based normal ferroelectrics. It would be useful to study fatigue anisotropy in another normal ferroelectric to clarify this point.

3.3.3.2 $Pb(Yb_{1/2}Nb_{1/2})O_3$-$PbTiO_3$ Single Crystals

Single crystals of perovskite $(1-x)Pb(Yb_{1/2}Nb_{1/2})O_3$-$xPbTiO_3$ (PYN-xPT) were grown by a conventional high temperature solution method.[48] Temperature dependence of the dielectric constant and dielectric constant at different frequencies for PYN-0.4PT single crystals are given in Figure 3.19.[49] The Curie temperature for compositions near the morphotropic phase boundary (x=0.5) is in the range of 300-400 °C due to compositional variations.[48] The PYN-0.4PT single crystals used in this study are rhombohedral with a T_c of about 300 °C.[48] At the absence of an applied field PYN-0.4PT

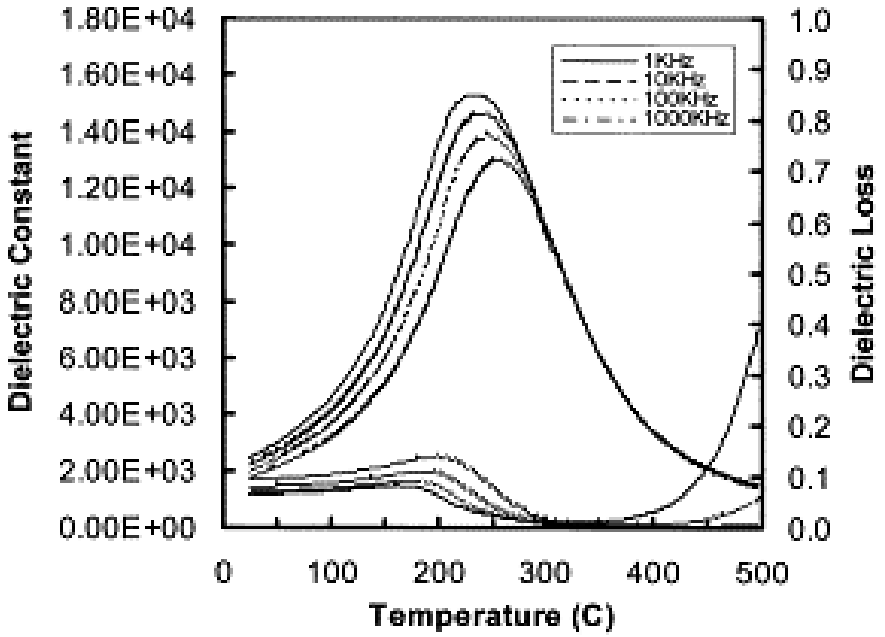

Figure 3.19 Temperature dependence of the dielectric constant and dielectric loss at different frequencies for PYN-0.4PT single crystals.[49]

is reported to be a relaxor ferroelectric as the dielectric properties change from relaxor to normal ferroelectric behavior with increasing PT content ($0.2 < x < 0.8$).[48]

Fatigue characteristics of heteroepitaxial PYN-0.4PT thin films have been studied as a function of crystalline orientation. It was reported that $[001]_C$-heteroepitaxial thin films demonstrate a fatigue free behavior up to 10^{11} cycles, while $[111]_C$-oriented heterostructures exhibit fatigue.[42]

As shown in Figure 3.20 and Figure 3.21, the fatigue behavior of PYN-0.4PT single crystals is very similar to PZN-PT single crystals and PYN-PT thin films. Figure 3.4 shows polarization-electric field hysteresis loops of PYN-0.4PT single crystals after 10 and 10^5 cycles in both $[001]_C$ and $[111]_C$ orientations. The coercive field values of virgin $[111]_C$- and $[001]_C$-oriented PYN-0.4PT single crystals were ~20.4 kV/cm and ~8.6 kV/cm, respectively. After 10^5 cycles at ac fields about two times their respective coercive fields at 0.1 Hz, the coercive field increased to ~23.4 kV/cm in $[111]_C$-oriented crystals and decreased to ~5.9 kV/cm in $[001]_C$-oriented crystals. On the other hand, as fatigue occurs in $[111]_C$-oriented crystals, the remanent polarization values dropped about 60% after 10^5 cycles. Only a negligible change was observed in remanent polarization values of $[001]_C$-oriented PYN-0.4PT single crystals.

Overall, self consistently with the fatigue anisotropy observations in relaxor based rhombohedral PZN-PT single crystals and PYN-PT single crystals, fatigue is suppressed in the $[001]_C$ orientation in PYN-0.4PT single crystals. These observations lead us to a primary conclusion that fatigue anisotropy could be related to the relaxor nature of ferroelectrics. Further studies need to be performed in several other ferroelectric systems

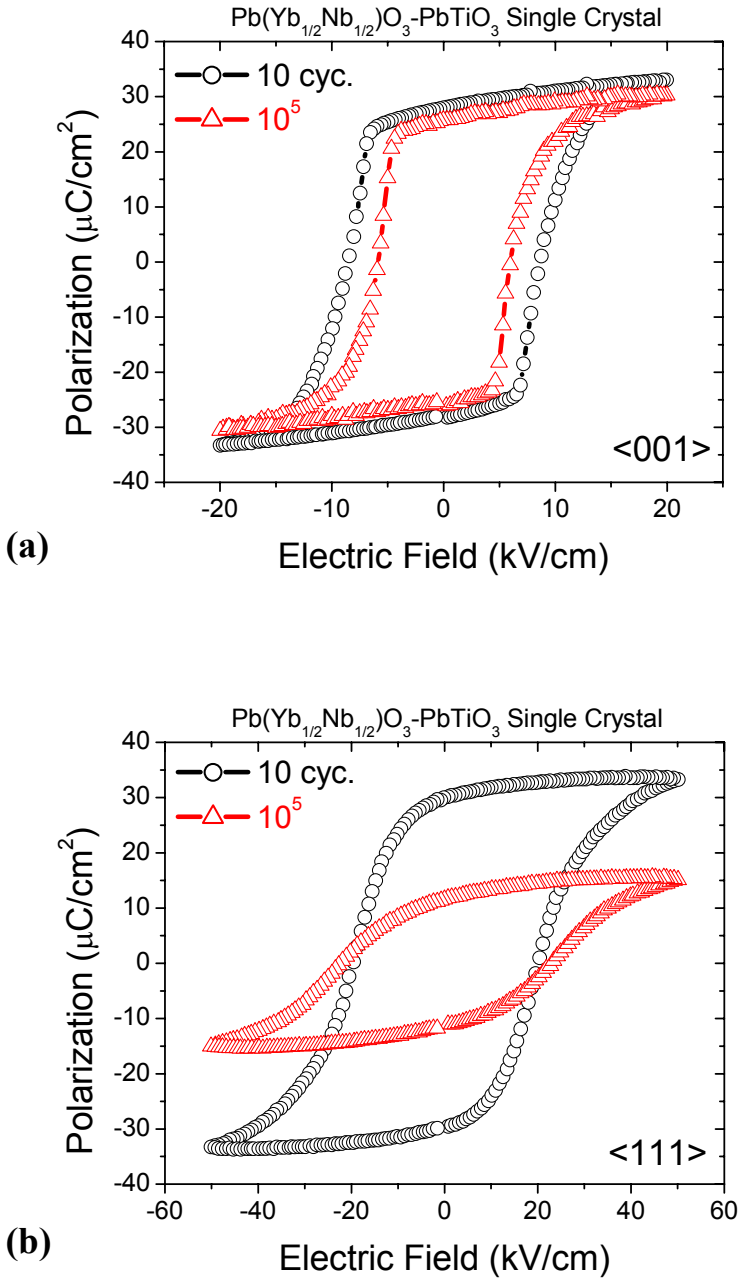

Figure 3.20 Polarization-Electric field hysteresis loops in $Pb(Yb_{1/2}Nb_{1/2})O_3$-$PbTiO_3$ single crystals after 10 and 10^5 cycles along the a) $[001]_C$, and b) $[111]_C$ orientations.

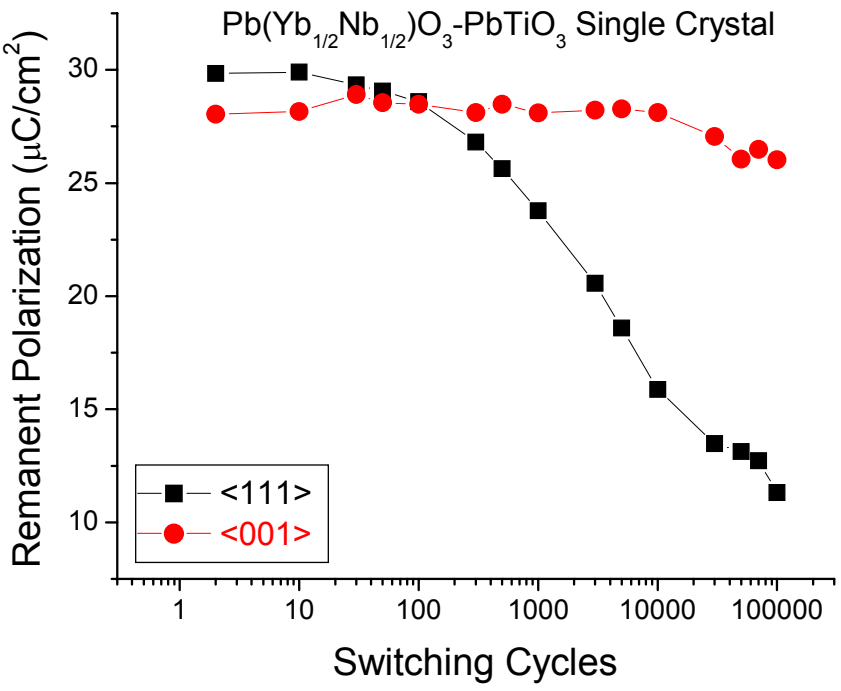

Figure 3.21 Polarization fatigue anisotropy in $Pb(Yb_{1/2}Nb_{1/2})O_3$-$PbTiO_3$ single crystals.

both from relaxor and normal ferroelectric families. In the next section, study of fatigue in a tungsten bronze type ferroelectric $Sr_{0.61}Ba_{0.39}Nb_2O_6$ single crystals is described.

3.3.3.3 $Sr_{0.61}Ba_{0.39}Nb_2O_6$ Relaxor Single Crystals

The tungsten bronze type ferroelectric crystals have a structure similar to tetragonal tungsten bronze K_xWO_3 ($x<1$).[50] $Sr_{0.61}Ba_{0.39}Nb_2O_6$ (SBN) belongs to the family of tungsten bronze type ferroelectric and exhibits relaxor character. In contrast to the cubic perovskite family (i.e, PZN), the polarization of the strontium-barium niobate $Sr_xBa_{1-x}Nb_2O_6$ (SBN) family is a single-component vector directed along the tetragonal *c*-direction, which drives the symmetry point group from 4/*mmm* to 4*mm* at the phase transition into the polar phase at low temperatures.[51]

Polarization fatigue properties of SBN single crystals were measured in two samples. The first crystal was cycled with the electric field applied along the c-direction. To study the influence of orientation in tungsten bronze SBN, one crystal was cut 45° off the c-direction. Polarization-electric field hysteresis loops of *c*-plate and the 45° off cut SBN single crystals were measured after increasing number of cycles are shown in Figure 3.22. The crystal which was cut 45° off from the *c*-direction has a slightly lower remanent polarization and higher coercive field as seen in Figure 3.23, which also shows how these values change with the number of ac cycles. Both crystals experience a very sharp drop with the first cycle of the electric field and then a steady state is reached and maintained throughout the cycling. Interestingly the drastic loss of polarization with the first ac cycle does not involve a notable change in the coercive field (as it usually increases with the loss of switchable polarization in bulk ferroelectrics).

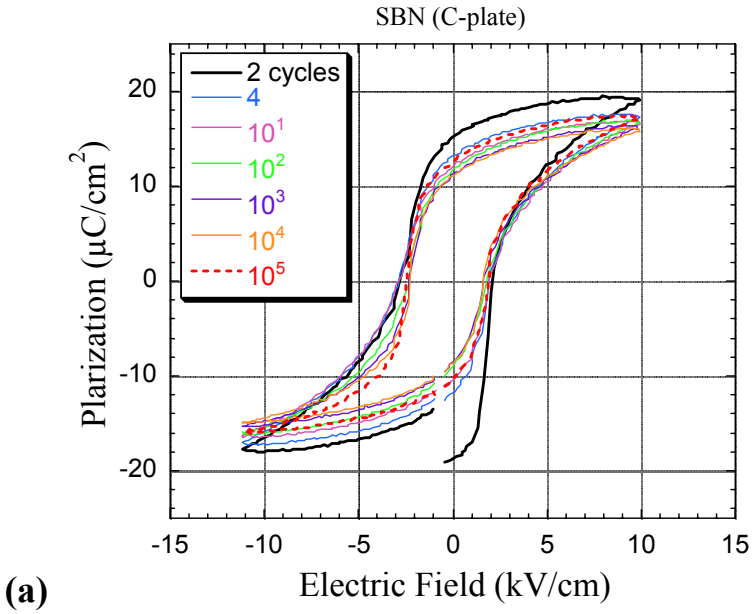

(a)

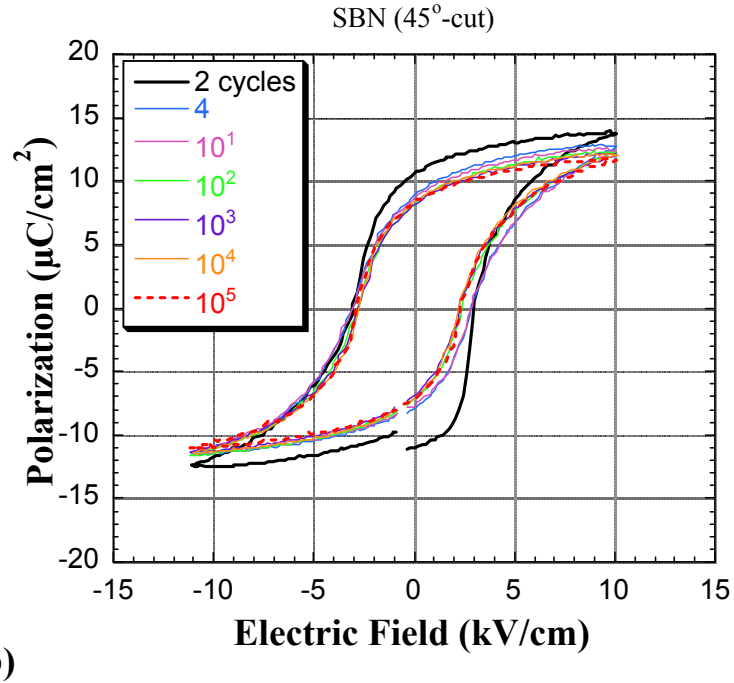

(b)

Figure 3.22 Polarization-Electric field hysteresis loops in a) c-plate, and b) 45°-off c-axis cut $Sr_{0.61}Ba_{0.39}Nb_2O_6$ (SBN) single crystals.

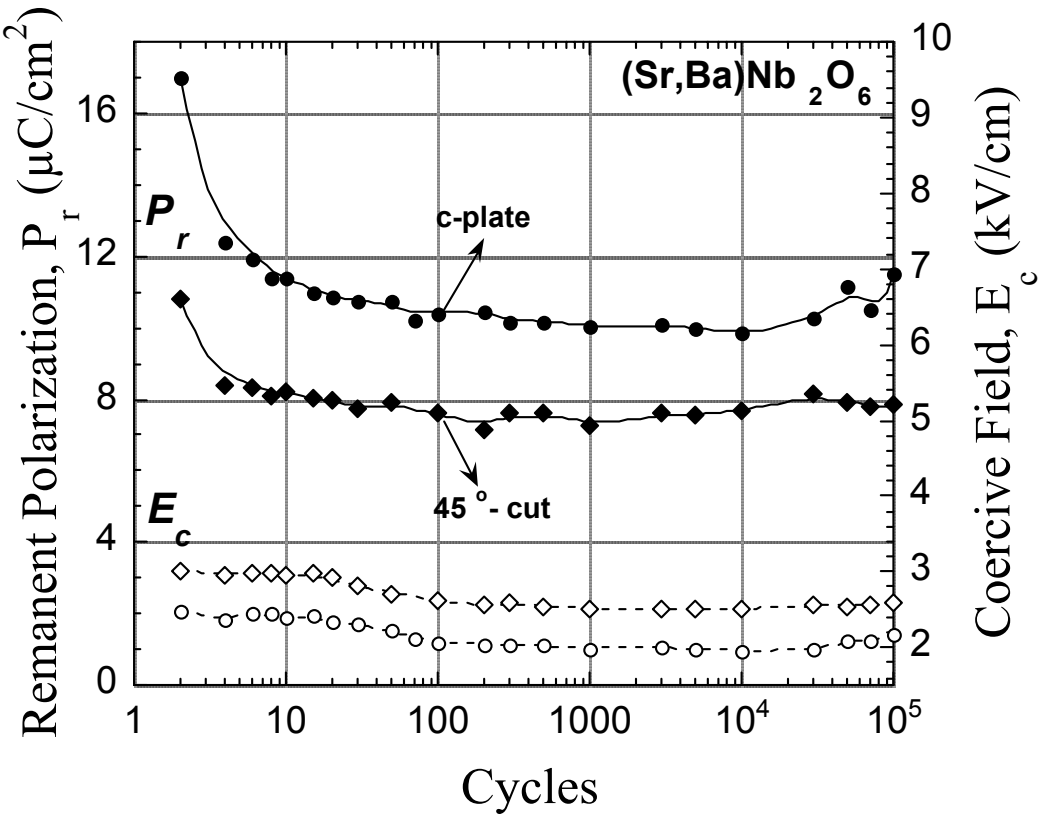

Figure 3.23 Switching cycle dependence of remanent polarization, P_r, and E_c of a c-plate, and b) 45°-off c-axis cut $Sr_{0.61}Ba_{0.39}Nb_2O_6$ (SBN) single crystals.

Fatigue is commonly observed in SBN single crystals. A similar drastic decrease was also observed in $Sr_{0.75}Ba_{0.25}Nb_2O_6$ single crystals.[52] These single crystals usually possess imperfections such as striation bands (perpendicular to the *c*-direction) that are mainly introduced during crystal growth, as the system has incongruent melting.[52,53] A slight offset is present in the *P-E* loops indicating the existence of an internal bias field but both P_r and E_c values remained almost constant with increasing number of cycles. Especially E_c did not even change with the first electric field cycle. This is not well understood at this moment. SBN seems to present a unique case, which makes it difficult to make general conclusions, especially for the focus of this research.

3.3.3.4 $Na_{1/2}Bi_{1/2}TiO_3$ Textured Ceramics

Sodium bismuth titanate $Na_{1/2}Bi_{1/2}TiO_3$ (NBT) is closely related to relaxor ferroelectrics and has a perovskite structure.[54] It is also a non-lead based piezoelectric material with a high Curie temperature (T_c~320°C) and remanent polarization (38 $\mu C/cm^2$).[55] In contrast to PMN, the NBT crystals exhibit a sequence of ferroelastic transformations at higher temperatures, so the ferroelectric phase emerges after a (paraelectric-paraelastic) --> (paraelectric - ferroelastic) --> (ferroelectric-ferroelastic) at room temperature.[54]

Polarization fatigue was studied in NBT ceramics of random orientation and of grain oriented (textured) along the $<001>_C$. The degree of orientation in samples tested here was about 70%.[56] Polarization-electric field hysteresis loops of $<001>_C$-textured NBT ceramics are seen in Figure 3.24. After 5×10^3 cycles, remanent polarization

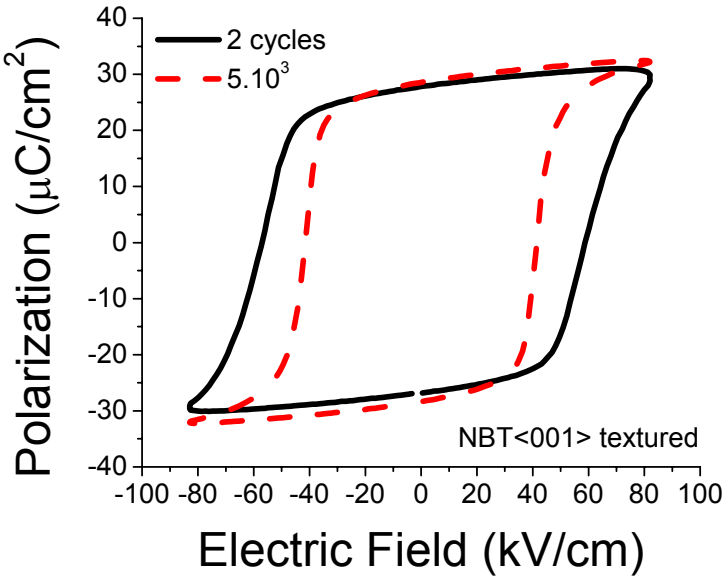

a)

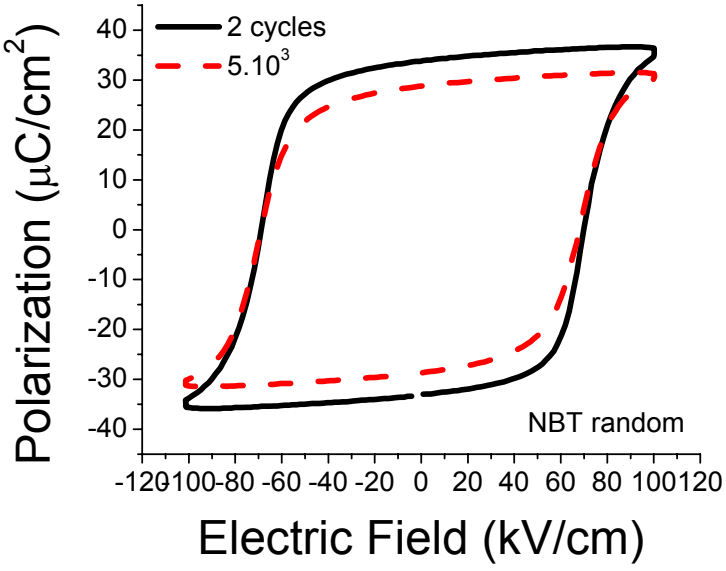

b)

Figure 3.24 Comparison of virgin and ac cycled (5.10^3 cycles) *P-E* loops of a) $<001>_C$-textured, b) randomly oriented $Na_{1/2}Bi_{1/2}TiO_3$ ceramics.

decreases in randomly oriented NBT but the coercive field remains constant. On the other hand, 70% $<001>_C$-textured NBT demonstrate better fatigue resistance as the remanent polarization remains constant and coercive field substantially decreases with cycling. There is an indication of fatigue anisotropy in a lead-free relaxor type ferroelectric NBT.

One interesting point should be noted is that in all the ferroelectrics demonstrating fatigue anisotropy, ac cycling in the fatigue resistant $<001>_C$ orientations decreases the coercive field. This may be an important subject of further study. Nonetheless, all the relaxor type ferroelectrics exhibit an orientation dependent fatigue behavior. For SBN and NBT, with further studies the results presented here can be enriched. Especially the very high coercive fields in textured NBT ceramics were problematic and inhibited further cycling in many cases due to dielectric breakdown.

If coercive fields can be reduced with quality improvements, texturing could take a new phase also for the switching properties of ferroelectric ceramics.

3.3.4 Influence of Temperature on Fatigue and Rejuvenation

One of the factors which may influence polarization switching and fatigue behavior is temperature.[57] Temperature dependence of fatigue (from 23 to 145 °C) was studied in PZN-4.5PT single crystals along $[111]_C$ orientation. Figure 3.25 shows the virgin hysteresis loops and loops after 10^5 cycles at different temperatures: 23, 65, 75, 85, and 100 ˚C, respectively, in PZN-4.5PT crystals with the $[111]_C$ orientation. Fatigue is observed at room temperature, and temperatures below 85 ˚C. At higher temperatures no fatigue was observed. In the $[111]_C$ rhombohedral case, the fatigue rate is reduced at higher temperatures as shown in Figure 3.26. The higher temperatures enable domain

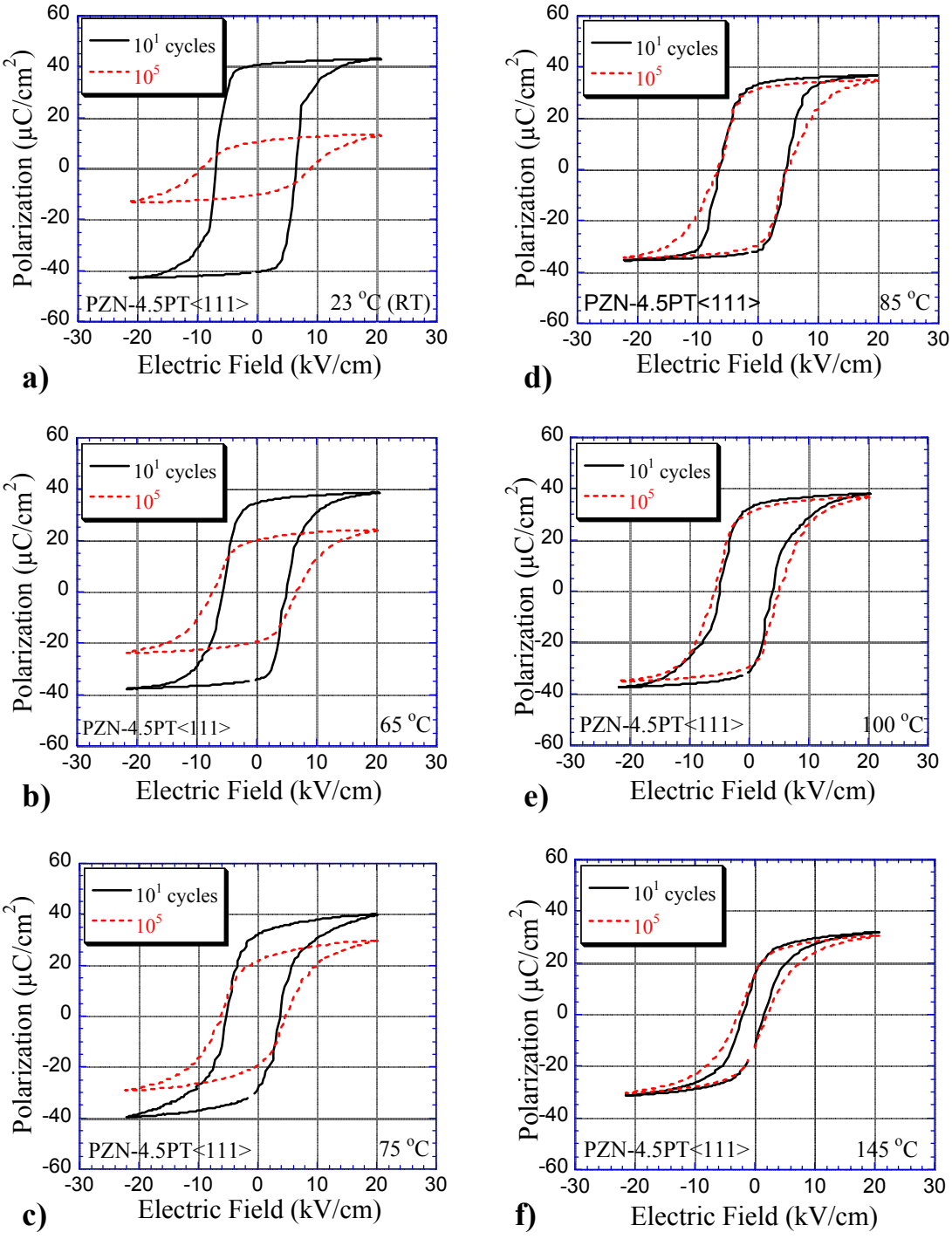

Figure 3.25 The influence of fatigue switching temperature on fatigue in rhombohedral PZN-4.5PT crystals along with $[111]_C$ orientation; (a) room temperature (23 °C), (b) 65 °C, (c) 75 °C, (d) 85 °C, (e) 100 °C, (f) 145 °C.

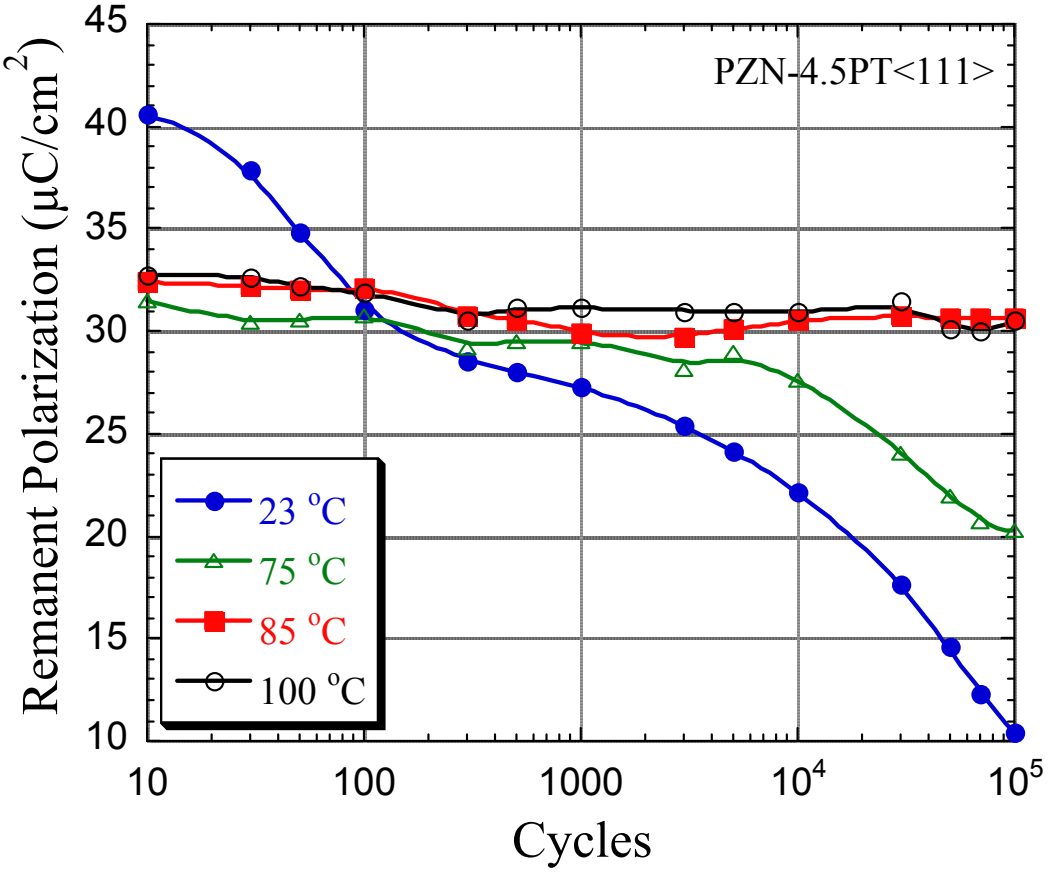

Figure 3.26 Fatigue rates as a function of temperature and the number of switching cycles in $[111]_C$-oriented PZN-4.5PT.

switching to overcome the pinning forces of the accumulated defects or space charge. Also at high temperatures, the probability of nucleation (or activating more preexisting nuclei) increases (see equation 1.7), thereby enabling polarization switching to occur throughout the ferroelectric crystals. Collectively, at these higher temperatures the spontaneous polarization does not fatigue at rates as fast as at lower temperatures.

Furthermore, in the case of tetragonal PZN-10PT (at 75 ˚C) crystals undergo fatigue in the $[001]_C$ direction; again the fatigue rate is reduced as temperature is increased (for similar reasons as explained above for $[111]_C$ rhombohedral crystals) at temperatures of 75 ˚C and above. In the case of tetragonal PZN-PT switching studies at room temperature, the switching frequently causes microcracking, the stress fields about the microcracks can pin polarization switching and is an additional source of fatigue. In single crystal samples undergoing fatigue, it is important to separate the influence of microcracking over space charge or point defect domain pinning. This can be readily done by a heat treatment that rejuvenates the polarization switching, the thermal energy here would not repair the cracks but can redistribute point defects and space charge by simple diffusion. So rejuvenation of polarization infers that no microcracking is involved in the fatigue of the polarization switching.

Figure 3.27 shows that annealing improves the P_r value of a fatigued $[111]_C$-oriented PZN- 4.5 PT crystal. When a fatigued crystal was annealed at 300 °C for 5 h in air, P_r increased to more than 95 % of the initial P_r value. Thermal annealing is believed

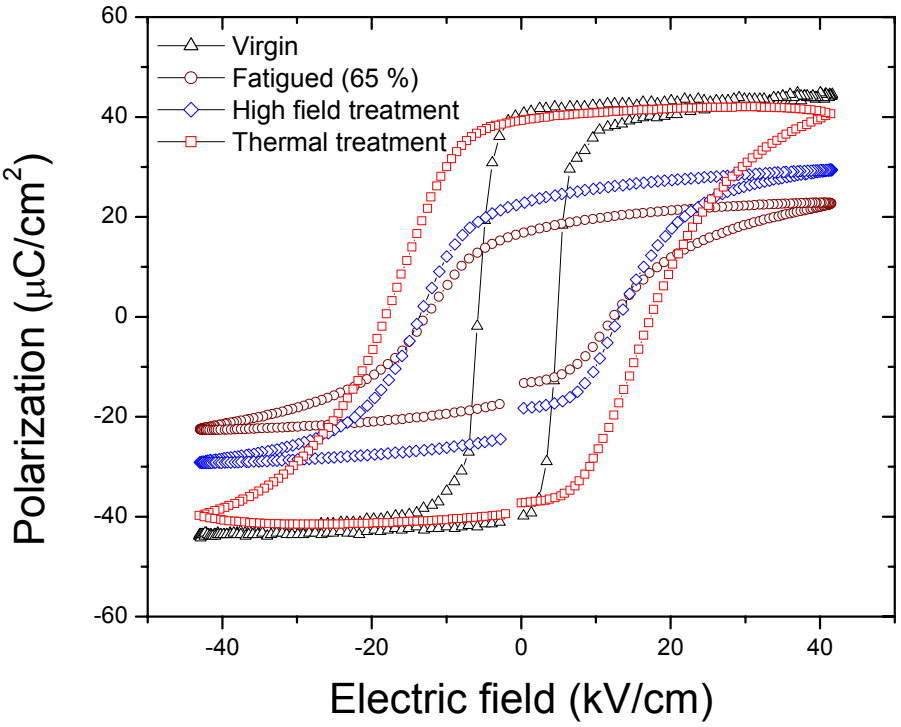

Figure 3.27 Rejuvenation of fatigue by thermal annealing.

to randomize defects inhomogeneously distributed during fatigue cycling. More discussion on thermal annealing will be presented in chapter 4. This result here proves that the fatigue observed in the present study is recoverable, and rules out fatigue by microcracking. Therefore, fatigue in the $[111]_C$-oriented PZN - 4.5 PT single crystals is believed to result from domain wall pinning via defects during polarization reversal, as has been reported in earlier single crystal studies. In orientations that have fast fatigue rates, this can be reduced by raising the temperature.

3.4 Summary and Conclusions

Polarization switching and fatigue behavior of PZN-PT single crystals was studied at various temperatures, compositions, and electric field strengths as a function of crystallographic orientations. It is observed that the rhombohedral PZN-PT crystals oriented with the field along $[001]_C$ has no fatigue. At room temperature, $[111]_C$- oriented rhombohedral PZN-PT fatigues as does tetragonal PZN-PT in $[001]_C$ and $[111]_C$ directions. In the $[111]_C$ rhombohedral case, the fatigue rate is reduced at higher temperatures.

All of the above illustrate the role of fatigue anisotropy and domain engineering in $Pb(Zn_{1/31}Nb_{2/3})O_3$–$PbTiO_3$ crystals. Fatigue is induced if a polarization vector is normal to the electrode plane and is parallel to the electric field vector. Fatigue rates are suppressed in some directions, provided the thermal energy can overcome pinning effects or alter active nucleation probability at the electrode interface without inducing

polarization parallel to the applied field. In the compositions close to the MPB, alternating electric fields can induce a ferroelectric phase with polarization parallel to the electric field direction, e.g. a rhombohedral to tetragonal phase transition in a $[001]_C$ crystal. This then can give rise to polarization fatigue. In special directions, such as $[110]_C$, a rhombohedral phase can be field induced into a metastable orthorhombic phase that has polarization parallel to the normal of the electrode plane and thereby undergo fatigue. In the case of electric fields inducing mixed ferroelectric phases, the fatigue is dominated by the polarization direction parallel to the electric field direction. It is hypothesized that if a ferroelectric crystal has engineered domains with polarization inclined to the electrode normal, charge injection is either reduced and/or charge is redistributed, and/or domain switching mobility is enhanced, thereby limiting fatigue.

Following these studies, fatigue anisotropy was also studied in other single crystal normal and relaxor based ferroelectrics systems of $Pb(Yb_{1/2}Nb_{1/2})O_3$–$PbTiO_3$ and $BaTiO_3$. Fatigue anisotropy was exhibited only in relaxor type ferroelectrics. Epitaxial ferroelectric thin films of $Pb(Yb_{1/2}Nb_{1/2})O_3$–$PbTiO_3$ also verify fatigue anisotropy at higher switching frequencies and thinner crystals.[42]

A comprehensive mechanism that explains fatigue is still awaiting the ferroelectrics community, however, these studies on ferroelectric phase and orientation, builds up the experimental background that ultimately has to be explained in a complete fatigue model.

3.5 References

[1] W. J. Merz, and J. R. Anderson, Bell Lab.Record **33**, 335 (1955).
[2] J. R. Anderson, G. W. Brady, W. J. Merz, and J. P. Remeika, J. Appl. Phys. **26**, 1387 (1955).
[3] H. L. Stadler, J. Appl. Phys. **29**, 743 (1958).
[4] D. S. Campbell, Phil. Mag. **79**, 1157 (1962).
[5] R. Williams, J. Phys. Chem. Solids **26**, 399 (1965).
[6] W.C. Stewart, and L.S. Cosentino, Ferroelectrics **1**, 149 (1970).
[7] D. B. Fraser, and J. R. Maldonado, J. Appl. Phys. **41**, 2172 (1970).
[8] S. B. Desu, Phys. Stat. Sol.(A) **151**, 467 (1995).
[9] F. Scott, and C. A. Paz De Araujo, Science **246**, 1400 (1989).
[10] K. Amanuma, T. Hase, and Y. Miyasaka, Jpn. J. Appl. Phys., **33**, 5211 (1994).
[11] T. Haccart, D. Remiens, and E. Cattan, Thin Solid Films **423**, 235 (2003).
[12] D. P. Vijay and S. B. Desu, J. Electrochem. Soc. **140**, 2640 (1993).
[13] H. N. Al-Shareef, K. R. Bellur, A. I. Kingon, and O. Auciello, Appl. Phys. Lett. **66**, 239 (1995).
[14] T. Nakamura, Y. Nakano, A. Kanisawa, and H. Takasu, Jpn. J. Appl. Phys., **33**, 5207 (1994).
[15] T. Nakamura, Y. Nakano, A. Kanisawa, and H. Takasu, Appl. Phys. Lett. **64**, 1522 (1994).
[16] K. Kushida-Abdelghafar, M. Hiratani, and Y. Fujisaki, J. Appl. Phys. **85**, 1069 (1999).
[17] J. T. Cheung, P. E. D. Morgan, and R. Neurgaonkar, Proceedings of the 4th International Symposium on Integrated Ferroelectrics, Colorado Springs, CO, 518 (1992).
[18] C. B. Eom, R. B. Van Dover, J. M. Phyllips, D. J. Werder, C. H. Chen, R. J. Cava, R. M. Fleming, and D. K. Fork, Appl. Phys. Lett. **63**, 2570 (1993).
[19] R. Ramesh, H. Girchlist, T. Sands, V. G. Keramidas, R. Haakenaasen, and D. K. Fork, Appl. Phys. Lett. **63**, 3592 (1993).
[20] R. Dat, D. J. Lichtenwalner, O. Auciello, and A. I. Kingon, Appl. Phys. Lett. **64**, 2873 (1994).
[21] J. Yin, T. Zhu, Z. G. Liu, and T. Yu, Appl. Phys. Lett. **75**, 3698 (1999).
[22] R. Dat, J. K. Lee, O. Auciello, and A. I. Kingon, Appl. Phys. Lett. **67**, 572 (1995).
[23] C. A. Pas de Araujo, J. D. Cuchiaro, L. D. McMillan, M. C. Scott and J. F. Scott, Nature (London) **374**, 627 (1995).
[24] R. E. Newnham, R. W. Wolfe, R. S. Horsey, F. A. Diaz-Colon, and M. I. Kay, Mat. Res. Bull **8**, 1183 (1973).
[25] J. F. Scott, Ferroelectrics, **206–207**, 365 (1990).
[26] S.-E. Park and T. R. Shrout, J. Appl. Phys. **82**, 1804 (1997).
[27] J. Kuwata, K. Uchino, and S. Nomura, Jpn. J. Appl. Phys. **21**, 1298 (1982).
[28] S. Wada, S.-E. Park, L. E. Cross and T. R. Shrout, Ferroelectrics **221**, 147 (1999).
[29] H. Yu and C. A. Randall, J. Appl. Phys. **86**, 5733 (1999).
[30] M. Shen and W. Cao, Appl. Phys. Lett. **75**, 3713 (1999).

[31] J. Yin, B. Jiang, and W. Cao, IEEE Trans. Ultrason. Ferroelectr. Freq. Control **47**, 285 (2000).
[32] S. Wada, S. Suzuki, T. Noma, T. Suzuki, M. Osada, M. Kakihana, S.-E. Park, and T. Shrout, Jpn. J. Appl. Phys. **38**, 5505 (1999).
[33] H. Yu, V. Gopalan, J. Sindel, and C. A. Randall, J. Appl. Phys. **89**, 561 (2001).
[34] J. Yin and W. Cao, J. Appl. Phys. **87**, 7438 (2001).
[35] M. L. Mulvihill, S.-E. Park, G. Rish, and T. R. Shrout, Jpn. J. Appl. Phys., **35**, 561 (1996).
[36] B. D. Cullity, Elements of X-Ray Diffraction-2nd Edition, Addison-Wesley Pub. Co., Reading, MA, 1978.
[37] X. Du and I.W. Chen, J. Appl. Phys. **83**, 7789 (1998).
[38] I. K. Yoo and B. Desu, Phys. Stat. Sol. **133**, 565 (1992).
[39] S.-F. Liu, S.-E. Park, T. R Shrout, and L. E. Cross, J. Appl. Phys. **85**, 2810 (1999).
[40] M. K. Durbin, E. W. Jacobs, J. C. Hicks, and S.-E. Park, Appl. Phys. Lett. **74**, 2848 (1999).
[41] M. K. Durbin, J. C. Hicks, S.-E. Park, and T. R. Shrout, J. Appl. Phys. **87**, 8159 (2000).
[42] V. Bornand, S. Trolier-McKinstry, K. Takemura, and C. A. Randall, J. Appl. Phys. **87**, 3965 (2000).
[43] P. W. Rehrig, "Templated Grain Growth of $BaTiO_3$-Based Perovskite Single Crystals," Ph.D. Thesis, The Pennsylvania State University, University Park, (1999).
[44] H. L. Stadler, J. Appl. Phys. **29**, 743 (1958).
[45] G. Arlt and H. Neumann, Ferroelectrics **87**, 109 (1988).
[46] U. Robels, R. Lohkamper, and G. Arlt, Proc. ISAF'90, Urbana, USA (1990).
[47] U. Robels and G. Arlt, J. Appl. Phys. **73**, 3454 (1993).
[48] S. Zhang, S. Rhee, C. A. Randall, and T. R. Shrout, Jpn. J. Appl. Phys. **41**, 722 (2002).
[49] S. Zhang, P. W. Rehrig, C. A. Randall, and T. R. Shrout, J. Cryst. Growth **243**, 415 (2002).
[50] A. Safari, R. K. Panda, and V. F. Janas, Key Eng. Mater. **122-124**, 35 (1996).
[51] J. R. Oliver, R. R. Neurgaonkar, and L. E. Cross, J. Appl. Phys. **64**, 37 (1988).
[52] B. Jimenez, C. Alemany, J. Mendiola, and E. Maurer, Ferroelectrics **38**, 841 (1981).
[53] T. W. Cline, "Domain Contributions to the Dielectric Response in Ferroelectric Crystals," Ph.D. Thesis, The Pennsylvania State University, University Park, (1977).
[54] G. Siny, E. Husson, J. M. Beny, S. G. Lushnikov, E. A. Rogacheva, and P. P. Syrnikov, Physica B: Cond. Matter **293**, 382 (2001).
[55] T. Takenaka and H. Nagata, Key Eng. Mater. **157-158**, 57 (1999).
[56] H. Yilmaz, "Texturing of $Na_{1/2}Bi_{1/2}TiO_3$-$BaTiO_3$ Ceramics by Templated Grain Growth," Ph.D. Thesis, The Pennsylvania State University, University Park, (2002).
[57] Q. Y. Jiang, E. C. Subbarao, and L. E. Cross, J. Appl. Phys. **75**, 7433 (1994).

Chapter 4

INFLUENCE OF ELECTRICAL CYCLING ON POLARIZATION REVERSAL IN $Pb(Zn_{1/3}Nb_{2/3})O_3$-$PbTiO_3$ FERROELECTRIC SINGLE CRYSTALS AS A FUNCTION OF ORIENTATION

$(1-x)Pb(Zn_{1/3}Nb_{2/3})O_3$-$xPbTiO_3$ (PZN-PT) ferroelectric single crystals with rhombohedral symmetry demonstrate a wide variety of anisotropic behavior under both unipolar and bipolar electrical switching. Specifically, PZN-4.5PT crystals demonstrate exceptional polarization switching fatigue resistance along $[001]_C$ (-c; pseudocubic), as opposed to normal fatigue in $[111]_C$ directions in the rhombohedral ferroelectric state.[1] The role of relaxor characteristics for fatigue anisotropy was discussed in the previous chapter. One of the aspects of relaxors is that their ferroelectric properties depend on the measurement frequency. The field and frequency dependence of switching polarization was studied as a function of cycling (fatigue) history in PZN-4.5PT crystals along $[001]_C$ and $[111]_C$ orientations. The field and frequency dependence of switching polarization can be described by a power law, where greater electrical field strength and frequency dependence are shown for $[111]_C$ crystals. As fatigue evolves in the $[111]_C$ orientation, higher electric fields are required for switching due to the changes in microscopic switching mechanisms and buildup of local internal electric fields. However, negligible changes are observed in $[001]_C$ oriented crystals as a function of cycling. These differences are consistent with switching current and strain-field analyses. From strain-

field data, asymmetry can be detected in bipolar strain loops accompanying the suppression of the polarization-electric field switching. The asymmetry is localized, as noted by region to region changes in strain-field loops across the surface of the $[111]_C$ PZN-PT crystal.

4.1 Introduction

Ferroelectric materials have been considered for use in non-volatile ferroelectric random access memories (NVFRAM). These devices use the switchable spontaneous polarization which is the defining characteristic of a ferroelectric material.[2, 3, 4] In ferroelectric thin film studies, fatigue [5, 6, 7] as well as imprint [8, 9, 10, 11, 12, 13, 14] and retention [15, 16, 17, 18, 19] are widely recognized as problems to overcome with NVFRAMs.[5, 6, 7] The details of polarization switching and associated issues were discussed in the previous chapters.

Voltage (or electric field) shifts induced by either thermal, optical, or electrical processes in thin films have been extensively investigated as a signature for imprint.[11,12,13,14] Voltage shifts have been attributed to the role of charged defects, asymmetry in the electrode structure, bombardment during growth, and/or defect-dipole alignment in the films. Donor dopants have been suggested to minimize imprint by suppressing the oxygen vacancy concentration.[11,12,14] Thermally induced voltage shifts are reported to be smaller in $SrBi_2Ta_2O_7$ (SBT) compared to $Pb(Zr,Ti)O_3$ (PZT). This was ascribed to the smaller oxygen vacancy concentration in the perovskite sublattice of SBT

as compared to that of PZT.[14] In spite of the many technical advances with NVFRAM, the fatigue and imprint mechanisms are still not fully understood.

In bulk ferroelectric ceramics, fatigue-associated strain hysteresis asymmetry has been reported, and it was related to a preferred orientation set by the first poling state.[20, 21] *Nuffer et al*. reported that by thermally annealing the samples before and after each cycling step, this preferred orientation due to first poling can be removed. Despite thermal treatments, one of the branches of the bipolar strain hysteresis degraded more strongly. An alternative explanation of the asymmetry in strain loops is the existence of a unidirectional frozen-in polarization.[22]

In bulk lead zirconate titanate ceramics, bipolar strain asymmetry can be induced by either bipolar or unipolar cycling.[23, 24] Acoustic emission tests show that these defect agglomerates hinder the domain wall mobility.[23] Bipolar cycling also results in loss of switchable polarization. It was reported that ceramics which are exposed to unipolar drive ($3x10^8$ cycles) also exhibit an asymmetric bipolar strain, but no loss of switchable polarization.[24] Bipolar drive induced offsets are easily recovered by cycling at elevated electric fields but are fairly stable under thermal treatments up to 400 °C. On the other hand, unipolar cycling induced bipolar strain asymmetry can be completely recovered at much lower temperatures, i.e., 250 °C. High electric fields, though, are not very effective for regaining the symmetry. A large number of bipolar cycles at high field are needed to improve the unipolar cycling induced symmetry degradation.

In this paper, the evolution of bipolar strain loops was studied in both "fatiguing" $[111]_C$ and "fatigue-free" $[001]_C$ orientations.[1,25] Use of single crystals provides the opportunity to study electrical switching within "a single grain" (in contrast to work on

polycrystalline ceramics) and allows the orientation dependence to be investigated. Furthermore, unlike thin films deposited by vapor deposition methods or sol-gel, the symmetry is not influenced by the substrate or the thermal processes used in growth, crystallization, and electroding of the films.[26, 27, 28 29, 30]

4.2 Experimental Procedure

Square plate shape 95.5%Pb($Zn_{1/3}Nb_{2/3}$)O_3-4.5%$PbTiO_3$ (PZN-4.5PT) single crystals (grown by a high temperature flux technique[31]) were mirror polished and fully electroded with silver paint on both surfaces. Polarization and bipolar strain hysteresis (*P-E and* x*-E*) measurements were performed simultaneously by using a modified Sawyer-Tower circuit and linear variable differential transducer (LVDT) driven by a lock-in amplifier (Stanford Research Systems, Model SR830). Fatigue tests were performed under ac fields with a triangular wave form. The applied fields amplitudes for the fatigue tests were 15 or 20 kV/cm at 10 Hz for <001> and <111> crystals, respectively.

As shown by Viehland et al., switching at different frequencies and field strengths is sensitive to random fields in the lead relaxor materials. In this study, different orientations were studied as a function of cycling. After cycling in the $[001]_C$ or $[111]_C$ direction, the samples were then tested by analyzing the variation of switching behavior for drive frequencies between 0.01 Hz and 100 Hz, and at different maximum field levels from 1kV/cm up to 20 kV/cm, depending on orientation and fatigue level.

To further access polarization dynamics, switching currents were obtained by a derivative of the charge data from the *P-E* hysteresis measurements. The fatigue tests were interrupted for *P-E* measurements at varying electric field and frequencies after 10^1, 10^2,10^3, 10^4, and 10^5 switching cycles.

4.3 Result and Discussion

4.3.1 Influence of cycling on polarization switching with electric field strength and driving frequency

Local random fields in relaxor ferroelectrics are created from breaks in translational symmetry, which can occur due to intermediate level cation order and strain variations owing to different size cations.[32, 33, 34, 35] These random fields give rise to broad time constant distributions of the nucleation and domain switching processes.[36, 37] Viehland et al. showed qualitatively that driving the switching under different frequencies and field strengths reveals changes associated with the time constant distributions.[38] To quantitatively interpret the random fields, a deconvolution of the driving field has to be performed; this, though, is difficult, given the fact that distribution depends on the field level applied. In this study, we used the method applied by Viehland et al. to investigate polarization switching as a function of fatigue and orientation dependence.

Figure 4.1 and Figure 4.2 show the changes in the switching behavior following 10^1 and 10^5 cycles in $[001]_C$ and $[111]_C$ oriented PZN-PT crystals, respectively. It is clear that in $[111]_C$ crystals, fatigue is accompanied by a substantial increase in the field

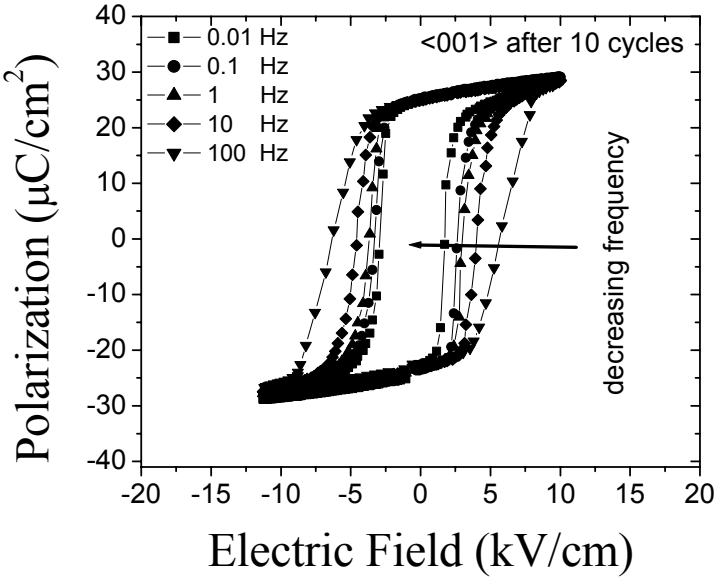

(a)

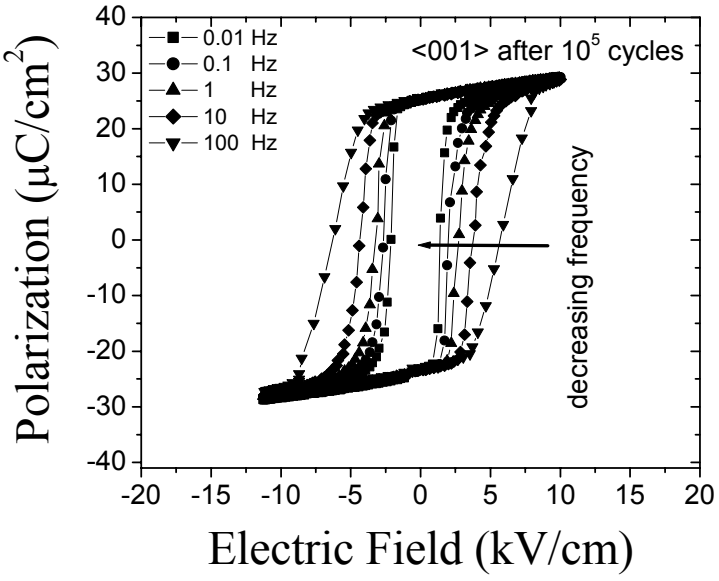

(b)

Figure 4.1 P-E loops for $[001]_C$ oriented PZN-4.5PT single crystals measured at 10 kV/cm in a range of frequencies: a) virgin $[001]_C$ crystal after 10 cycles, b) fatigue free $[001]_C$ crystal measured after 10^5 cycles.

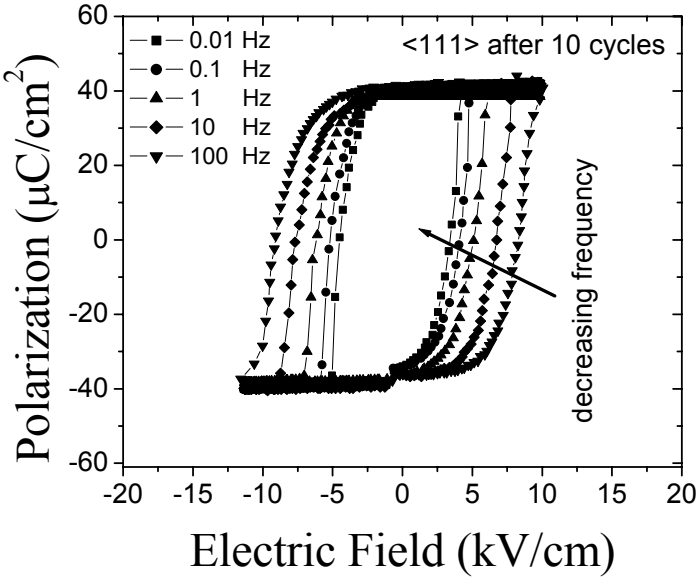

(a)

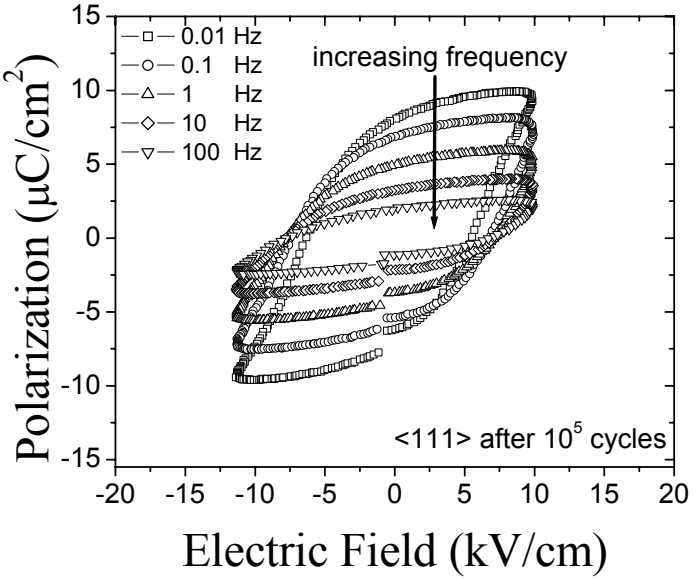

(b)

Figure 4.2 P-E loops for $[111]_C$ oriented PZN-4.5PT single crystals measured at 10 kV/cm in a range of frequencies: a) virgin $[111]_C$ crystal after 10 cycles with saturated polarization, b) fatigued $[111]_C$ crystal after 10^5 switching cycles showing strong frequency dependence of both P_r and E_C.

dependence of the switching. In contrast, the $[001]_C$ crystals show very similar behavior before and after cycling. These differences were quantified by plotting the remanent polarization of the hysteresis loops as a function of switching cycling for each applied electric field over a range of frequencies. The results are presented in Figure 4.3. In $[001]_C$ oriented PZN-4.5PT crystals, we note that the remanent polarization is effectively frequency independent above a critical bipolar field strength. For all cycling histories, the 5 kV/cm data is frequency independent for $[001]_C$ over the frequency range measured.

After 10 cycles, the critical field drops to 3 kV/cm. This is consistent with an earlier investigation[39], where preconditioning switching was observed to lower the coercive field. The frequency independence between 0.01 Hz and 100 Hz demonstrates that there are no rate-limiting processes associated with the underlying switching mechanisms of the $[001]_C$ PZN-PT materials or the external circuit for this field range. In the case of $[111]_C$, the curves demonstrate a stronger frequency dependence. Furthermore, for a given field strength, the frequency dependence grows stronger as fatigue progresses. This implies that there are internal rate limiting switching mechanisms operating in the $[111]_C$ switching PZN-4.5PT crystals, and they systematically become more dominant as a crystal is cycled in this direction.

A simple power law empirically describes the scaling laws relating remanent polarization and cycling frequency in these crystals in both $[001]_C$ and $[111]_C$ directions.

$$\mathrm{P_r} = a \times f^{n} \tag{4.1}$$

where : "P_r" is the remanent polarization,

"*f*" is the driving frequency,

"a" is a constant at a specific field strength, and

"n" is a power law exponent for a specific field strength amplitude.

The constants "a" and "n" are tabulated in Table 4.1 for both orientations as a function of the number of cycles at 10 kV/cm in a range of frequency from 0.01 to 100 Hz. It is seen here that as fatigue evolves in $[111]_C$ oriented crystals, the constants change; this contrasts with the stable values for $[001]_C$.

To further understand the switching process as a function of the cycling history of $[001]_C$ and $[111]_C$ PZN-4.5PT crystals, the current changes were studied. Figure 4.4 shows the switching currents in both orientations as a function of the cycling history. The $[001]_C$ crystal again shows an initial conditioning effect in the switching behavior, with the current-time behavior stabilizing after 10 cycles or so, and subsequently remaining constant up to 10^5 cycles and most likely far beyond this. The maximum in the current peaks for these drive conditions occurs at about 0.3 seconds for cycling at 0.1 Hz. The distribution about this characteristic time is also constant throughout all the cycles. This behavior is very different from the $[111]_C$ switching current data. In Figure 4.4(b), the current curves are shifted to longer times and have broader distributions when measured later in the cycling process. This is consistent with a fatigue mechanism in which the initial fast switching mechanisms slow down and slower components eventually get frozen in and no longer contribute to the ferroelectric switching. Figure 4.5 summarizes the trend in the characteristic switching time for the $[111]_C$ and $[001]_C$ orientations. The characteristic switching time shifts to longer times as fatigue evolves in the $[111]_C$ orientation. A major shift in the characteristic switching becomes apparent after 10^4

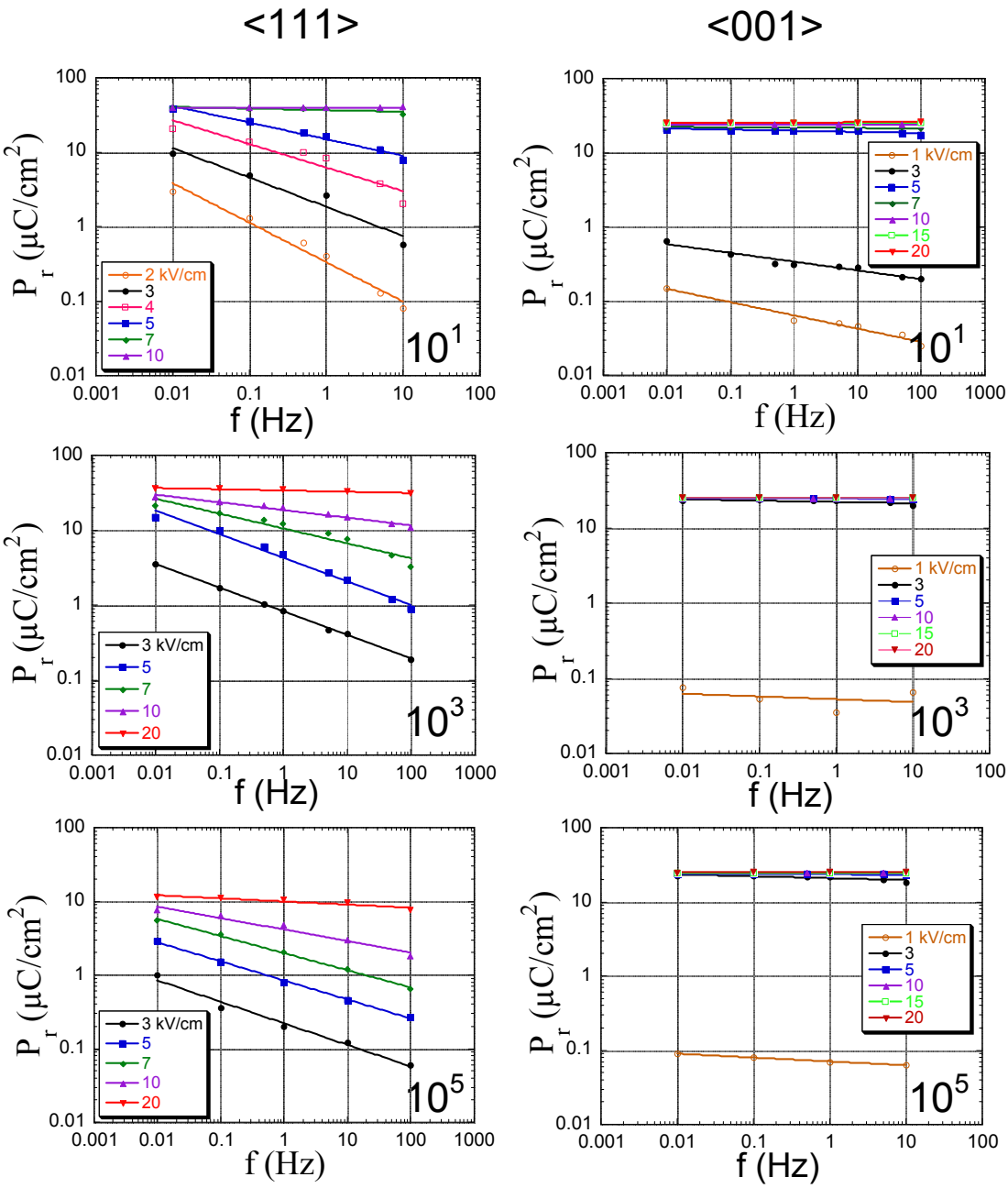

Figure 4.3 Field and frequency dependence of polarization switching in PZN-4.5PT single crystals as a function of cycling in $[111]_C$ and $[001]_C$ orientations.

Table 4.1 Power law constants for PZN-4.5PT single crystals at 10 kV/cm for different orientations and switching history.

$P = a \times f^n$		Number of switching cycles				
Constants	**Orientation**	10^1	10^2	10^3	10^4	10^5
a ($\mu C/cm^2$)	**<001>**	24.03±0.09	24.66±0.02	24.81±0.017	24.81±0.02	24.31±0.02
	<111>	39.85±0.13	-	18.56±0.47	14.81±0.57	4.13±0.19
n (exponent)	**<001>**	0.001±0.0013	0.000±0.0003	0.001±0.0002	0.001±0.0003	0.000±0.0003
	<111>	0.001±0.0011	-	-0.091±0.008	-0.095±0.013	-0.142±0.015

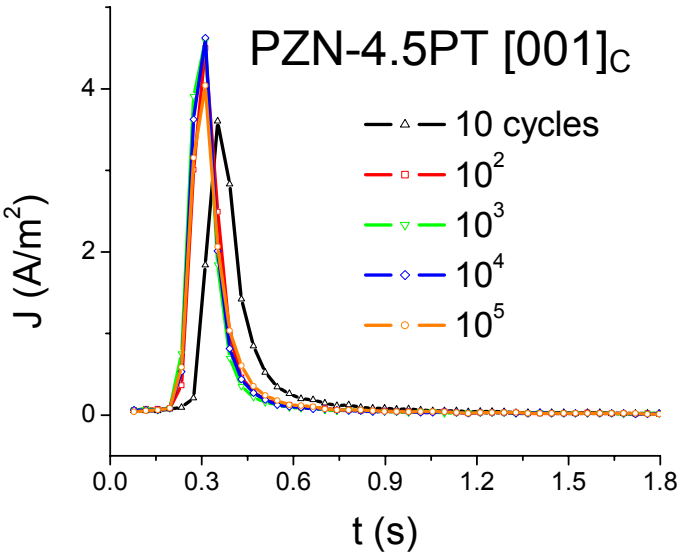

(a)

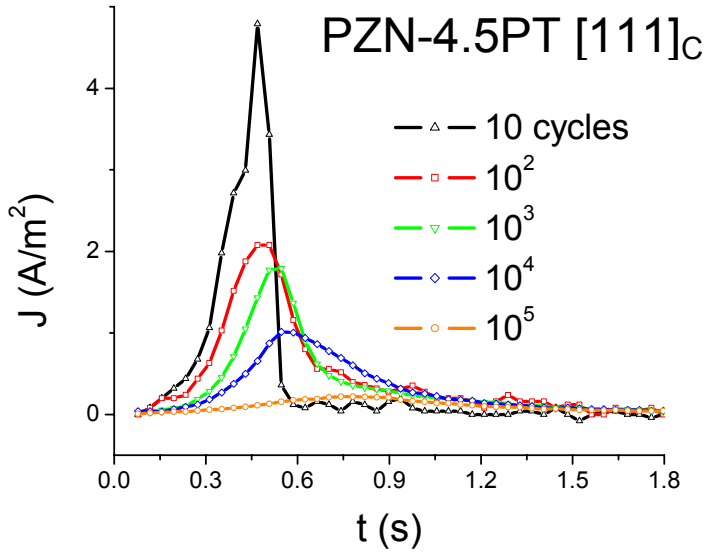

(b)

Figure 4.4 Switching current densities with bipolar cycling/fatigue in PZN-4.5PT crystals in a) $[001]_C$, b) $[111]_C$ directions.

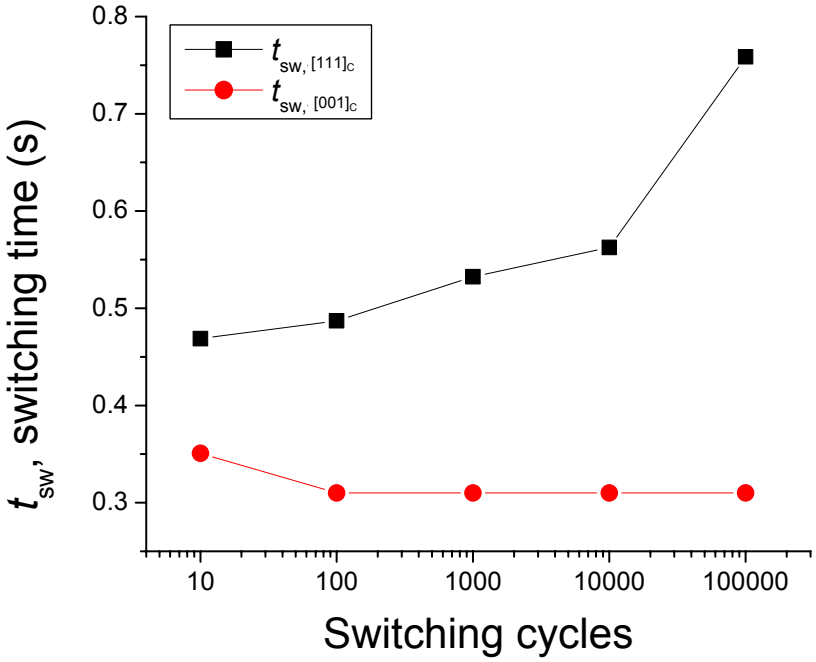

Figure 4.5 Characteristic switching times during bipolar switching in PZN-4.5PT crystals along the $[111]_C$ and $[001]_C$ orientations .

cycles. After this point, generally faster fatigue rates are observed. Consequently, greater field strengths are required for a constant frequency to either induce reversed polarization or more domain walls for polarization switching in the [111] direction.

4.3.2 Fatigue induced asymmetry in [111] oriented crystal

Kholkin et al.[40,41] successfully utilized strain-field switching to study fatigue processes in ferroelectric thin films. This is a useful tool, since the presence of an internal electric field strongly perturbs the strain-field switching curves. Comparable measurements were made on PZN-PT crystals in this work for different crystallographic directions as a function of bipolar cycling. It was found that $[111]_C$ oriented crystals show the onset of a strain field asymmetry, which grows as cycling continues as shown in Figure 4.6(a). In contrast, $[001]_C$ crystals shows symmetrical strain-field curves throughout cycling, as seen in Figure 4.6(b). This suggests that no net internal fields develop in the $[001]_C$ non-fatiguing directions. Small and homogeneously distributed internal fields may exist. These, though, if they do exist, do not effectively stabilize domains and give rise to fatigue. The internal fields that develop in $[111]_C$ crystals are locally inhomogeneous, as deduced by positional changes across the surface of the PZN-PT crystal. These differences are sufficiently large that the asymmetry in the strain field switching can develop with either orientation. This implies that local internal fields vary across the $[111]_C$ crystals, producing islands of frozen domains (as shown in Figure 4.7). Unlike earlier studies in polycrystalline materials, PZT, the asymmetry is not induced by the polarity of first switching. The lateral resolution of the LVDT used in this

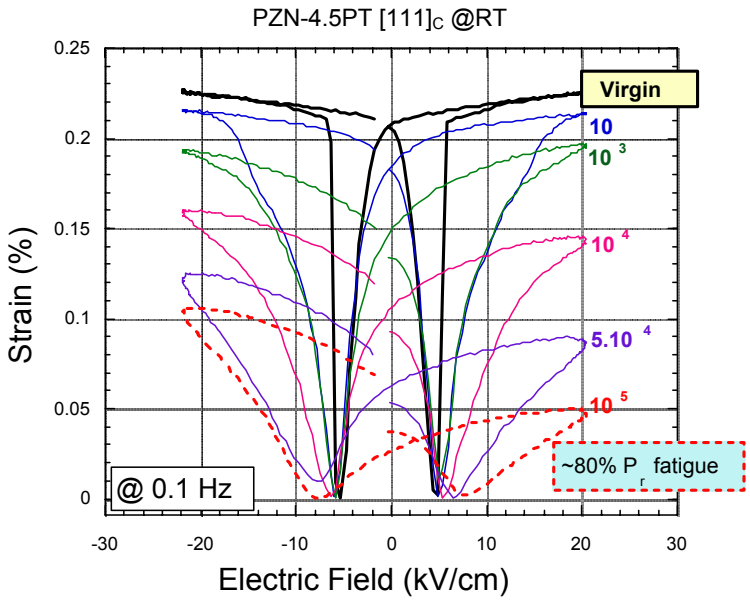

(a)

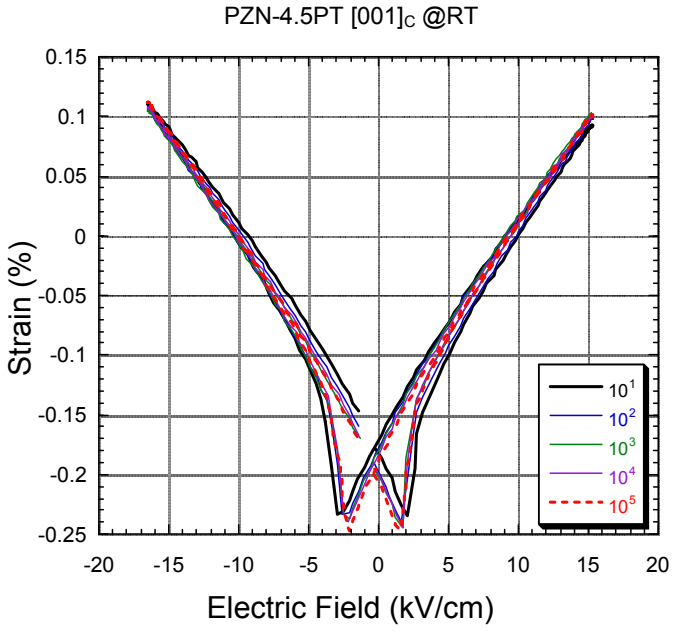

(b)

Figure 4.6 Bipolar strain loops as a function of cycling (up to 10^5 cycles) in a) $[111]_C$ and b) $[001]_C$ orientations. Fatigued $[111]_C$ crystals show asymmetric switching.

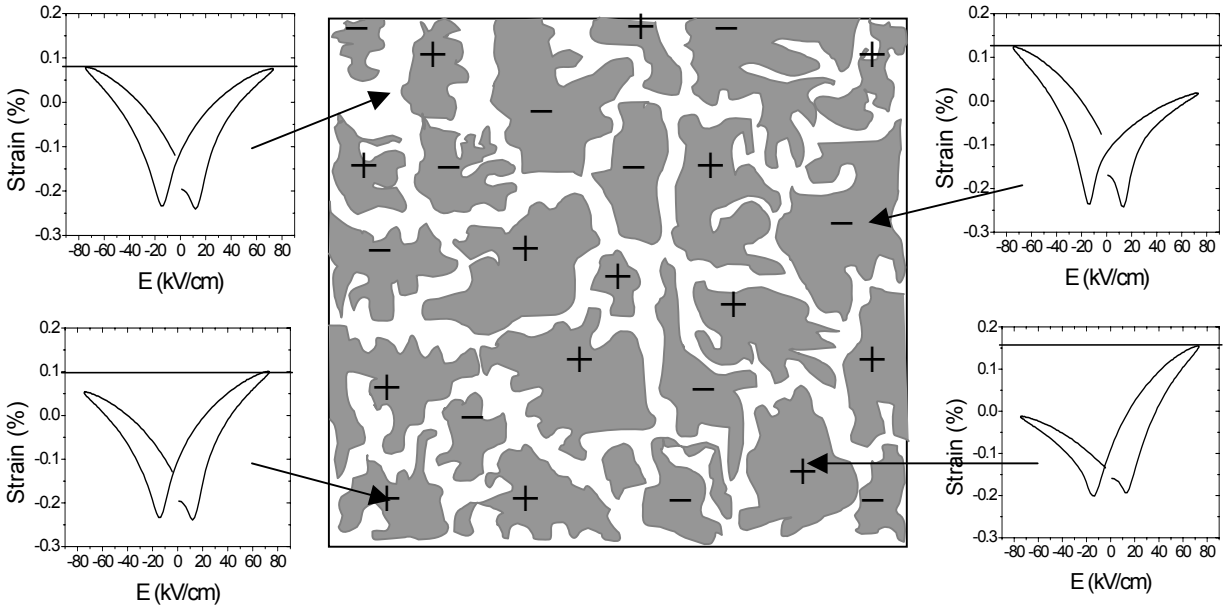

Figure 4.7 Fatigued $[111]_C$ crystal PZN-PT (x=0.045) demonstrated a heterogeneous nature for switching as asymmetry changes its polarity throughout the same surface.

investigation was relatively coarse; given this, the scale of the islands is on a millimeter scale. The observation of island formation in PZT thin films undergoing fatigue was first reported by Colla et al. on a micron scale, as detected by atomic force microscopy.[42] The origin of the islands may be the same in both cases, but the difference in the size of the islands might be a result of the relative difference in thickness of the ferroelectrics or the spatial resolution of the probe utilized.

4.3.3 Electrical and Thermal Rejuvenation of Fatigue

In earlier studies on fatigue in ferroelectric bulk and thin films, it was observed that fatigue can often be rejuvenated either by annealing the material above the Curie temperature or applying larger electric fields to overcome internal fields. Comparable measurements were made on the single crystal system studied here. The magnitude of the applied field was increased from 20 kV/cm up to 70 kV/cm in an attempt to recover the symmetry, but the asymmetry remained even at the high electric fields, as shown in Figure 4.8. However, in other regions, it was possible to get near symmetric strain hysteresis or curves with reversed asymmetry, as depicted in Figure 4.7. So it is concluded that in $[111]_C$ directions, fatigue cannot be recovered by simply applying higher field. This is consistent with local regions having frozen in domain structures clamped by an internal bias. However, thermal annealing at 300˚C for 5h in air completely recovers both the magnitude of the switchable polarization and symmetry in the hysteresis loops in fatigued crystals, as shown in Figure 4.10. This can be attributed to redistribution and/or reduction of the defects that can control freezing of domains.

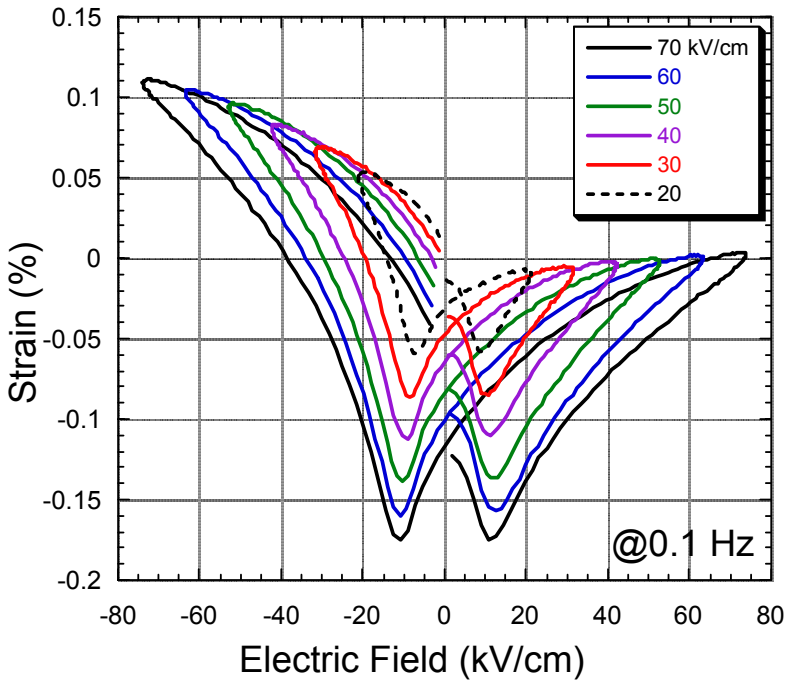

Figure 4.8 Asymmetry is retained at increased field levels in fatigued PZN-4.5PT[111]$_C$.

However, the coercive field remains large; the defects, although now randomized in space throughout the ferroelectric, limit domain motion and increase the coercive field. This is supported by the high characteristic time constant, after fatigue and rejuvenation observed in current-time curve, Figure 4.10(b).

4.4 Summary and Conclusions

Fatigue anisotropy in PZN-PT crystals in $[001]_C$ and $[111]_C$ orientations has been studied. In this investigation, the dependence of the switching behavior on driving frequency and the driving field strength was measured. There is a conditioning process that is required in the $[001]_C$, but after about 10 cycles with field $\geq$ 3 kV/cm, the switching is very stable over a large number of cycles with no evidence of fatigue. In the $[111]_C$ orientation, the remanent polarization changes as a function of drive frequency and field strength through cycling. As the ferroelectric material fatigues, higher fields and slower cycling times are required to maximize the remanent polarization. The decay rate of the remanent polarization follows a simple scaling law. The same conclusions can be reached in analyzing the switching current under a.c. drive.

Through measurement of strain electric field switching, an asymmetry in $[111]_C$ fatiguing crystals was observed. This is considered to be the result of an internal electric field. No net internal fields are found in $[001]_C$ oriented crystals, even after large numbers of cycles. Local changes in the amount of asymmetry and also reversal in the asymmetry across the same crystal indicates the internal field is the result of statistical events and not broken by symmetry from the first injection process. Once the asymmetry evolves, it

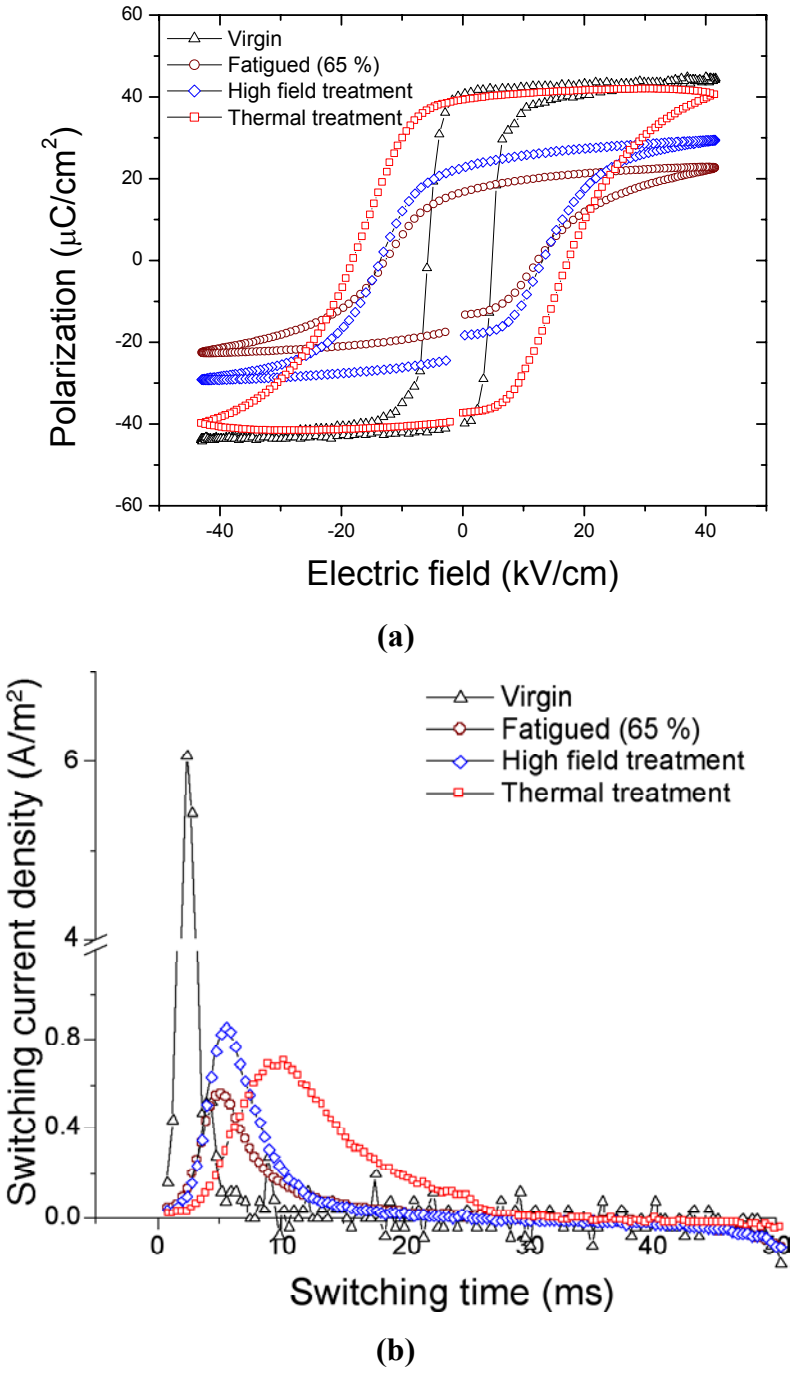

Figure 4.9 Rejuvenation of fatigue induced effects by high electric field and thermal annealing at 300 ˚C treatments: a) P-E hysteresis loops, b) switching currents

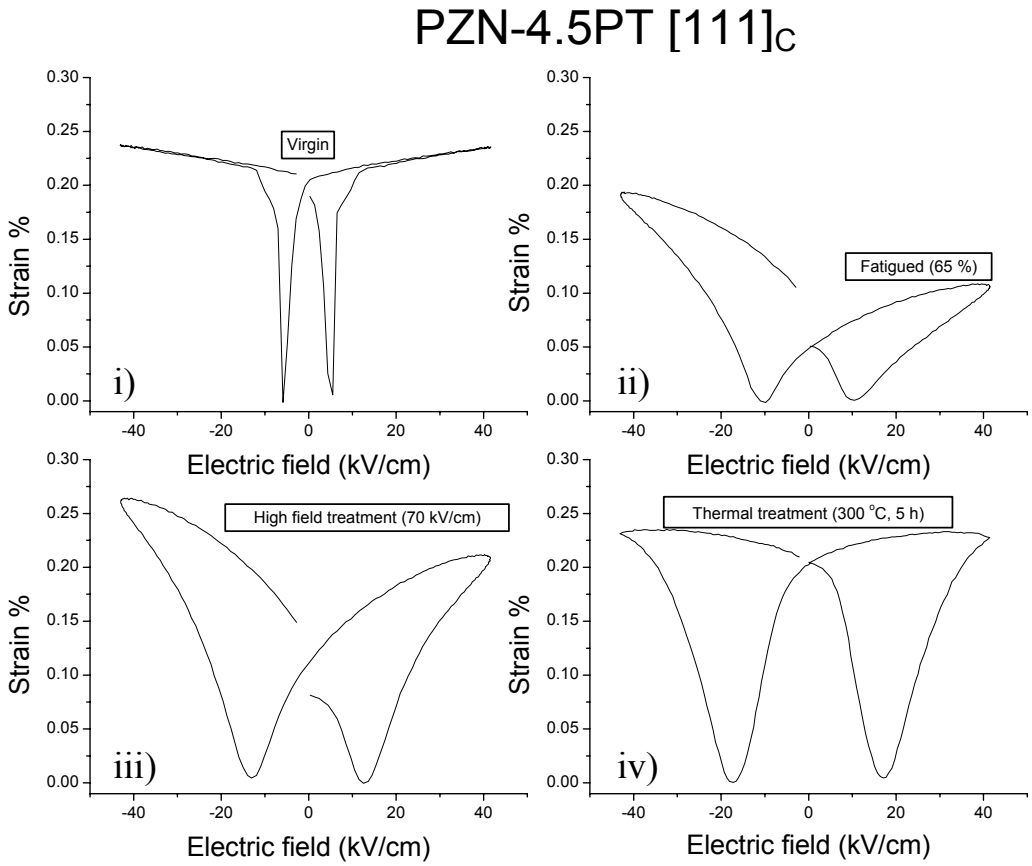

Figure 4.10 Rejuvenation of fatigue induced effects in bipolar strain hysteresis loops, (i) virgin, (ii) at the 65% fatigue, (iii) no recovery after 70 kV/cm field application, and (iv) symmetrical after thermal anneal at 300˚C for 5 hours.

cannot be recovered by stronger electric fields up to 70 kV/cm. However, thermally annealed crystals regain symmetry in the strain-field curves if the driving electric field is high enough to give polarization saturation, $E \geq 2 \times E_c$. It is believed that the thermal annealing randomizes the defects. In $[111]_C$ orientation, rejuvenation anneals yield a symmetrical hysteresis, but with enhanced coercive fields.

4.5 References

[1] J. F. Scott and C. A. Paz de Araujo, Science **246**, 1400 (1989).
[2] J. T. Evans and R. Womack, IEEE J. Solid State Circuits **23**, 1171 (1988).
[3] A. Kingon, Nature **401**, 658 (1999).
[4] J. F. Scott, Ferroelectric Memories, Springer, New York, 2000.
[5] A. K. Tagantsev, I. Stolichnov, E. L. Colla, and N. Setter, J. Appl. Phys. **90**, 1387 (2001).
[6] B. H. Park, B. S. Kang, S. D. Bu, T. W. Noh, J. Lee, and W. Jo, Nature (London) **401**, 682 (1999).
[7] B. H. Park, S. J. Hyun, C. R. Moon, B.-D. Choe, J. Lee, C. Y. Kim, W. Jo, and T. W. Noh, J. Appl. Phys. **84**, 4428 (1998).
[8] M. Grossmann, O. Lohse, D. Bolten, U. Boettger, T. Schneller, and R. Waser, J. Appl. Phys. **92**, 2680 (2002).
[9] S.-H. Kim, D.-S. Lee, C. S. Hwang, D.-J. Kim, and A. I. Kingon, Appl. Phys. Lett. **77**, 3036 (2000).
[10] W. L. Warren, D. Dimos, G. E. Pike, B. A. Tuttle, M. V.Raymond, and J. T. Evans, Appl. Phys. Lett. **67**, 866 (1995).
[11] W. L. Warren, B. A. Tuttle, D. Dimos, G. E. Pike, H. N. Al-Shareef, R. Ramesh, and J. T. Evans, Jpn. J. Appl. Phys. **35**, 1521 (1996).
[12] A. Gruverman, B. J. Rodriguez, R. J. Nemanich, and A. Kingon, J. Appl. Phys. **92**, 2734 (2002).
[13] H. N. Al-Shareef, D. Dimos, W. L. Warren, B. A. Tuttle, J. Appl. Phys. **80**, 4573 (1996).
[14] Y. Shimada, K. Nakao, A. Inoue, M. Azuma, Y. Uemoto, E. Fujii, and T. Otsuki, Appl. Phys. Lett. **71**, 2538 (1997).
[15] Z. Zhang, Y. N. Wang, J. S. Zhu, F. Yan, X. M. Lu, H. M. Shen, and J. S. Liu, Appl. Phys. Lett. **73**, 3674 (1998).
[16] K. Nakao, Y. Judai, M. Azuma, Y. Shimada, and T. Otsuki, Jpn. J. Appl. Phys. **37**, 5203 (1998).

[17] K.-M. Lee, H.-G. An, J.-K. Lee, Y.-T. Lee, S.-W. Lee, S.-H. Joo, S.-D. Nam, K.-S. Park, M.-S. Lee, S.-O. Park, H.-K. Kang, and J.-T. Moon, Jpn. J. Appl. Phys. **40**, 4979 (2001).
[18] B. S. Kang, J.-G. Yoon, T. W. Noh, T. K. Song, S. Seo, Y. K. Lee, and J. K. Lee, Appl. Phys. Lett. **82**, 248 (2003).
[19] W. L. Warren, D. Dimos, B. A. Tuttle, G. E. Pike, and H. N. Al-Shareef, Integrated Ferroelectrics **16**, 77 (1997).
[20] W. L. Warren, B. A. Tuttle, and D. Dimos, Appl. Phys. Lett. **67**, 1426 (1995).
[21] J. Nuffer, D. C. Lupascu, and J. Rodel, Acta Mater. **48**, 3783 (2000).
[22] J. Nuffer, D. C. Lupascu, and J. Rodel, Appl. Phys. Lett. **80**, 1049 (2002).
[23] C. Verdier, D. C. Lupascu, and J. Rodel, Appl. Phys. Lett. **81**, 2596 (2002).
[24] K. Takemura, M. Ozgul, V. Bornand, S. Trolier-McKinstry, and C. A. Randall, J. Appl. Phys. **88**, 7272 (2000).
[25] M. Ozgul, K. Takemura, S. Trolier-McKinstry, and C. A. Randall, J. Appl. Phys. **89**, 5100 (2001).
[26] W. L. Warren, H. N. Al-Shareef, D. Dimos, B. A. Tuttle, and G. E. Pike, Appl. Phys. Lett. **68**, 1681 (1996).
[27] S.-H. Kim, D.-J. Kim, S. K. Streiffer, and A. I. Kingon, J. Mater. Res. **14**, 2476 (1999).
[28] J. Lee and R. Ramesh, Appl. Phys. Lett. **68**, 484 (1996).
[29] W. Liu, J. Ko, and W. Zhu, Mater. Lett. **49**, 122 (2001).
[30] J. Lee, C. H. Choi, B. H. Park, T. W. Noh, and J. K. Lee, Appl. Phys. Lett. **72**, 3380 (1998).
[31] M. L. Mulvihill, S.-E. Park, G. Risch, Z. Li, K. Uchino, and T. Shrout, Jpn. J. Appl. Phys., Part 1 **35**, 3984 (1996).
[32] Y. Imry and S. Ma, Phys Rev. Lett. **35**, 1399 (1975).
[33] G. Smolenski and A. Agranovskaya, Sov. Phys. Solid State **1**, 1429 (1960).
[33] L. E. Cross, Ferroelectrics **76**, 241 (1987).
[35] C. Randall, A. Bhalla, T. Shrout, and L. E. Cross, J. Mater. Res. **5**, 829 (1990).
[36] V. Y. Shur, E. L. Rumyantsev, E. I. Shishkin, I. S. Baturin, Phys. Solid State **44**, 2145 (2002).
[37] V. Y. Shur, E. L. Rumyantsev, E. V. Nikolaeva, E. I. Shishkin, I. S. Baturin, J. Appl. Phys. **90**, 6312 (2001).
[38] D. Viehland and Y.-H. Chen, J. Appl. Phys. **88**, 6696 (2000).
[39] M. Ozgul, E. Furman, S. Trolier-McKinstry, and C. A. Randall, presented at 27th Annual Cocoa Beach Conference and Exposition on Advanced Ceramics & Composites meeting of the American Ceramic Society Electronics and Engineering Ceramics divisions meeting in Jan. 27-30, 2003 at Cocoa Beach, FL.
[40] A. L. Kholkin, M. L. Calzada, P. Ramos, J. Mendiola, N. Setter, Appl. Phys. Lett. **69**, 3602 (1996).
[41] A. L. Kholkin and M. L. Calzada, Journal de Physique IV **8**, 195 (1998).
[42] E. L. Colla, S. Hong, D. V. Taylor, A. K. Tagantsev, and N. Setter, Appl. Phys. Lett. **72**, 2763 (2000).

Chapter 5

POLARIZATION RELAXATION ANISOTROPY IN $Pb(Zn_{1/3}Nb_{2/3})O_3$-$PbTiO_3$ SINGLE CRYSTAL FERROELECTRICS AS A FUNCTION OF FATIGUE HISTORY

An asymmetry evolution and its local nature were observed in a fatigued crystal as discussed in the previous chapter. Consistent with the inhomogeneity, an increased frequency dependence was also noted. Polarization switching can be influenced by the existing perturbation sources in a ferroelectric crystal. Polarization relaxation was studied in $Pb(Zn_{1/3}Nb_{2/3})O_3$-$PbTiO_3$ (PZN-PT) single crystals to probe the perturbations as a function of orientation. To excite pre-poled crystals, a modest dc voltage (< 1/2 of the coercive field) was applied along the poling direction. Upon removal of the voltage, the polarization decay in the time domain was measured. Experimental data were modeled with a stretched exponential function. Stretching exponent ($\beta_{<hkl>}$) and characteristic time ($\tau_{<hkl>}$) constants for polarization relaxation were determined from data over four decades in the time domain at different stages of bipolar cycling. $\beta_{<hkl>}$ values after 10^1 cycles were 0.146±0.002 and 0.247±0.0004 in the <001> and <111> orientations, respectively. The $\beta_{<111>}$ constant increased up to 0.453±0.104 after 10^5 cycles in <111> oriented crystals that show fatigue. However, much less change is observed in $\beta_{<001>}$ as a function of cycling for <001> crystals. Characteristic time constants for relaxation ($\tau_{<hkl>}$) were calculated for <001> and <111> orientations as 0.401±0.048 s and 57.46±0.10 s,

respectively. These results suggest a faster polarization relaxation in <001> than in the <111> orientation of rhombohedral PZN-PT ferroelectric crystals.

5.1 Introduction

Since the discovery of their extraordinary piezoelectric properties (d_{33} ~2500 pC/N) with large, electric field induced strain (~1.7 %) in rhombohedral crystals oriented along $[001]_C$ (where the subscript denotes measurements with respect to the cubic axes), numerous investigations have been made in the PZN-PT system.[1-8] It has been widely noticed that the measured properties of PZN-PT single crystals are strongly anisotropic. Park *et al.* explored the dependence of electric field – induced strains on crystallographic orientation in PZN-PT crystals. Large piezoelectric strains with extremely low hysteresis were observed in $[001]_C$ poled crystals, compared to lower strain with large hysteresis in the $[111]_C$ orientation. The very high strains, coupled with the low hysteresis of $[001]_C$ oriented crystals were attributed to the engineered-domain configuration in which the domain walls are not driven by applied fields in the poled state.[3] Electric field induced domain configurations and domain switching under pulsed electric field conditions have been investigated by Yu *et al.* in PZN-PT crystals oriented at various crystallographic directions. Both domain wall mobility and activation energies were reported to be higher in the $[001]_C$ direction than for $[111]_C$. The observed anisotropy in the switching under pulse conditions was believed to indicate that the engineered domain state along the $[001]_C$ direction is more stable than that in the $[111]_C$ direction. Consequently, a higher activation field is needed in $[001]_C$ oriented crystals. However, once the energy barrier is

overcome during the switching process, domain walls move faster in $[001]_C$ oriented crystals.[6,8]

Many ferroelectric materials show a progressive loss in switchable polarization on cycling through the hysteresis loop repeatedly. This process is known as polarization fatigue. Fatigue studies in PZN-PT crystals also revealed anisotropy.[9-11] It was found that $[001]_C$ oriented rhombohedral PZN-PT demonstrates excellent fatigue resistance, while $[111]_C$ oriented rhombohedral PZN-PT fatigues as shown in

Figure 5.1. Fatigue is also observed in $[001]_C$ crystals when tetragonal material is generated by changes in temperature or driving field strength.[11] The superior fatigue resistance along the $[001]_C$ direction is consistent with the observation of higher domain wall mobility (at least in the rhombohedral phase field).[8] It is important to note that in some studies, fatigue has been correlated with a slowing down of domain walls.[12]

There is likely to be a complex interaction between existing sources of depolarizing fields under switching conditions, and the evolution of domains and polarization after external field is removed (polarization relaxation from an excited state). One way in which this could be manifested is in time variation in the remanent polarization due to spontaneous polarization reversal. This is sometimes referred to as retention loss, and is widely studied in thin films.[13-16] Some of the recent studies on polarization relaxation focused on the physical origins of the relaxation kinetics during polarization reversal. Different retention studies covered different time frames, from very short times ($t < 1$ s) to long times ($t > 1$ s). The main concern in practical ferroelectric memory applications is the long-time retention. However, the short-time retention is also

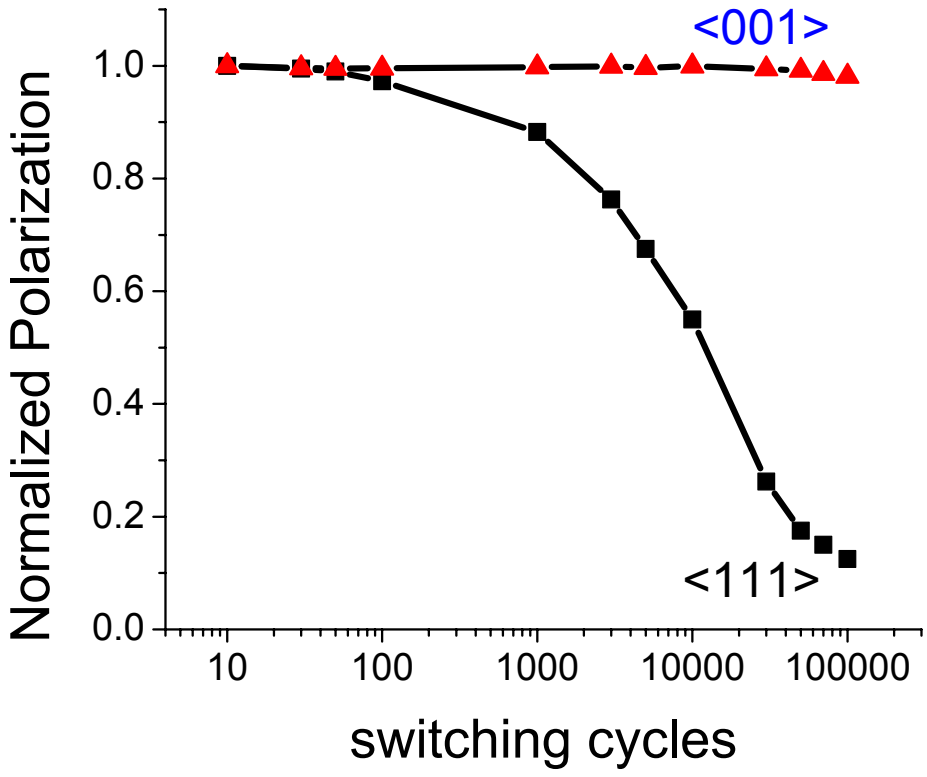

Figure 5.1 Fatigue anisotropy in PZN-4.5PT single crystal.

important in probing the polarization dynamics which govern the fast decay of polarization upon removal of the electric field. Kang *et al*. investigated the short-time retention loss properties and reported that fatigued capacitors showed a significant loss in retained polarization in the short-time regime. This was interpreted in terms of increasing depolarization fields with fatigue.[17] Thus, it appears that collective information on the polarization dynamics both in the presence and absence of external fields may be helpful to characterize and understand the polarization switching and fatigue anisotropy.

The purpose of this study is to gain insight into the anisotropy in PZN-PT and related materials by probing the relaxation of dc field excited domains upon removal of the electric field. The classical time decay approach is utilized to understand the effect of local perturbations on polarization as a function of orientation and cycling history.[18-22] Here, the focus is the relaxation kinetics of polarization in pre-poled crystals after exposure to a sub-coercive field level dc field perturbation applied along the poling direction. The polarization decay in the time domain was measured for two different crystallographic orientations in PZN-4.5PT single crystals which demonstrate different fatigue behavior, and in crystals that have experienced different switching histories. The aim of the work was to determine if there are differences in polarization relaxation in $[001]_C$ and $[111]_C$, as well as to determine how the relaxations change as a function of bipolar cycling.

The dynamic processes occurring in complex systems such as the PZN-4.5%PT relaxor crystals encompass different length and time scales for the polarization. Both fast and slow rearrangements take place within the microscopic, mesoscopic and macroscopic organization of the systems. A common aspect of relaxor or glassy ferroelectric systems

is a certain amount of order at an intermediate, so-called mesoscopic, scale while they are disordered at the microscopic scale and are homogeneous at the macroscopic scale.[23] A simple exponential relaxation law cannot describe the relaxation phenomena and kinetics in such materials. There are two mechanisms driving nonexponential relaxation in quenched, disordered media with stretched exponential relaxation. One is related to random pinning sites.[24] Secondly, in disordered systems such as spin glasses, complex relaxation is caused by the existence of frustrated antiferromagnetic/ferromagnetic-type interactions[25-27] which is a direct consequence of the quenched disorder[28]. A polarization analogy to spin glasses has been made in dipole glasses. In such materials, the nature of the polarization dynamics is influenced by a variety of perturbation sources (e.g., micro and mesoscopic chemical heterogeneities, random site occupancy and dipolar interactions). During relaxation from higher energy levels, domains will relax to lower energy configurations by multiple pathways influenced by perturbation sources. This study is intended to determine how polarization relaxation correlates with the orientation dependent fatigue behavior in PZN-PT crystals.

5.2 Experimental Procedure

Single crystals of $0.955Pb(Zn_{1/3}Nb_{2/3})O_3–0.045PbTiO_3$ (PZN-4.5PT) solid solutions were grown by a high temperature flux technique.[29] The crystals of this composition have a perovskite structure and are rhombohedral (pseudocubic) at room temperature. The crystals were oriented either along the $[111]_C$ or along the $[001]_C$ axes

to within ±2° by using a Laue Camera (Multiwire Laboratories Ltd., real-time Laue machine).

For electrical characterization, plate-shaped samples were cut from the oriented crystals and prepared by polishing with silicon carbide and alumina polishing powders (down to ~1 μm) to achieve flat and parallel surfaces onto which silver paste electrodes were applied. Silver paste electrodes were preferred because they can be removed easily by washing with acetone without changing the nature of the crystal/electrode interface after the electrode removal. The thickness of samples used in this study ranged from 450 μm to 600 μm. Coercive fields (measured at 20 kV/cm and 0.1 Hz) for the crystals are about 3 kV/cm and 5 kV/cm in <001> and <111> directions, respectively.

High field measurements utilized a modified Sawyer–Tower circuit. A high voltage amplifier (Trek Model 609C-6) was used in both poling and polarization fatigue measurements. The experimental procedure for the relaxation studies is shown in

Figure 5.2. Crystals were exposed to electric fields (*E*) as high as $5\times E_C$ for poling to achieve saturated polarization prior to time domain experiments. For fatigue measurements, electric fields were applied with a triangular bipolar wave form. The magnitude and the frequency of the applied field were 20 kV/cm and 10 Hz, respectively, for $[001]_C$ crystals. The applied field was higher (40 kV/cm) for $[111]_C$ samples to ensure full switching due to the increasing coercive field with fatigue. During measurements, the samples were submerged in Fluorinert, an insulating liquid, to prevent arcing.

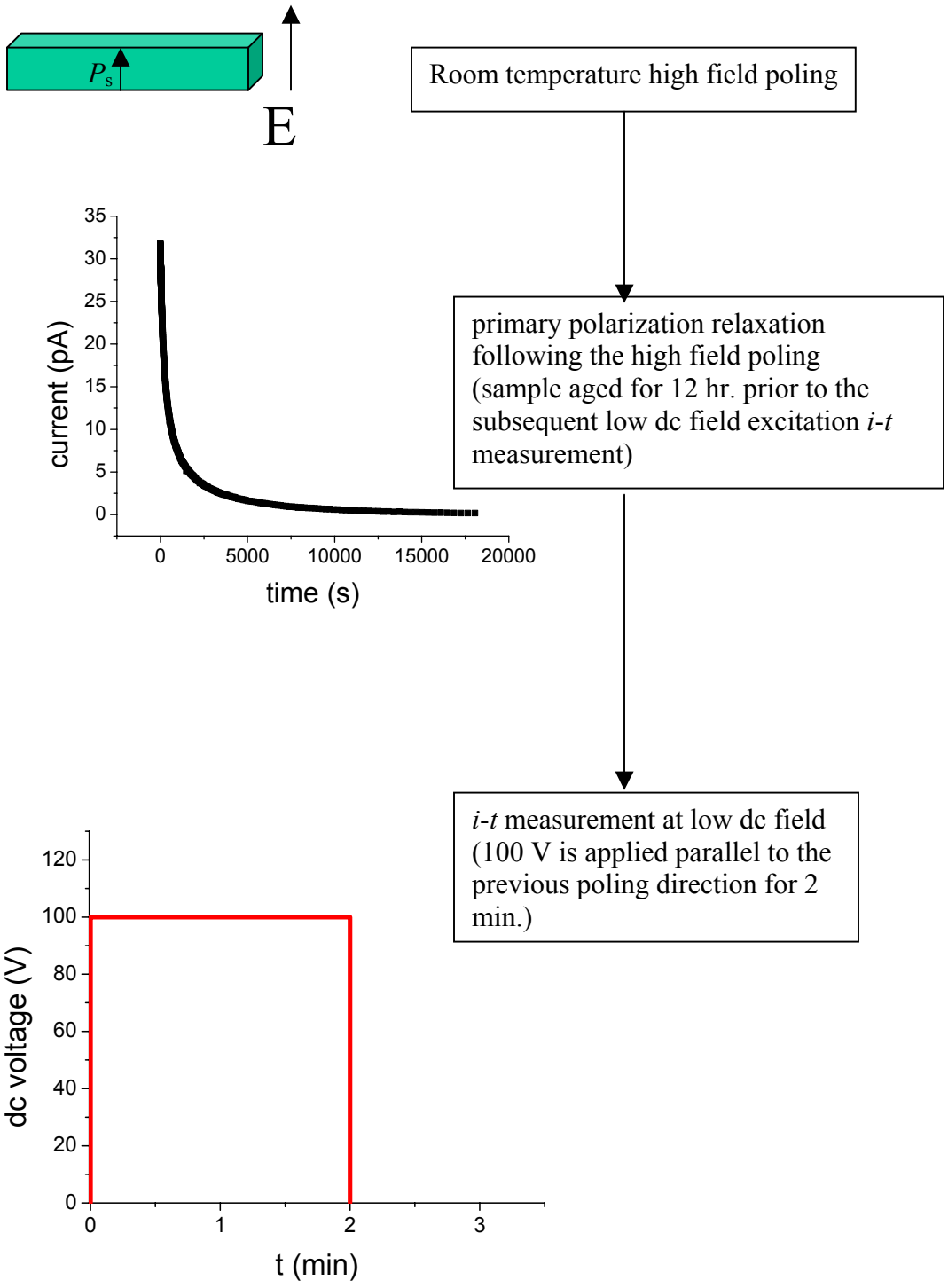

Figure 5.2 Experimental procedure for polarization relaxation measurements in pre-poled PZN-4.5PT single crystals.

To investigate the influence of continuous bipolar cycling on domain dynamics, the relaxation in the time domain was probed for both orientations at different stages in the cycling history, i.e., virgin, 1, 10, 10^2, 10^3, 10^4, and 10^5 cycles. That is, fatigue experiments were interrupted at these numbers of cycles to track the influence of cycling-induced changes on domain dynamics. To maintain as constant as possible a domain state for comparison, crystals were always repoled following bipolar cycling.

It should be mentioned here that the main concern in this study is to probe domain relaxation due to perturbation of the domain structure with a comparatively weak excitation field. Thus, it was important to separate this type of response from the primary relaxation that occurs in crystals following the high field poling process as schematically depicted in Figure 5.3(a). When a field much higher than a coercive field is applied to the crystal, domains are driven to a high energy level (2) from the lower energy level (1). Following high field poling, crystals will experience a primary relaxation (partial depoling) back to a lower energy state. In order to minimize the complication associated with these two different processes, prepoled crystals were given at least 12 hours to stabilize after the primary relaxation process. After reaching a more stable polarization configuration, a weak, constant (~1.6 kV/cm) dc field was applied for about 2 minutes in the poling direction to excite the polarization to a higher energy state as shown in Figure 5.3(b). After 2 minutes, the voltage source was turned off and the current decay due to the domain relaxation was measured by a HP4140B pA meter/dc voltage source. This setup was able to measure the current after about 0.5 second. In this study, current was monitored over four decades in the time domain.

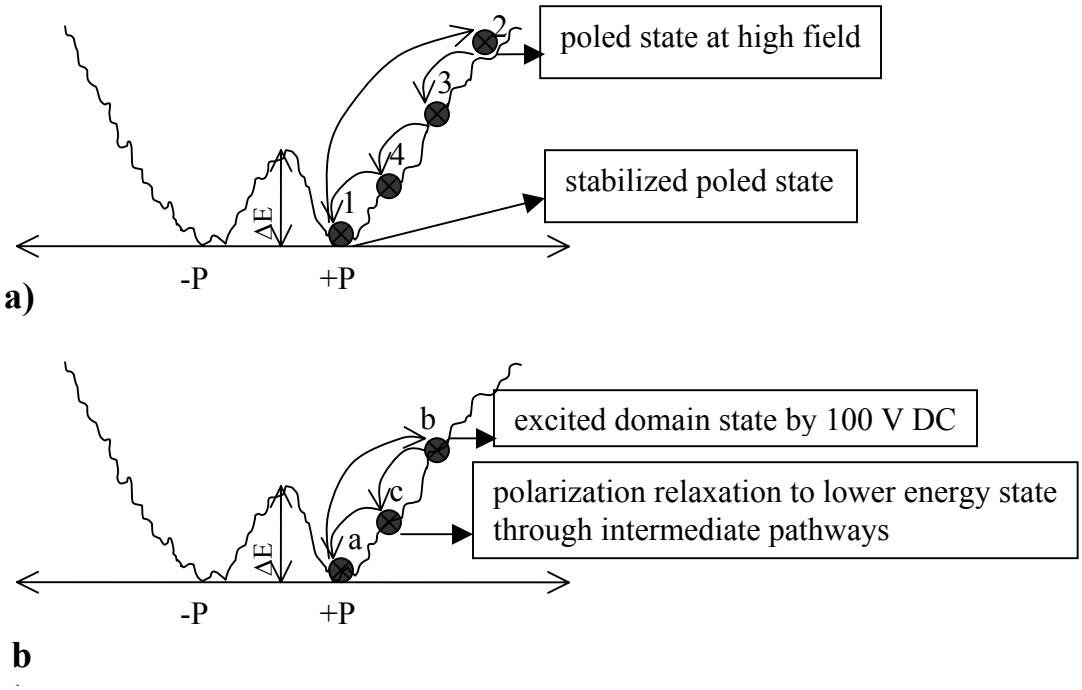

Figure 5.3 A schematic of polarization states during a) high field poling and partial depoling, b) low field excitation and relaxation in ferroelectric crystals.

In this case, the polarization is excited from a lower energy state (a) to a higher energy level (b) by a low dc field. Upon removal of the field, domains relax back to lower the crystal's total free energy through intermediate pathways via domain wall motion as well as mesoscopic and atomic scale rearrangements. These experiments were performed in both orientations to relate the fatigue anisotropy to domain dynamics. The measured currents in the time domain during relaxation reflect the nature of the domains in two distinct orientations.

The measured current vs. time (*i*-*t*) data were converted to polarization vs. time (*P*-*t*). The time dependence of the polarization *P*(t) was fitted to a stretched exponential function to extract the constants which give information about the relative polarization relaxation in both directions as a function of the cycling history (fatigue).

Polarization relaxation experiments are very dependent on the measurement conditions and techniques utilized to probe them. Time dependent processes can be influenced by temperature, the total time over which the properties probed, and the magnitude of the perturbation used to make the measurements. Consequently, the results reported here correspond to the specific measurement conditions described.

5.3 Results and Discussions

A typical time dependence for the measured current (*i*-*t*), along with the converted polarization data *P*(t), measured at room temperature is presented in Figure 5.4. In this case, a 1.6 kV/cm (< 1/2 of E_C) constant dc field acts as the driving force for the polarization excitation. The polarization relaxation (from an excited state) occurs when

the external field is removed as depicted in Figure 5.3(b). The measured polarization decay in the time domain (*P-t*) data was fitted to a well known phenomenological relaxation function, namely the Kohlrausch-Williams-Watts[30,31] (KWW) function

$$P(t) = P_1 - P_2 \cdot \exp[-(t/\tau)^{\beta}], \tag{5.1}$$

where τ is a characteristic relaxation time, and β is the stretched-exponent coefficient ranging from 0 to 1. Recently, this function has been used to analyze different types of relaxation data in the time domain.[14,15,32] It has also been suggested that there is a direct connection between the stretched exponential behavior and the fractal nature of the disordered material.[33] In recent years, dynamical heterogeneity was established as a possible source of stretched exponential relaxation.[21] The components of the relaxation response in most materials are related to the size distribution of relaxing entities (domains).[21] A droplet model was proposed to describe the existence of polarization irregularities (i.e., polar droplets) within the poled state.[34-36] Priya *et al.* have studied the mechanical aging behavior in relaxor-PT crystals close to the morphotropic phase boundary (MPB) and concluded that poled single crystals may not have simple domain states, but rather may have many irregular small polar regions within domains.[37] These domain structures are common in relaxor materials and solid solutions as previously reported.[38,39]

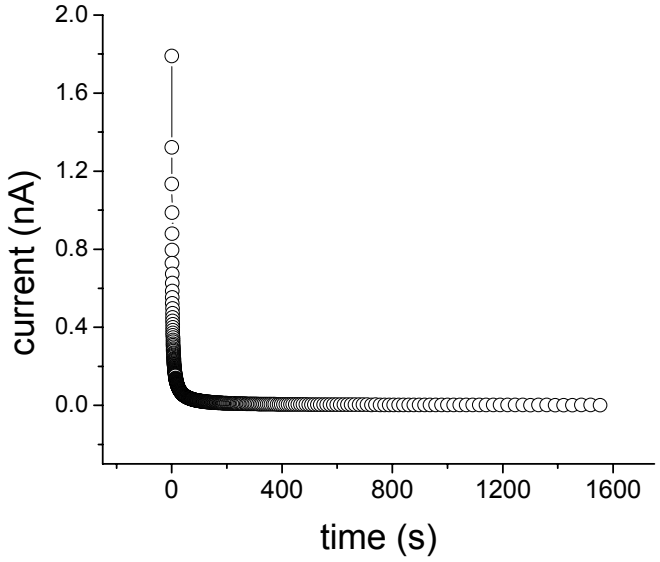

a)

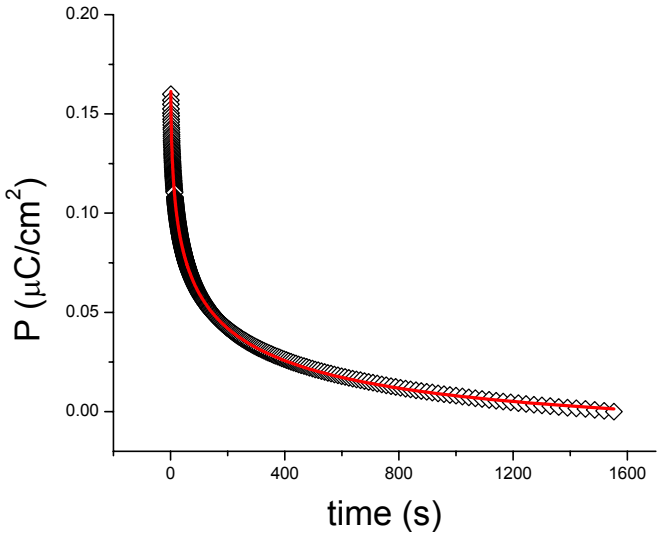

b)

Figure 5.4 Polarization relaxation probed by (a) direct current measurements in the time domain and (b) calculated decrease in polarization.

A typical KWW fit of experimental *P*(t) data for <001> and <111> orientation is shown (the solid line is the fitting, the symbols are the experimental data) in Figure 5.5. For both orientations, the magnitude of the polarization relaxation detected is modest, at most a few tenths of a $\mu C/cm^2$ when the fit is extrapolated back to t = 0 s. Thus, the polarization changes that are being probed in this measurement do, in fact, correspond to small perturbations, rather than to significant re-writing of the domain state. Furthermore, a relatively small difference in the magnitude of the polarization relaxation current was detected in <111> oriented crystals before and after the fatigue process (the amount of relaxing polarization decreases by about a factor of two after 10^5 cycles).

The fitting parameters β and τ were determined from the KWW fits as a function of the number of bipolar switching cycles and plotted in Figure 5.6 for both orientations. As shown in Figure 5.6(a), the stretching exponent (β) values are close for both orientations in virgin crystals, i.e., 0.146±0.002 for <001> and 0.247±0.0004 for <111> after 10 cycles. However, a remarkable increase was recorded in $\beta_{<111>}$ to 0.453±0.104 after 10^5 switching cycles. An average, low $\beta_{<001>}$ value (0.1545±0.0085) was maintained throughout the cycling experiments. Greatly different characteristic time constants (τ) were determined for the <001> and <111> orientations as 0.401±0.048 and 57.46±0.10 s, respectively. There is not much change in the relaxation time constant values during cycling, regardless of fatigue. This may be because only mobile domains contribute to the measured relaxation data in these conditions. These results are consistent with both the fatigue anisotropy observation shown in and the literature relating fatigue to the frozen islands of non-switching regions.[12,40,41]

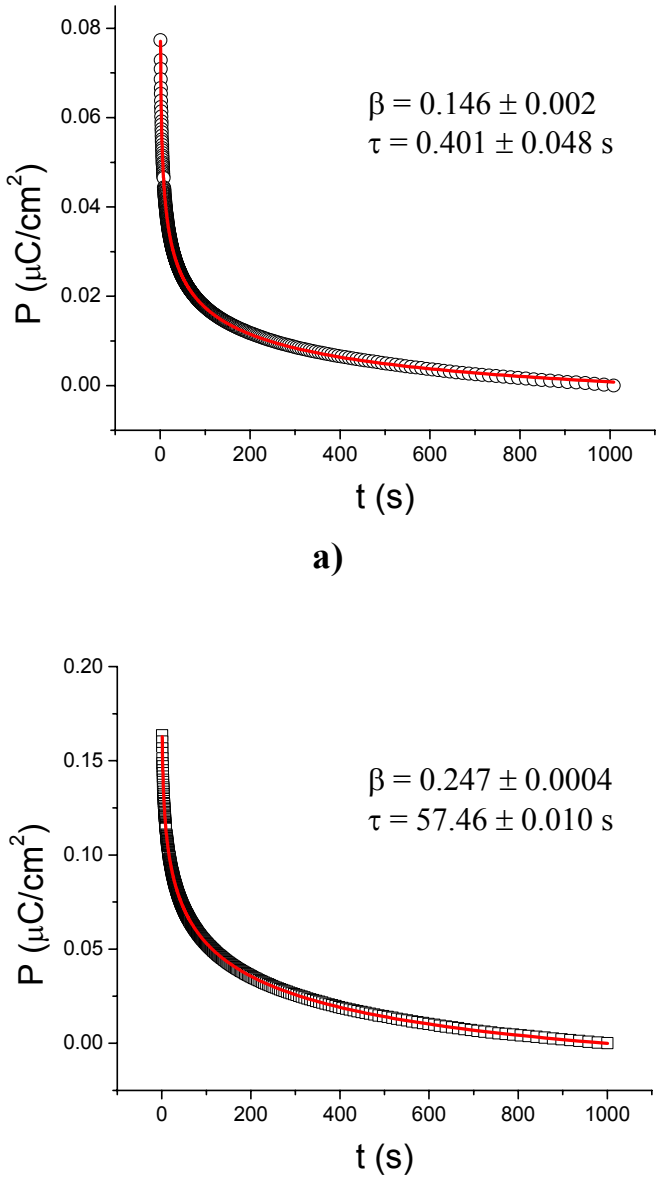

Figure 5.5 Polarization relaxation data fit to the stretched exponential function (KWW) for a) O<001>; b) □<111> orientations.

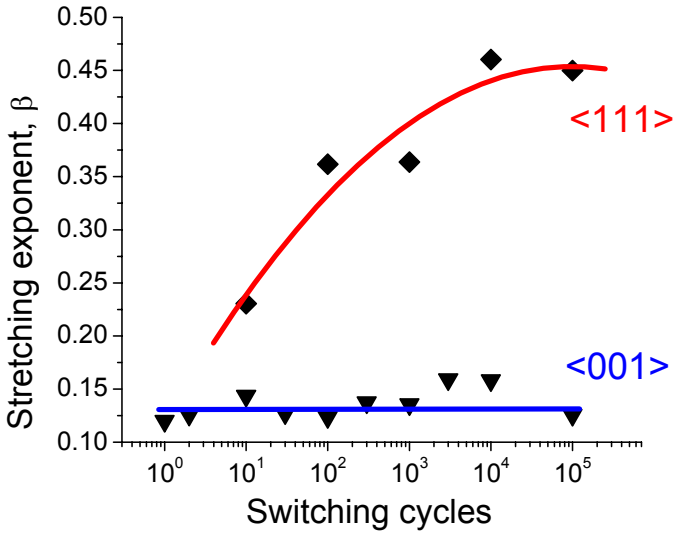

a)

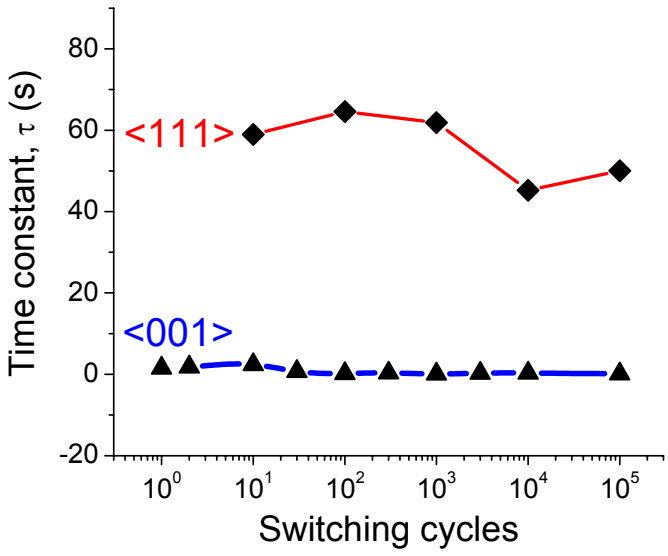

b)

Figure 5.6 Stretched exponential constants with the number of cycles for <001> and <111> orientations: a) stretching exponent, β, b) characteristic time for relaxation,τ.

As fatigue evolves in the <111> oriented crystal, it seems that the slow-moving domain walls are gradually frozen out and that their contribution to the total switching processes diminishes, reducing the total effective volume of switchable ferroelectric crystal. <111> oriented crystals may be more susceptible to fatigue because of the higher τ values. An increase in $\beta_{<111>}$ corresponds to a less stretched relaxation and this is observed in the fatiguing orientation. On the other hand, the low, stable $\beta_{<001>}$ values for <001> crystals are a reflection of a very broad time distribution for switching. These analyses are summarized schematically in Figure 5.7, where $g(\tau)$ is the distribution function for time constants, τ.

Comparable fitting constants were reported in other ferroelectric systems for long-time relaxation experiments.[15,17] Gruverman *et al.*[15] reported a stretching exponent in tetragonal $Pb(Zr_{0.2}Ti_{0.8})O_3$ (PZT) films of 0.24. Kang *et al.*[17] investigated short-time retention loss in PZT films before and after fatigue. The decay of retained polarization $\Delta P(t)$ was analyzed in terms of polarization relaxation with a distribution of relaxation time and found to follow a power law, $\Delta P(t) = \Delta P_\infty + \Delta P_0 [1+(t/t_0)]^{-n}$ where ΔP_∞ and $(\Delta P_\infty + \Delta P_0)$ are the asymptotic values of ΔP at $t = \infty$ and 0, respectively, and t_0 is a characteristic relaxation time. The power law exponent n values were 0.07 and 0.23±0.02 before and after fatigue, respectively. The relaxation parameters obtained in this study seem to be in a reasonable range and an increase with fatigue in stretching exponent is consistent with the study by Kang *et al*.

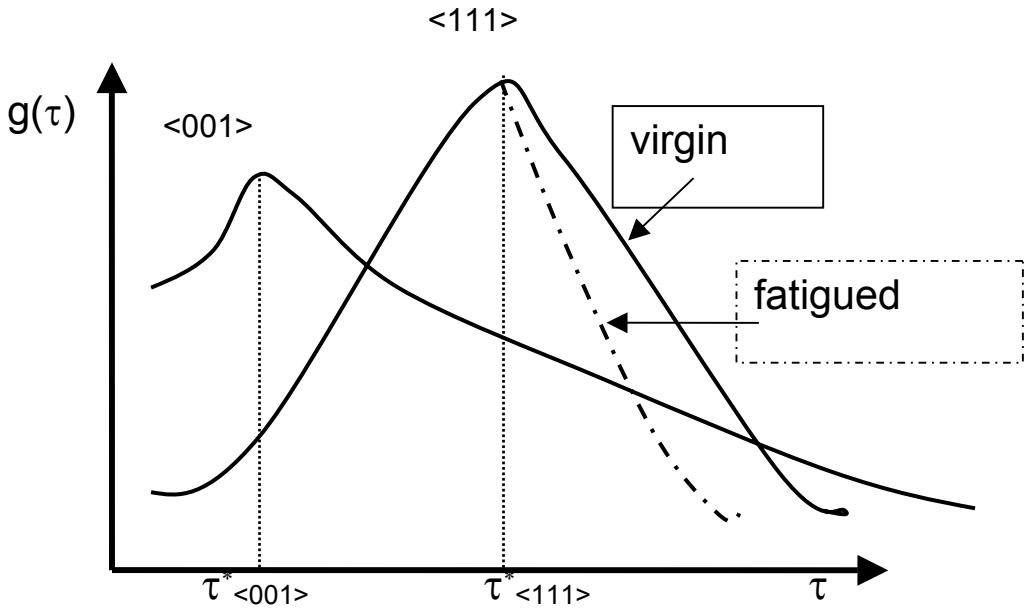

Figure 5.7 A schematic depiction of time constant distribution function for relaxation in <001> and <111> orientations based on fitting data.

It is difficult to make a sensible comparison of τ values with data from the literature, since relaxation processes in ferroelectrics take place over such wide time scales (τ values ranging over more than 10 orders of magnitude in time have been reported) and the field excitation is applied under different conditions. Any set of measurements samples only a portion of the distribution. Furthermore, it is not clear that the relaxation times associated with spontaneous polarization reversal (which are presumably governed by net internal fields) will be identical to those associated with polarization decay after weak excitation, or those associated with characteristic time constants for polarization reversal under applied fields. Consequently, comparisons should only be made for τ values of samples exposed to the same type of excitation.

Although it is difficult to make any comparison of the τ values measured here to those measured elsewhere, an internal comparison of $\tau_{<001>}$ and $\tau_{<111>}$ measured under the same conditions is revealing. It is clear that $\tau_{<001>}$ is appreciably smaller than $\tau_{<111>}$, which is consistent with prior reports of higher domain wall mobilities in <001> PZN-PT crystals.[6,8]

The major difference in relaxation response of crystals with different orientations could be related to the different domain configurations adopted. In poled rhombohedral crystals, the spontaneous polarization is along the <111> direction. Thus, at least one of the polarization vectors is parallel to the poling direction in <111> oriented crystals. This state is sampled during the (initial) switching and poling experiments, as evidenced by the large polarizations observed for <111> crystals. The instability of this domain state is, however, widely discussed, and at lower fields, the sample drops back to a multi-domain

configuration. Thus, it is likely that in the polarization relaxation experiments, excitation of the polarization is from the three canted polarization directions with one component parallel to [111]. Note that the magnitudes of the polarization currents in this case are small (comparable to those of the <001> crystals), suggesting that the polarization relaxation measurement is not probing a switching/depoling process. It is also interesting that there is now experimental evidence that <111> crystals switch through the inclined axes, rather than by 180° switching.[42] This would suggest that as the fatigue process proceeds, the sample has been cycled through states in which domains continually appear and disappear, presumably by nucleation and growth processes.

Pinning of domain walls in this case would be consistent with the observed fatigue and the increase in $\beta_{<111>}$, since the exponent β is characteristic of the domain size and shape distribution in the material.[17]

In contrast, all of the polarization vectors are inclined to the poling direction in <001> crystals. For this orientation, large concentrations of domain walls (many of them charged) are built in during the poling process, and the resulting domain states are known to be stable. The domain structures in <001> and <111> orientations are known to differ. The mechanisms of the polarization reversal process are not known for <001> crystals, but in any event, the large existing concentrations of domain walls (as well as the presence of a mechanism for absorbing and desorbing charges at the charged domain walls) may be related to the increase in fatigue resistance.

5.4 Conclusions

Single crystal PZN-PT exhibits a stretched exponential type relaxation in the time domain at room temperature. Relaxation data fit to a stretched exponential function (KWW) with small β values (<0.25), implying a relatively broad distribution of relaxation times. The crystallographic orientation dependence of the slow relaxation process has been studied as a function of bipolar switching cycles (fatigue). Stretched exponential analysis of the experimental results for <001> and <111> orientations at different levels of cycling demonstrated an orientation dependence of the stretching exponent β and characteristic relaxation time τ. Small values for β and τ were determined for the <001> orientation, and these remained relatively stable throughout the cycling. However, β increased with fatigue for the <111> orientation. The characteristic time constant, τ, is much higher for <111> crystals. Both $\tau_{<111>}$ and $\tau_{<001>}$ are independent of fatigue. These observations would be consistent with a picture in which the slow domains freeze out with fatigue, so that their contribution to the relaxation diminishes, for <111> oriented crystals. The polarization relaxation is much faster in <001> oriented PZN-PT. Constant and relatively small $\beta_{<001>}$ and $\tau_{<001>}$ values imply a broader distribution of relaxation processes in <001> crystals, peaked at a shorter time than for the <111> orientation. Additional work to clarify the relation between the polarization relaxation kinetics and differences in the domain structures is needed to clarify the impact of kinetics on the fatigue process.

5.5 References

[1] J. Kuwata, K. Uchino, and S. Nomura, Ferroelectrics **37**, 579 (1981).

[2] J. Kuwata, K. Uchino, and S. Nomura, Jpn. J. Appl. Phys. **21**, 1298 (1982).

[3] S.-E. Park and T. R. Shrout, J. Appl. Phys. 82, 1804 (1997).

[4] S.-E. Park and T. R. Shrout, Mater. Res. Innovations **1**, 20 (1997).

[5] S.-F. Liu, S.-E. Park, T. R. Shrout, and L. E. Cross, J. Appl. Phys. **85**, 2810 (1999).

[6] H. Yu and C. A. Randall, J. Appl. Phys. **86**, 5733 (1999).

[7] M. Shen and W. Cao, Appl. Phys. Lett. **75**, 3713 (1999).

[8] H. Yu, V. Gopalan, J. Sindel, and C. A. Randall, J. Appl. Phys. **89**, 561 (2001).

[9] V. Bornand, S. Trolier-McKinstry, K. Takemura, and C. A. Randall, J. Appl. Phys. **87**, 3965 (2000).

[10] K. Takemura, M. Ozgul, V. Bornand, S. Trolier-McKinstry, and C. A. Randall, J. Appl. Phys. **88**, 7272 (2000).

[11] M. Ozgul, K. Takemura, S. Trolier-Mckinstry, and C. A. Randall, J. Appl. Phys. **89**, 5100 (2001).

[12] V. Ya. Shur, E. L. Rumyantsev, E. V. Nikolaeva, E. I. Shishkin, and I. S. Baturin, J. Appl. Phys. **90**, 6312 (2001).

[13] J. F. Scott, C. A. Araujo, H. B. Meadows, L. D. McMillan, and A. Shawabkeh, J. Appl. Phys. **66**, 1444 (1989).

[14] T. Mihara, H. Yoshimori, H. Watanabe, and C. A. Araujo, Jpn. J. Appl. Phys. **34**, 2380 (1995).

[15] A. Gruverman, H. Tokumoto, A. S. Prakash, S. Aggarwal, B. Yang, M. Wuttig, R. Ramesh, O. Auciello, and T. Venkatesan, Appl. Phys. Lett. **71**, 3492 (1997).

[16] I. G. Jenkins, T. K. Song, S. Madhukar, A. S. Prakash, S. Aggarwal, and R. Ramesh, Appl. Phys. Lett. **72**, 3300 (1998).

[17] B. S. Kang, J. Yoon, T. W. Noh, T. K. Song, S. Seo, Y. K. Lee, and J. K. Lee, Appl. Phys. Lett. **82**, 248 (2003).

[18] A. T. Fiory, Phys. Rev. B **4**, 614 (1971).

[19] Y. Imry and S. Ma, Phys. Rev. Lett. **35**, 1399 (1975).

[20] V. Westphal, W. Kleemann, and M. Glinchuk, Phys. Rev. Lett. **68**, 847 (1992).

[21] R. V. Chamberlin, Phase Transitions **65**, 169 (1998).

[22] T. Granzow, U. Dorfler, Th. Woike, M. Wohlecke, R. Pankrath, M. Imlau, and W. Kleemann, Phys. Rew. B **63**, 174101 (2001).

[23] Y. Feldman, A. Puzenko, and Y. Ryabov, Chem. Phys. **284**, 139 (2002).

[24] A. Diaz-Sanchez, A. Perez-Garrido, A. Urbina, and J. D. Catala1, Phys. Rev. E **66**, 031403 (2002).

[25] M. Randeria, J. P. Sethna, and R. G. Palmer, Phys. Rev. Lett. **54**, 1321 (1985).

[26] F. Cesi, C. Maes, and F. Martinelli, Commun. Math. Phys. **188**, 135 (1997).

[27] G. Franzese and A. Coniglio, Phys. Rev. E **58**, 2753 (1998).

[28] A. Fierro, A. de Candia, and A. Coniglio, Phys. Rev. E **56**, 4990 (1997).

[29] M. L. Mulvihill, S.-E. Park, G. Risch, Z. Li, K. Uchino, and T. Shrout, Jpn. J. Appl. Phys., Part 1 **35**, 3984 (1996).

[30] R. Kohlrausch, Ann. Phys. Chem. **91**, 179 (1854).

[31] G. Williams and D. C. Watts, Trans. Faraday Soc. **66**, 80 (1970).

[32] A. A. Bokov, M. M. Kumar, Z. Xu, and Z.-G. Ye, Phys. Rev. B **64**, 2241 (2001).

[33] P. Jund, R. Jullien, and I. Campbell, Phys. Rev. E **63**, 036131 (2001).

[34] W. McMillian, Phys. Rev. B **30**, 476 (1980).

[35] A. Bray and M. Morre, J. Phys. C **17**, L463 (1984).

[36] D. Fisher and D. Huse, Phys. Rev. Lett. **56**, 1601 (1986).

[37] S. Priya, J. Ryu, K. Uchino, and D. Viehland, Appl. Phys. Lett. **79**, 2624 (2001).

[38] C. A. Randall, D. J. Barber, and R. W. Whatmore, J. Microsc. **145**, 275 (1987).

[39] A. D. Hilton, C. A. Randall, D. J. Barber, and T. R. Shrout, Ferroelectrics **93**, 379 (1989).

[40] E. L. Colla, S. Hong, D. V. Taylor, A. K. Tagantsev, N. Setter, and K. No, Appl. Phys. Lett. **72**, 2763 (1998).

[41] E. L. Colla, I. Stolichnov, P. E. Bradely, and N. Setter, Appl. Phys. Lett. **82**, 1604 (2003).

[42] J. Yin and W. W. Cao, Appl. Phys. Lett. **79,** 4556 (2001).

Chapter 6

INFLUENCE OF ELECTRIC FIELD CYCLING AND FATIGUE ON DOMAIN STRUCTURE IN RELAXOR LEAD ZINC NIOBATE - LEAD TITANATE (PZN-PT) SINGLE CRYSTALS

As discussed in the first chapter, ferroelectric materials experience polarization fatigue as the polarization direction is continuously reversed by application of an ac field. This is reflected in the polarization– electric field loops as a decrease of switchable (or remanent) polarization and a slight increase in coercive field. Both imply difficulty in the polarization (domain) reversal process. Fatigue is generally agreed to be tied to the changes in domain structures and their response to the switching conditions. The domain structures of $Pb(Zn_{1/3}Nb_{2/3})O_3$–4.5%$PbTiO_3$ (PZN-PT) single crystals have been studied under different conditions by a variety of observation techniques. The goal in this research is to observe the changes in domain configurations of $<111>_C$ and $<001>_C$ - oriented PZN-PT crystals as a function of fatigue history. Transmission mode polarized light microscopy is utilized for domain observations through the crystal thickness. The observations made here will be evaluated in light of the fatigue anisotropy observations discussed in the preceding chapters.

6.1 Introduction to the Role of Domains in the Properties of Pb(Zn1/3Nb2/3)O3-PbTiO3 Single Crystals

PZN-4.5PT crystals exhibit relaxor type ferroelectric behavior with a broad and frequency dependent phase transition near 140 °C as discussed in chapter 1. Relaxor ferroelectrics are known to be comprised of nanometer scale microdomains when cooled through the Curie temperature range under no external electric or mechanical fields.[1] Once an electric field is applied, randomly oriented nanometer size small microdomains transform to micrometer scale macrodomains. Cold-stage TEM studies revealed the existence of microdomains by freezing in of such polar regions. Microdomain to macrodomain phase transitions were also confirmed by the 'in-situ' switching by means of electron beam inducing local stresses and charged regions to align the domains.[2,3] Application of an electric field to a relaxor ferroelectric results in several other developments such as a hysteresis loop, and an increase in the elastic and dielectric compliances and associated loss factors due to the formation of long-range dipole ordering. The macrodomains also exhibit anisotropic behavior such as birefringence which continues after the field is removed until the temperature is raised to the Curie temperature range.[4,5]

Recently gained insights into macroscopic behavior through crystallographic engineering (by applying an electric field toward non-polar $<001>_C$ direction) generated additional interest in the polarization switching behavior of ferroelectric single crystals.[6,7,8] The very high electromechanical coupling coefficient ($k_{33} > 93\%$) and

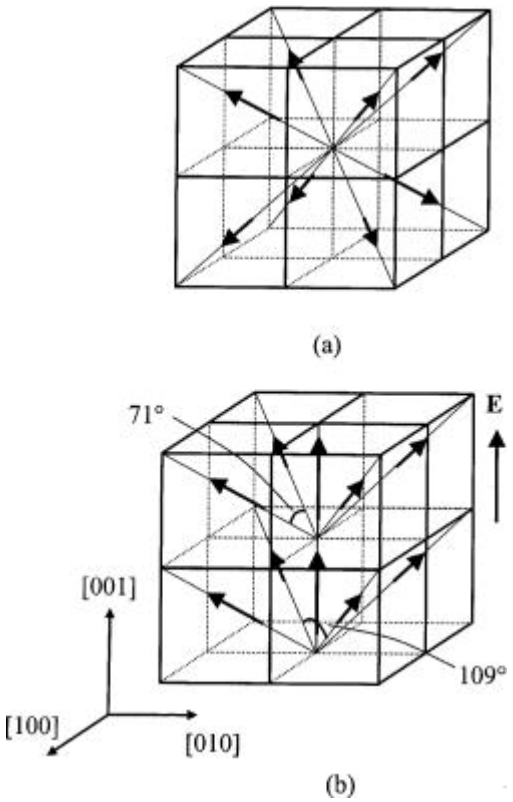

Figure 6.1 Illustration of the assumed domain structure with intersecting charged domain walls for a PZN-4.5PT crystal: (a) Eight possible polarization orientations at zero field (E=0), (b) Four polarization orientations remain after electric field is applied parallel to $[001]_C$ orientation.[12]

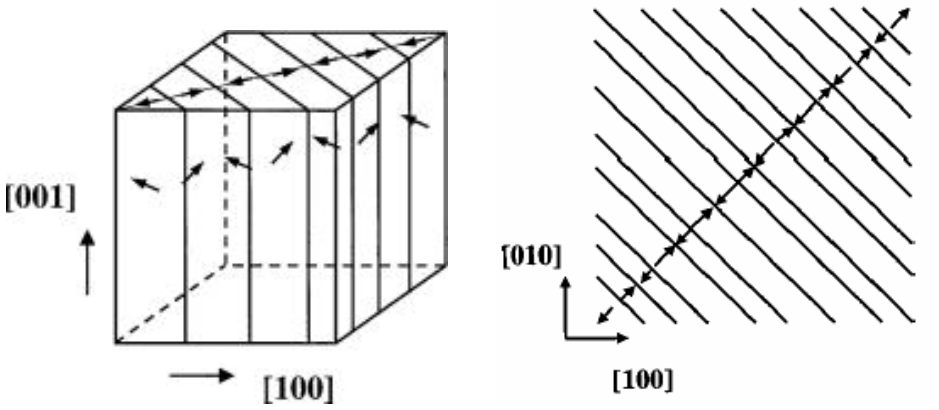

Figure 6.2 An illustration of a twin domain structure commonly observed in $<001>_C$ poled PZN-4.5PT crystals.[12]

piezoelectric coefficient ($d_{33} \geq 2600$ pC/N) reported in PZN-PT crystals are attributed to the engineered domain structures and the switching of polarization. Extensive research has been conducted on the electrical properties of relaxor ferroelectric materials and many theories have been proposed to understand the underlying physics. Yet a full understanding of these complex materials requires the knowledge of domain structures and the changes that occur at varying conditions such as temperature and electric field history. Domain configuration, as in the case of other ferroelectrics, plays an important role in the polarization and strain behavior and in turn their coupling to control electromechanical performance of rhombohedral PZN-PT crystals.

Because the dipoles of the PZN-4.5PT crystals form along the body diagonals of the parent cubic perovskite structure at the paraelectric-ferroelectric phase transition, the crystal structure has rhombohedral symmetry with the point group symmetry 3*m* in the ferroelectric state within each domain variant.[9,10] When an electric field is applied along the $[001]_C$ axis of the cubic coordinates, four of the eight possible polarization orientations remain i.e., $[111]_C$, $[\bar{1}11]_C$, $[1\bar{1}1]_C$, $[\bar{1}\bar{1}1]_C$ as shown in Figure 6.1. Statically such a system would have a macroscopic pseudo-tetragonal symmetry considering the energy degeneracy of these four domain states. Contrary to the earlier studies assuming 4*mm* symmetry,[6,11] Yin and Cao concluded that two-domain type structures are more likely to occur in poled PZN-4.5PT, particularly in samples with non-cubic macro-geometry or slight misorientations in the crystal cutting. A commonly observed domain pattern with a two-domain variant is shown schematically in Figure 6.2.[12] This domain configuration includes charged domain-wall twinning on (110) planes. A charged domain

wall involves a head to head (or tail to tail) polarization, and these walls are typically less mobile and act as sinks for local charge accumulation.[12,13]

It has been proposed that the applied electric field direction affects the domain stability in rhombohedral PZN-PT crystals.[8,14] In comparison with electric field exposure along the $<111>_C$ direction, an electric field applied along the $<001>_C$ direction induces a stable "averaged" domain configuration with little domain motion under dc bias, resulting in hysteresis-minimized strain behavior. Yin and Cao[15] also reported that electric field application along the $<001>_C$ direction could cause the domain boundaries to be in a charged state, resulting in L and T shaped domain walls on observation via optical microscopy.

In PZN-4.5PT crystals, the macroscopic domain structure appears only following an external electric field application inducing the micro- to macro-domain transition. Virgin crystals not exposed to an electric field do not present normal ferroelectric type domains. The configuration of the macroscopic domains will reflect the crystal structure of the ferroelectric phase under the electric field. The characteristics of the domains, observed during and after electric field exposure along the $<001>_C$ direction, are intriguing because the crystal structure under the $<001>_C$ electric field must possess a symmetry lower than rhombohedral, such as c-axis unique monoclinic.[16] The domain configuration constructed (in a monoclinic structure) will also affect the nature of the polarization reversal process and consequently influence the piezoelectric and dielectric properties of PZN-PT crystals.[14]

It is also important to understand the influence of continuous electric field cycling on the domain configuration, particularly in light of the very different polarization fatigue

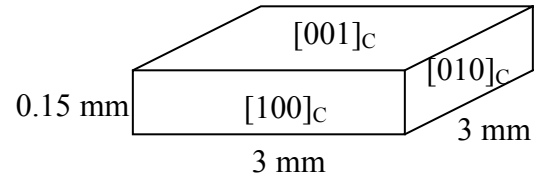

a)

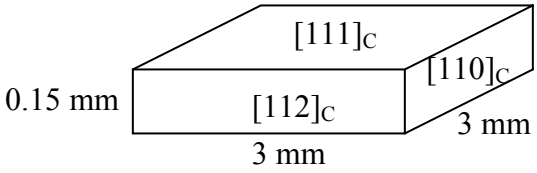

b)

Figure 6.3 Plane orientations in PZN-4.5PT single crystals with (a) $[001]_C$, and (b) $[111]_C$ major surfaces.

behaviors demonstrated by $<111>_C$ and $<001>_C$ rhombohedral PZN-PT single crystals, the latter being "fatigue free".[17] Collective information can be gained from the earlier domain studies in both virgin and poled crystals as a function of composition, temperature, orientation, and electric field exposure. In this research, the focus is to develop an understanding from the observation of changes occurring in the domain configurations as a function of electrical cycling (fatigue) history in both $<111>_C$ and $<001>_C$ orientations. The results will be used to better understand the polarization fatigue anisotropy in rhombohedral PZN-PT crystals.

6.2 Experimental Procedure

Square, plate-shaped $Pb(Zn_{1/3}Nb_{2/3})O_3$-4.5%$PbTiO_3$ single crystals (grown by a high temperature flux technique) were prepared with three pairs of perpendicular surfaces. Crystal orientations were checked by the Laue x-ray technique, as described in Chapter 3. For each composition, samples were prepared with two types of orientations: $[001]_C/[010]_C/[100]_C$ and $[111]_C/[1\bar{1}0]_C/[11\bar{2}]_C$. Samples were thinned to a thickness of about 150 microns to achieve optical transparency by polishing parallel to the major $[001]_C$ or $[111]_C$ surfaces. For submicron polishing, diamond paste is used with a final finishing polish with 0.05 μm colloidal silica gel. Transparent crystals were cleaned using acetone and dried in air. Sample geometries and orientations are sketched in Figure 6.3.

As a first step, prior to thermal annealing, as grown crystals were investigated under the transmission optical microscope with polarizers.[18,19] In the second step, crystals

were annealed at 400 ^{o}C for 5 hours to eliminate processing and sample preparation induced stresses. Polishing media can easily act to impose local stress on a relaxor ferroelectric and induce local alignment to form macrodomain structures.

After this initial microscopy observation, thermally annealed crystals were electroded with silver paste for electric field application. Silver paste electrodes were preferred due to the fact that they can be removed easily by washing with acetone. This will permit the observation to be performed on bare crystals, which give the best light transmission through the thickness. It could also prevent any complication from using sputtered metal electrode which may interfere with the light even if it is very thin. Crystals were poled along their major surfaces using 30 kV/cm at 0.1 Hz at room temperature. The same electrical measurement setup was used as described in chapter 3 for polarization fatigue measurements. Domain configurations were observed in $<001>_C$ and $<111>_C$ poled crystals.

In the next step, crystals with both orientations were cycled in the same way as the earlier fatigue measurements were performed (See chapter 3). In this case, domains were observed in crystals exposed to 10 or 10^5 cycles to compare the influence of fatigue history on domain shape, configuration, size, and density. Domains were investigated on the crystals as they were cycled (i.e. no subsequent poling was performed). Upon removal of the electric field in the cycling experiments, crystals were submerged into acetone to gently wash away the silver electrodes from the surfaces. To investigate whether the observations were affected by any of the cleaning and handling steps, one of the

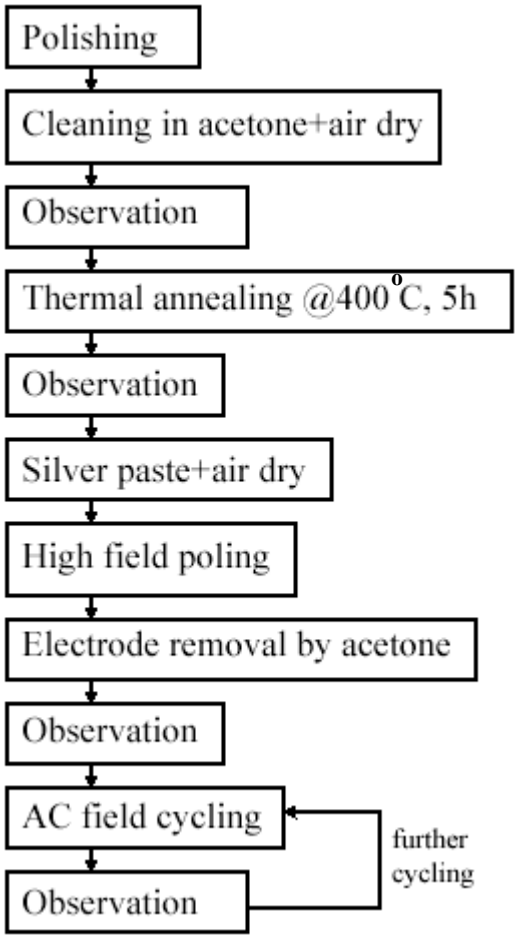

Figure 6.4 Domain observation procedure.

thermally annealed crystals was taken as a reference and observations were made on the same sample after exposing the crystal to intentionally harsh cleaning and handling procedures.

Domain structure comparisons were made for $<001>_C$ and $<111>_C$ oriented as-grown crystals, after high electric field poling, and after 10 cycles and 10^5 cycles. After checking the domains as cycled, the samples were repoled with a unipolar field and remeasured. A domain observation procedure flow chart is given in Figure 6.4, for convenience.

6.3 Results and Discussion

Figure 6.5, and Figure 6.6 show visible domain structures in as-polished $[001]_C$, and $[111]_C$ oriented crystals, respectively. Intersecting domains are seen even at low magnification in $[001]_C$ oriented crystals (Figure 6.5.a). However in $[111]_C$ oriented crystals, only at high magnifications were domain patterns detected in optical observations (

Figure 6.6.c).

After thermal annealing, domains observed in polished crystals disappeared in both orientations. Figure 6.7 shows thermally annealed crystal pictures at different magnifications. This indicates that polishing stresses can induce macrodomain states.

An important point of caution to be made here is that the domain structures in the thin ferroelectric single crystals could be altered due to external mechanical stresses given the ferroelastic nature of the relaxor ferroelectrics. These could originate from

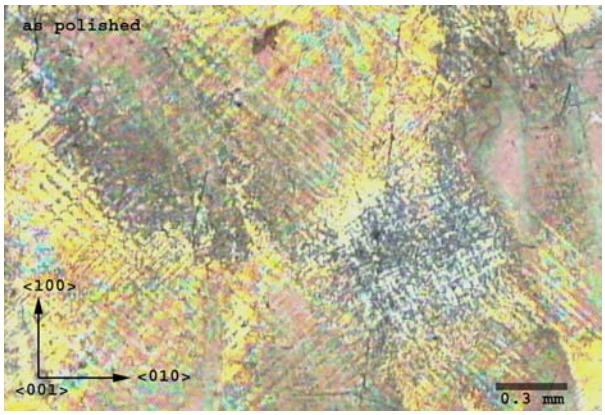

a) 25X

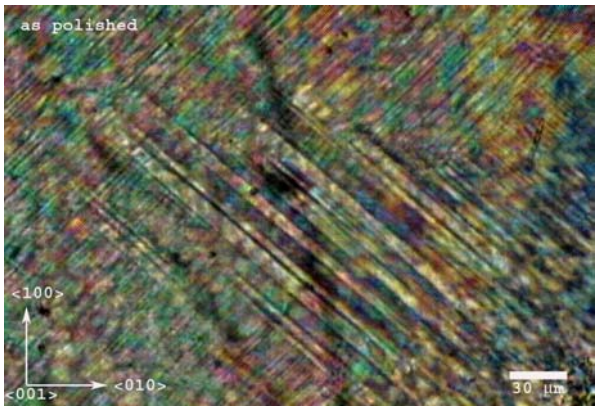

b) 200X

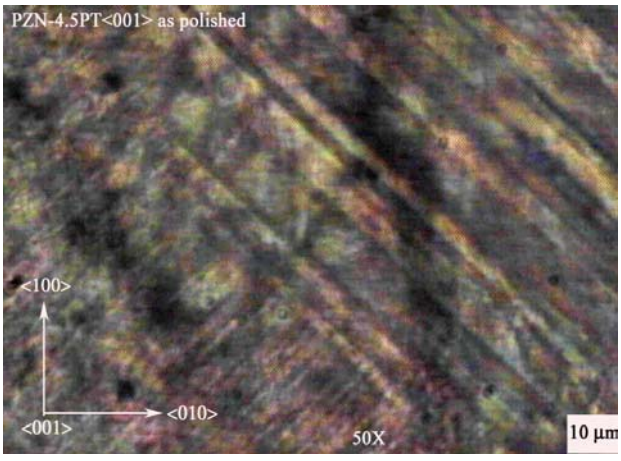

c) 500X

Figure 6.5 Domains in as grown PZN-4.5PT<001> prior to thermal annealing (no electric field exposure), at a variety of magnifications.

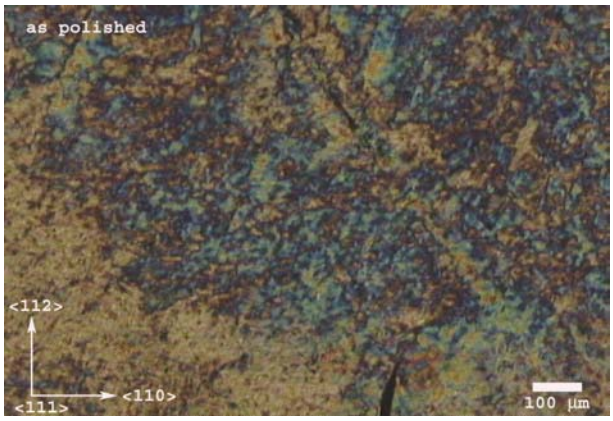

a) 50X

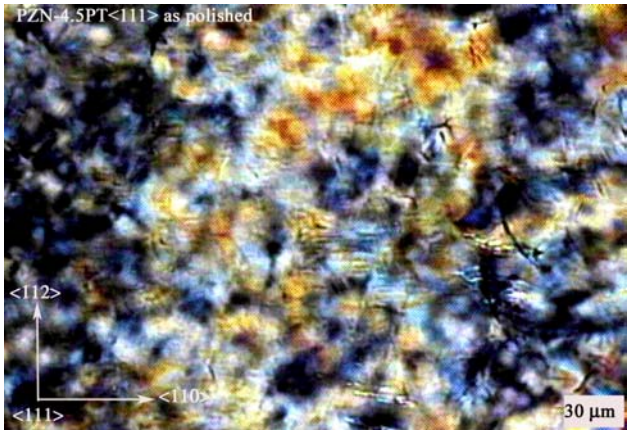

b) 200X

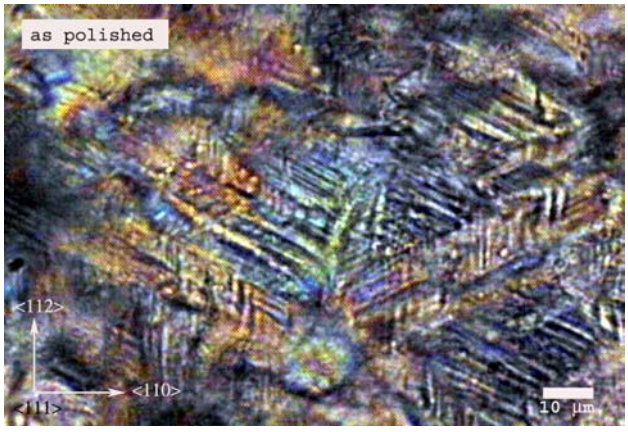

c) 500X

Figure 6.6 Domains in as grown PZN-4.5PT<111> prior to thermal annealing (no electric field exposure).

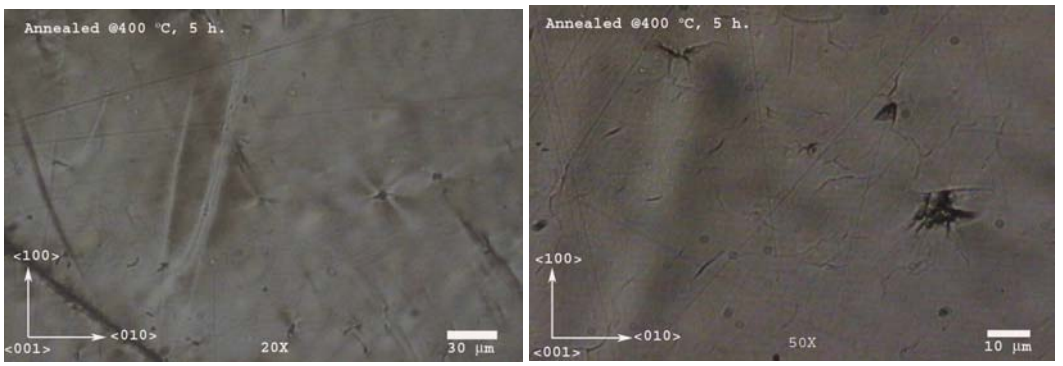

a)

200X 500X

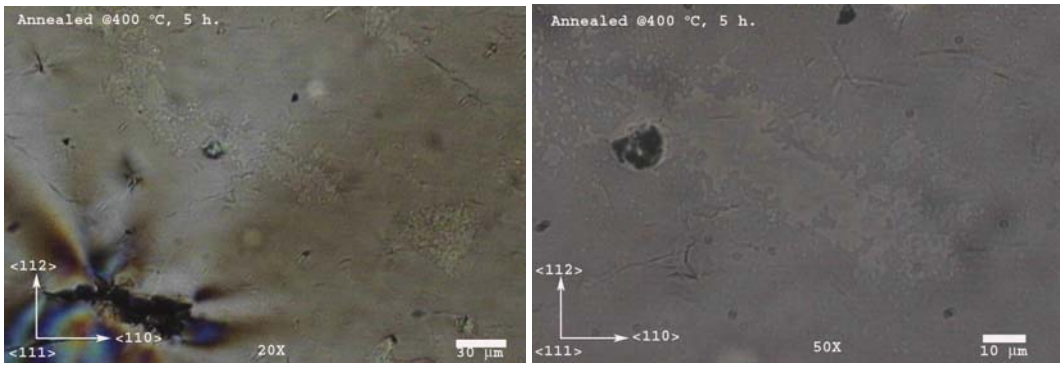

b)

200X 500X

Figure 6.7 Domain patterns disappear with thermal treatment at 400 ^{o}C for 5 hours in PZN-4.5PT single crystals: (a) <001> single crystal, (b) $<111>_C$ single crystal at two different magnifications.

handling, applying and removing the silver paint electrode, cleaning etc. To understand the sensitivity of the samples to these types of pressures, thermally annealed samples were exposed to a certain degree of stressing involved in the processes mentioned above. No indication of any domain pattern or any other change was noted in any of the crystals, implying that such stresses are not contributing to the observed domain patterns in this study, and thereby not contributing artifacts that distort interpretation of the fatiguing crystals.

Single crystals were then poled by applying a unipolar triangular wave electric field at room temperature to field amplitudes of ~30 kV/cm. Figure 6.8 and Figure 6.1 show the domain structures in $[001]_C$ and $[111]_C$ poled crystals, respectively. Electric field exposure is expected to induce micro- to macro-domain transitions in relaxor ferroelectrics. Thermally annealed crystals present no macroscopic domains, consistent with the relaxor behavior; upon poling domains appeared in both crystals poled along $<001>_C$ or $<111>_C$.

As shown in Figure 6.8, upon poling in this $[001]_C$ oriented crystal, only one set of twins out of a possible four dominates. A <110> orientation twin structure is formed by $[111]/[\bar{1}\,\bar{1}\,1]$ vectors of $\boldsymbol{P}_s$ with a 109° angle between them. Large size (~8 μm) and low density domains are homogeneously distributed across the sample surface. Large size domains with $\{110\}_C$ -oriented domain walls were also reported by Yin and Cao in PZN-4.5PT single crystals. Possible orientations of domain walls in rhombohedral PZN-4.5PT crystals are summarized in Table 6.1. The observed large twin domains and coexistence of both charged and uncharged domains, indicated by L- and T-shape domain walls, is considered to invalidate the assumption of the 4*mm* macroscopic tetragonal symmetry.[7,11]

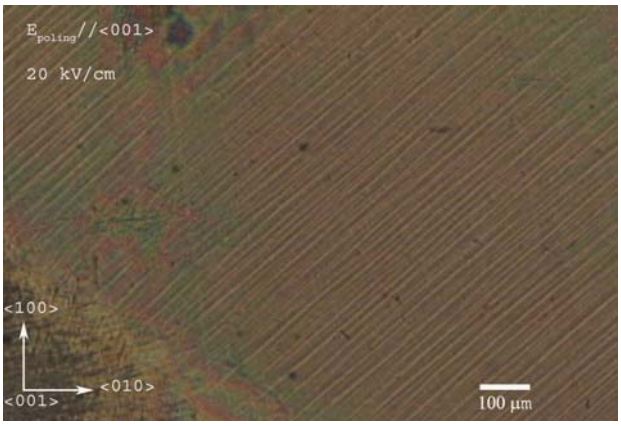

a) 50X

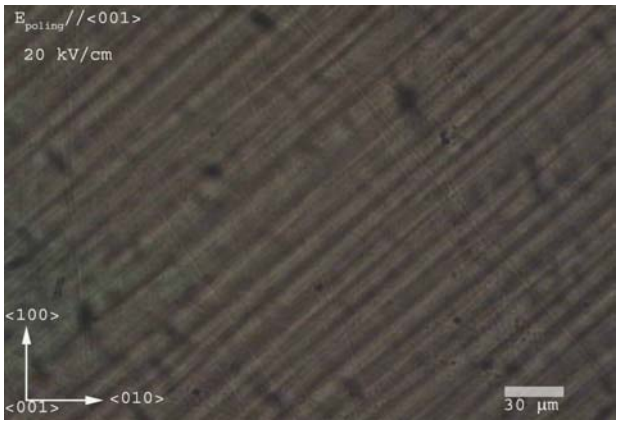

b) 200X

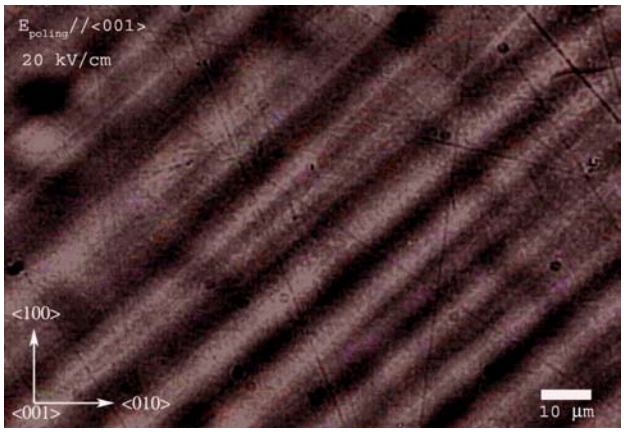

c) 500X

Figure 6.8 Domains in $[001]_C$ poled PZN-4.5PT<001> single crystal. (Domain size is ~8 μm.)

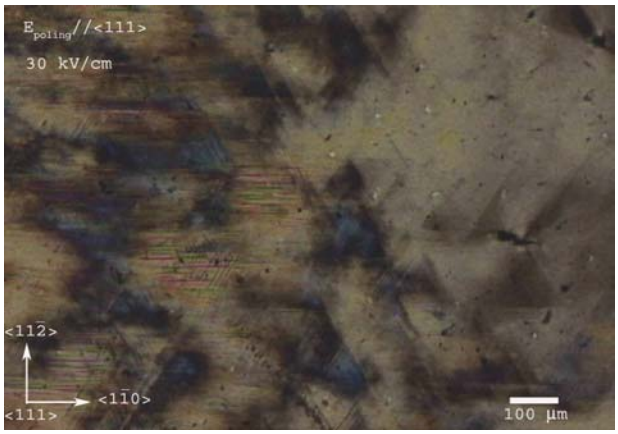

50X

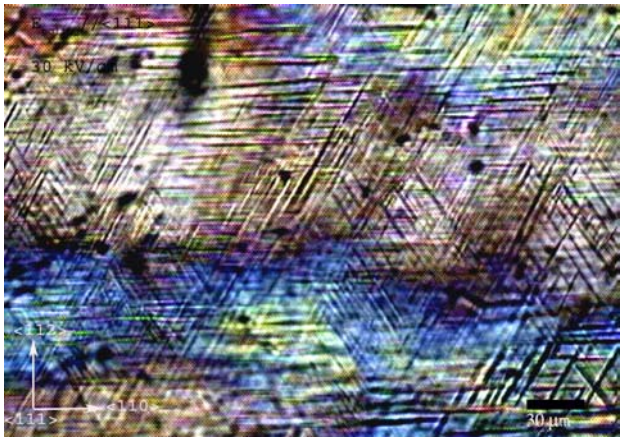

200X

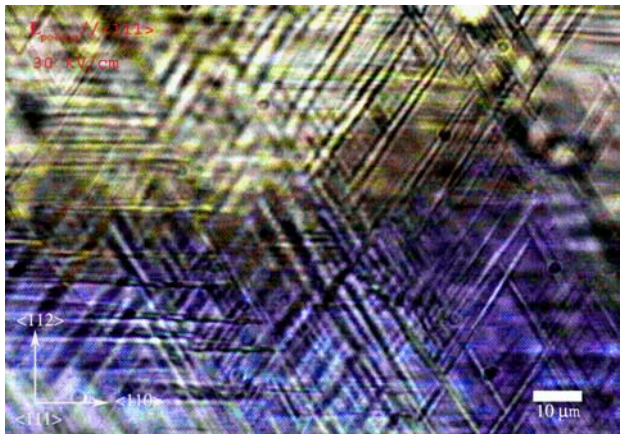

500X

Figure 6.9 Domains in $[111]_C$ poled PZN-4.5PT<111> single crystal. (Domain size is ~2 μm.)

Table 6.1 Possible domain wall orientations in rhombohedral PZN-4.5PT<001> crystal.

P_s / P_s'	Charged	Uncharged
[111]/[$\bar{1}\bar{1}$1]	[110]	[001]
[111]/[1$\bar{1}$1]	[010]	[101]
[111]/[$\bar{1}$11]	[100]	[011]
[1$\bar{1}$1]/[$\bar{1}\bar{1}$1]	[100]	[0$\bar{1}$1]
[$\bar{1}$11]/[1$\bar{1}$1]	[1$\bar{1}$0]	[001]
[$\bar{1}$11]/[$\bar{1}\bar{1}$1]	[010]	[$\bar{1}$01]

On the other hand, rather small size (~2 μm) domains appear in $[111]_C$ poled PZN-4.5PT<111> single crystal as shown in Figure 6.10. The intersection lines of domain walls form a characteristic angle in all samples in this observation. The angles between domain-walls were measured as ~71 or 109 degrees. High density finer domains in $[111]_C$ poled crystal may be due to single domain instability and a partial depolarization upon the removal of electric field.[14]

After these basic observations (that were used to compare the domain study protocol and crystals to earlier studies), the investigations were extended to develop an the understanding of ac cycling on both orientations. As discussed in the first chapter,

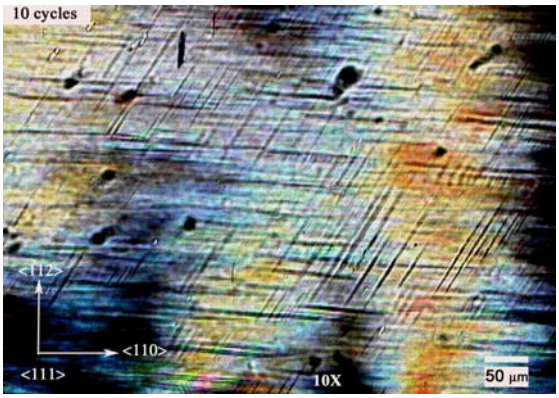

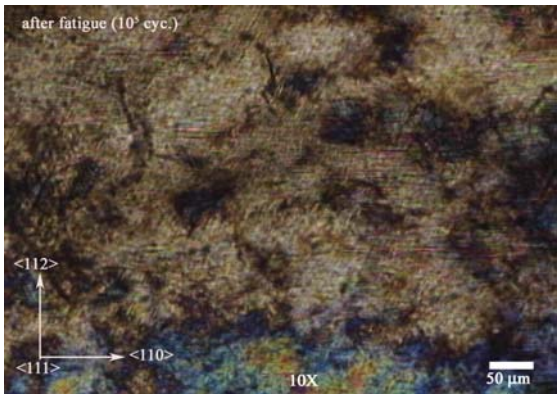

10 cycles (No fatigue) 100X 10^5 cycles (Fatigued)

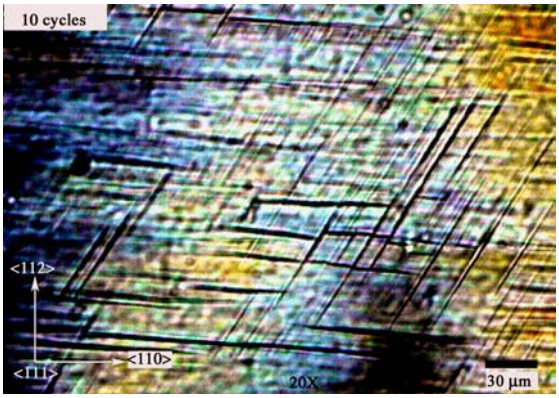

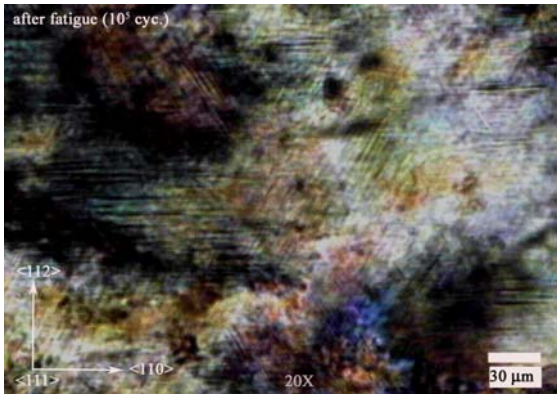

10 cycles (No fatigue) 200X 10^5 cycles (Fatigued)

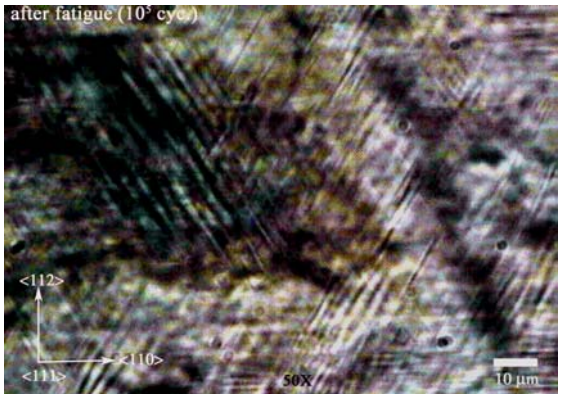

10 cycles (No fatigue) 500X 10^5 cycles (Fatigued)

Figure 6.10 Domain structures in PZN-4.5PT<111> single crystals after10 cycles (left-hand side pictures) and 10^5 cycles (right side pictures) at different magnifications.

polarization switching occurs in relaxor type ferroelectric single crystals through several steps with island region formations.[5]

Figure 6.10 shows domain structures in a PZN-4.5PT<111> single crystal after 10 and 10^5 cycles. As presented in chapter 3, continuous ac cycling systematically reduces the amount of switchable polarization when the cycling field is applied along a non-$<001>_C$ orientation. When compared to the domains after few cycles (no fatigue), crystals cycled 10^5 times exhibit a slight refinement in domain structure coupled with an increase in the density.

Domain structures of PZN-4.5PT$<001>_C$ crystals are seen in Figure 6.11 after 10 and 10^5 cycles. In this orientation, ac cycling does not induce polarization loss after 10^5 cycles. It can be concluded from these results that cycling applied along the $<001>_C$ orientations induces a coarsening of macro-domains, minimizing the surface energy associated with domain-walls. In particular, a reduction in the charged domain-wall density is anticipated. It should be noted that a uniform, finer texture exists within the larger domains and does not change throughout the cycling. Another point which has to be made here is that uncycled $[001]_C$ -poled crystals present a uniform domain configuration across the sample surface (Figure 6.8). This changes once the crystal is cycled as seen in Figure 6.11. On cycling, different regions of the crystal take on different domain orientations. These regions are about several hundred microns in lateral extent. On the same surface, domain orientation changes giving rise to island formation. Domains in different orientations from region to region enable the estimation of the size of the islands.

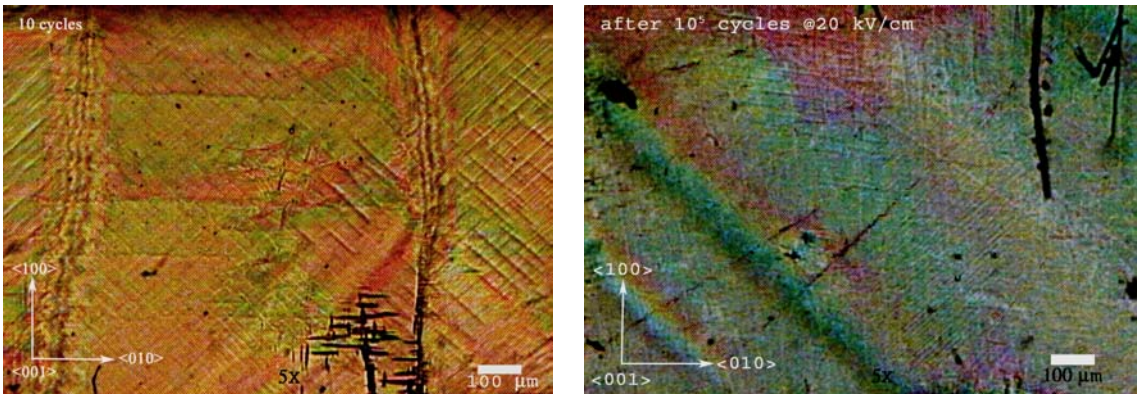

10 cycles 50X 10^5 cycles

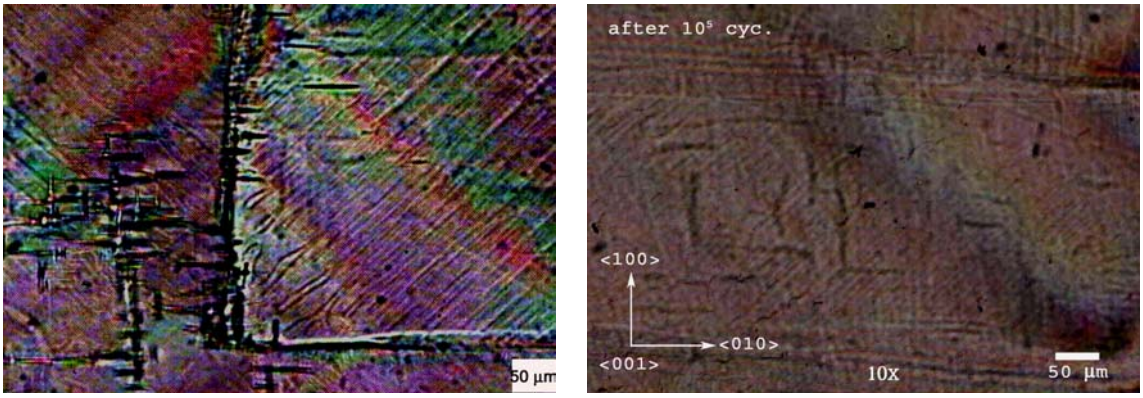

10 cycles 100X 10^5 cycles

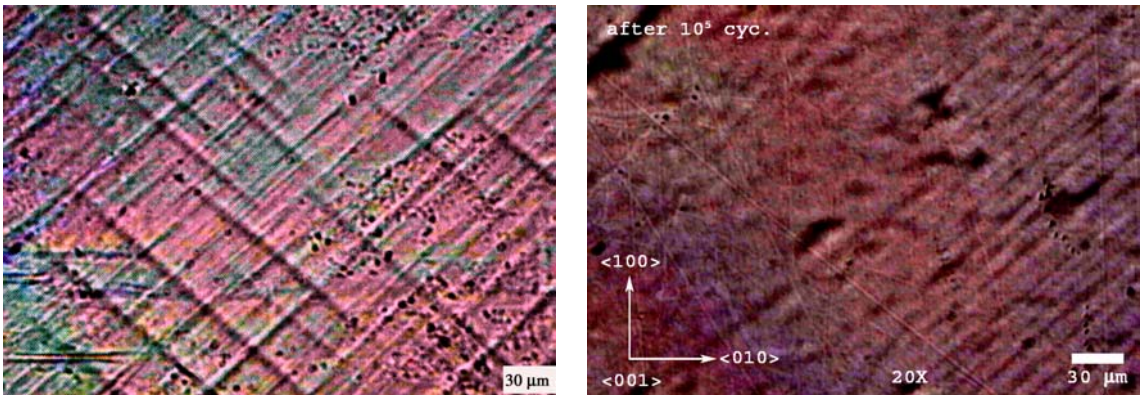

10 cycles 200X 10^5 cycles

Figure 6.11 Domain structures in PZN-4.5PT<001> single crystals after10 cycles (left-hand side pictures) and 10^5 cycles (right-hand side pictures) at different magnifications.

It is critical to mention that after cycling, poling again leads to a microstructure favoring one set of domain variants again. When $<001>_C$ oriented PZN-4.5PT single crystals are poled after a few ac cycles, the number of visible domain-walls is reduced.

This can be seen in Figure 6.12 which shows the poling effect in $<001>_C$ exposed to 10 and 10^5 ac cycles. For the $<111>_C$ crystal no remarkable domain modification is induced by poling either in virgin (10 cycles) and fatigued (10^5 cycles) crystals as shown in Figure 6.13.

6.4 Conclusions

Thermally annealed crystals of both $<111>_C$ and $<001>_C$ orientation do not present any macroscopic domain pattern visible in optical microscopy. Application of an electric field induced ferroelectric domains in both orientations. Classical 109° and 71° domains are observed in PZN-4.5PT rhombohedral crystals on either poling or electric field cycling along the $<111>_C$ orientations.

Continued cycling to 10^5 cycles induces a high density of domains in crystals which exhibit polarization fatigue. This can be readily understood in terms of a classical nucleation model. The $<111>_C$ -oriented crystal which undergoes fatigue eventually develops domain-walls that can no longer respond to the external field. These domains are frozen in. To continue the switching process, nucleation of new domains is necessary, eventually these are also lost to the fatigue process. The net result is that the crystal continues to increase its domain density, but the domains may not all contribute to the switching process. A similar result was obtained through polarization relaxation

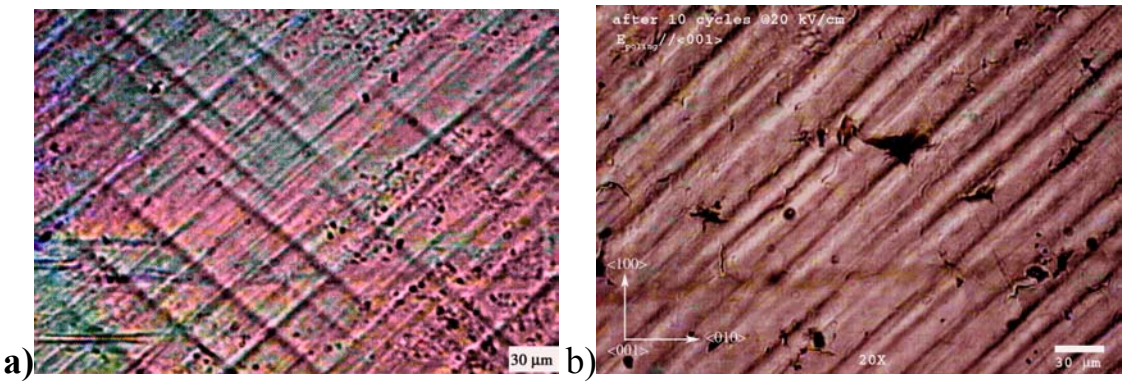

10 cycles (No poling) 200X 10 cycles + poling

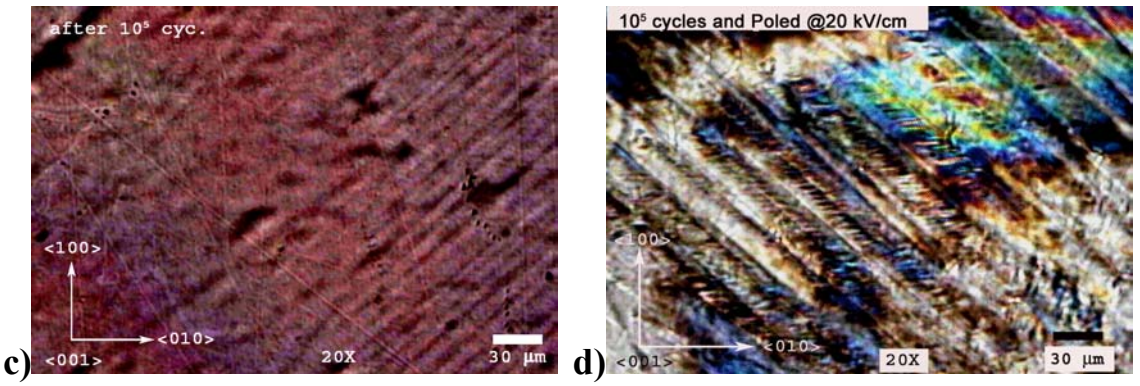

10^5 cycles (No poling) 200X 10^5 cycles + poling

Figure 6.12 Influence of poling on domain configurations in PZN-4.5PT<001> single crystal after a) 10 cycles, b) 10 cycles and poling, c) 10^5 cycles, d) 10^5 cycles and poling. (Pictures at different magnifications)

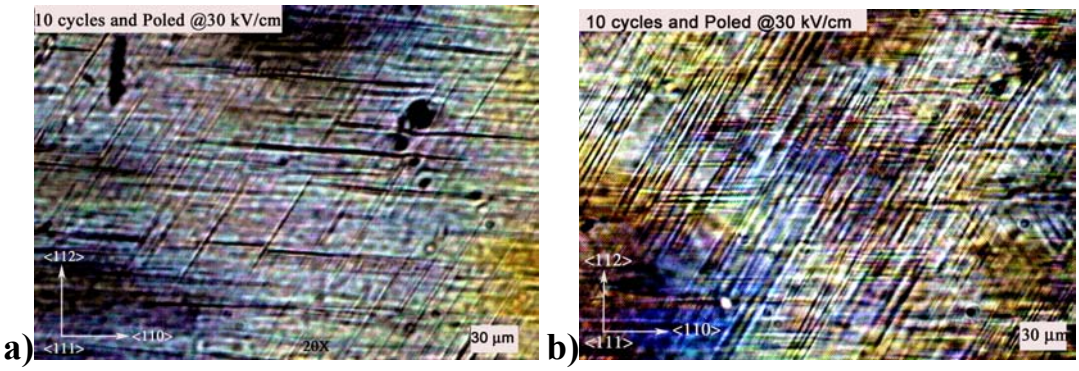

10 cycles (No poling) 200X 10 cycles + poling

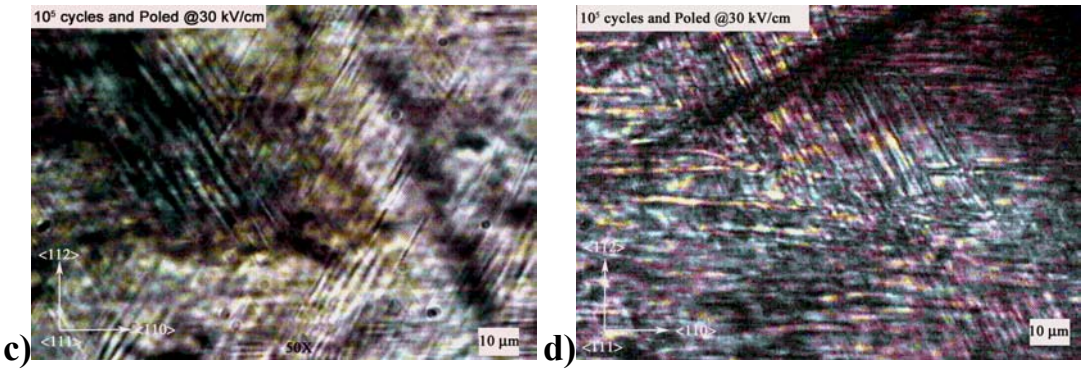

10^5 cycles (No poling) 500X 10^5 cycles + poling

Figure 6.13 Influence of poling in PZN-4.5PT<111> single crystal after a) 10 cycles, b) 10 cycles and poling, c) 10^5 cycles (fatigued), d) 10^5 cycles (fatigued) and poling.

experiments when weak field perturbation is probed in crystals before and after fatigue. As discussed in chapter 5, fatigued crystals demonstrated a less stretched relaxation behavior for weak field perturbation. As the crystal experiences fatigue and growth of frozen in domains, eventually the probability of nucleation may become the rate-limiting process and limit total polarization switching. This then requires higher fields to induce nucleation and move less mobile domain-walls. All of these in the $<111>_C$ crystal is consistent with the above model and observations.

The $<001>_C$ -oriented crystals in the unpoled state appear macroscopically isotropic, consistent with the relaxor behavior. Then an application of an ac or direct field induces domains. The observed domain pattern may imply that there are charged domain-walls and furthermore domain regions on poling may not possess 4*mm* symmetry, as only a few domain variants are observed. On bipolar cycling, 4 variants are observed with the appearance of both T and L-shaped domains. Contained within these domains is a smaller domain contrast. From the earlier studies with transmission electron microscopy, nanometer lamellar domains are found in relaxor ferroelectric $Pb(Sc_{1/2}Ta_{1/2})O_3$.[20] In essence there is a broad scale of domain size in the $<001>_C$. Such complex domain structures may coarsen and the islands may also coarsen. However the finer domains that are observed in the optical microscopy seem to show no major change. The interfaces at islands and T- and L-shaped domain configurations may be problematic for charge trapping, on cycling these eventually seem to disappear and decrease in density. At this time, the nature of the switching process in $<001>_C$ is not clear. Earlier work from Yu and Randall shows fractal clustering under pulsed fields.[21] It may be that classical

nucleation and growth that controls the switching process in $<111>_C$ is not present in $<001>_C$ directions. This may be the origin of the fatigue-free nature in $<001>_C$.

6.5 References

[1] G. A. Smolenski and A. I. Agranovskya, Sov. Phys. Sol. -State. **1**, 1429 (1959).
[2] C. A. Randall, D. J. Barber, R. W. Whatmore, and P. Groves, Ferroelectrics **76**, 277 (1987).
[3] C. A. Randall, D. J. Barber, and R. W. Whatmore, J. Micro. **145**, 235 (1987).
[4] L. E. Cross, Ferroelectrics **76**, 241 (1987).
[5] M. L. Mulvihill, "In-situ Observation of the Domin Behaviors in Normal and Relaxor Ferroelectric Single Crystals Under Applied Electric Field and Temperature," Ph.D. Thesis, Pennsylvania State University, 1996.
[6] S.-E. Park and T. R. Shrout, J. Appl. Phys. **82**, 1804 (1997).
[7] S.-E. Park and T. R. Shrout, IEEE Trans. Ultrason. Ferroelectr. Freq. Contro**l 44**, 1140 (1997).
[8] S. Wada, S.-E. Park, L. E. Cross and T. R. Shrout, Ferroelectrics **221**, 147 (1999).
[9] S. Nomura, T. Takahashi, and Y. Yokomizo, J. Phy. Soc. Jpn. **27**, 262 (1969).
[10] J. Kuwata, K. Uchino, and S. Nomura, Jpn. J. Appl. Phys. **21**, 1298 (1982).
[11] J. Yin, B. Jiang, and W. Cao, IEEE Trans. Ultrason. Ferroelectr. Freq. Contro**l 47**, 285 (2000).
[12] J. Yin and W. Cao, J. Appl. Phys. **92**, 444 (2002).
[13] M. E. Lines and A. M. Glass, Principles and Applications of Ferroelectrics and Related Materials, Clarendon Press, Oxford 1977.
[14] J.-K. Lee, J. Y. Yi, K.-S. Hong, S.-E. Park, and J. Millan, J. Appl. Phys. **91**, 4474 (2002).
[15] J. Yin and W. Cao, J. Appl. Phys. **87**, 7438 (2000).
[16] S.-E. Park, S. Wada, L. E. Cross, and T. R. Shrout, J. Appl. Phys. **86**, 2746 (1999).
[17] M. Ozgul, K. Takemura, S. Trolier-McKinstry, and C. A. Randall, J. Appl. Phys. **89**, 5100 (2001).
[18] E. Wahlstrom, Optical Crystalloghraphy, 5th ed.,Wiley, New York 1979.
[19] H. Schmid, Polarized Light Microscopy (PLM) of Ferroelectric and Ferroelastic Domains in Transmitted and Reflected Light., Ferroelectric Ceramics, edited by N. Setter and E. L. Colla, Birkhauser Verlag, Basel 1993. p.107-126.
[20] C. A. Randall and A. Bhalla, Jpn. J. Appl. Phys. **29**, 327 (1990).
[21] H. Yu, V. Gopalan, J. Sindel, and C. A. Randall, J. Appl. Phys. **89**, 561 (2001).

Chapter 7

MAJOR CONCLUSIONS AND FUTURE WORK

Polarization fatigue anisotropy was discovered and then studied in detail in this research. Experimental work and following analyses were performed to characterize this anisotropic fatigue behavior in an attempt to encapsulate the underlying conditions in single crystal materials. Polarization fatigue behaviors of several ferroelectric materials were also studied to contrast and improve the understanding of structure-property relationships in terms of polarization switching processes and possible origins of the mechanisms.

7.1 Conclusions

Fatigue anisotropy was first discovered in PZN-4.5PT rhombohedral single crystals at room temperature. It was observed that relatively fast fatigue was characteristic of $[111]_C$ rhombohedral crystals. One of the attractive aspects of single crystals is that fatigue could be studied not only at a variety of temperatures, compositions, ferroelectric phases, applied field conditions, but also combination of these parameters with crystallographic orientation (which will eventually impact domain configurations). Only negligible cycling-induced changes were noted, after 10^5 cycles in $[001]_C$ crystals. This strong anisotropy was tested for stability at various conditions (i.e,

temperature, composition, electric field strength). All the results confirmed that PZN-PT crystals demonstrate a strong fatigue resistance when switched with an angle to the $[111]_C$ spontaneous polarization orientation, i.e., $[001]_C$, $[110]_C$, in the rhombohedral phase region. Fatigue reappears if a different phase (i.e., tetragonal, orthorhombic) is induced through variations in compositions, temperature, or electric field strength. Fatigue was observed in both orientations in tetragonal compositions. Two possibilities involve possible microcracking during cycling, or that the relaxor nature of the crystal may be an important factor for fatigue resistance along $[001]_C$ in rhombohedral compositions. Fatigue experiments in several other ferroelectrics including normal and relaxor types support the scenario of a relaxor contribution to fatigue anisotropy.

Polarization reversal dynamics was studied in terms of field and frequency dependence as a function of fatigue history in both orientations. Another approach was to probe polarization relaxation in time upon the removal of a dc excitation much lower than the coercive field of $[001]_C$- and $[111]_C$-oriented PZN-4.5PT single crystals. Both experiments revealed a very distinct behavior for different orientations of the single crystals of the same composition. $[001]_C$-oriented crystals exhibit minimized field and frequency dependence and a broad distribution of time constants. Relaxation processes were modeled with a stretched exponential function to determine relative time constants and distribution. On the other hand, $[111]_C$-oriented crystals show strong field and frequency dependence and a narrower distribution of time constants for switching. Both results are consistent with fatigue behavior of the crystals. Microscopic observations were also in support of these observations. PZN-PT crystals possess a domain structure with a wide range of finer domains within coarse domains. It is possible that the high domain

density in $[001]_C$ orientations provides a large number of nuclei for the switching process, making it very difficult to pin all of the active sites. Thus, even if some nuclei become inactive, the material can still be efficiently switched.

It seems that a combination of underlying relaxor structure and engineered domain switching may provide the optimum solution for improved fatigue in ferroelectrics leading to better reliability in applications.

7.2 Future Work

Future studies on fatigue anisotropy should involve the investigation of two possible hypotheses as summarized in Figure 7.1. Optical microscopy revealed an increased domain wall density in fatigued crystals. This could be due to continuous nucleation as some regions freeze and do not contribute switching. Newly formed domains will also be pinned requiring further nuclei and domain formation. The continuity of such processes would produce more fractal and higher density domain walls. Especially understanding of high fatigue resistance along orientations with an angle to the spontaneous polarization would be useful to reveal the origin of fatigue anisotropy in relaxor ferroelectrics. One possibility for high fatigue resistance in these orientations is the existence of the charged domain walls which may act as sink and absorb injected charges during high electric field cycling thereby inhibiting pinning of domain walls. Charge injection behavior in a particular orientation can be studied by applying a variety of metal electrodes with different work functions giving rise to

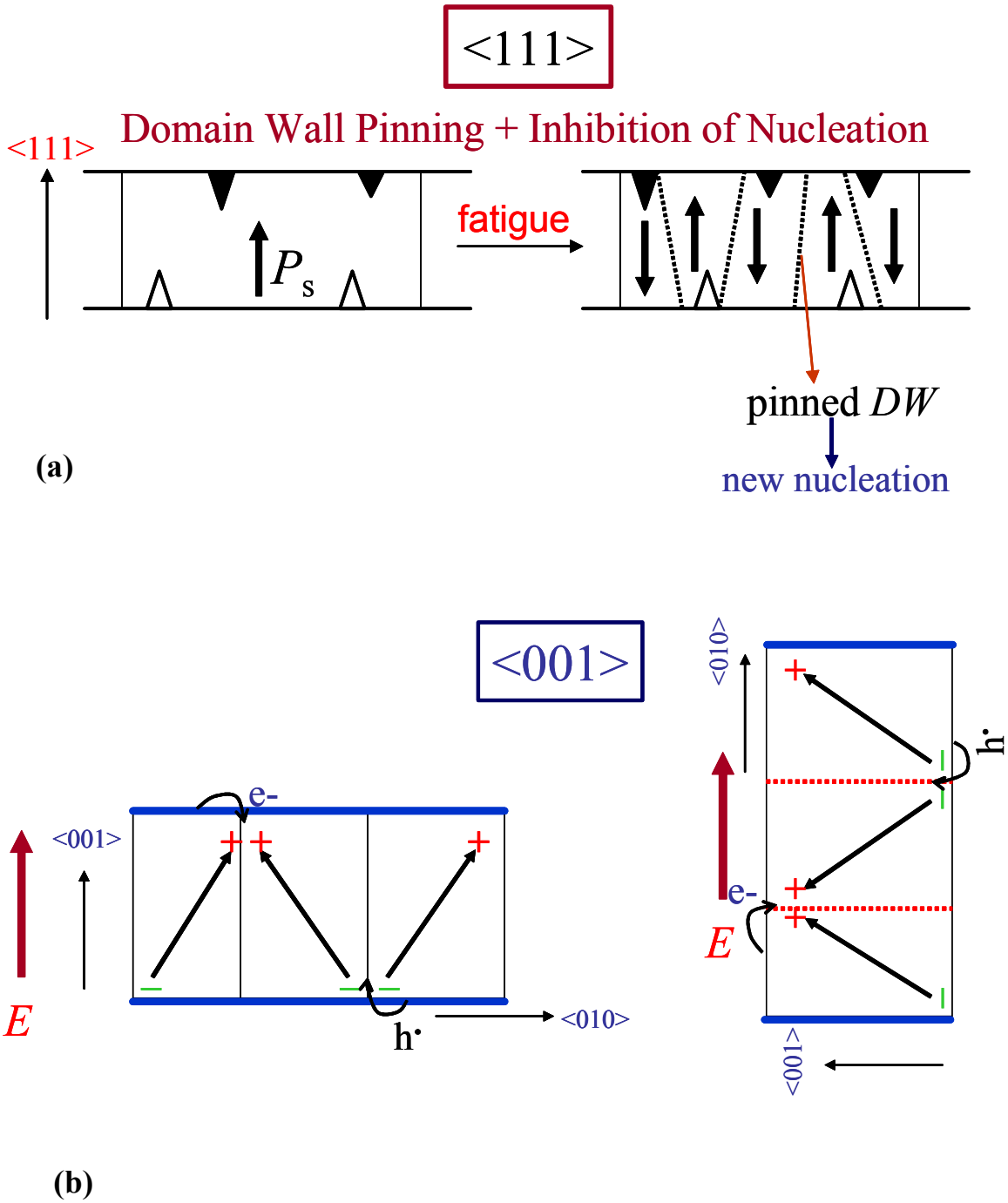

Figure 7.1 Two possible hypotheses for fatigue anisotropy in relaxor ferroelectric single crystals along a) $<111>_C$ and b) $<001>_C$ orientations.

different energy barriers for injection. Thermally stimulated current studies can also be useful to study charge injection with observation of charge release.

Another important factor is the relaxor characteristics providing a broad distribution of time constants for switching. A more systematic study of fatigue as a function of relaxor nature can be useful to clarify the criticality of underlying relaxor structure. Both frequency and time domain polarization relaxation and optical microscopy observations in this study suggested that broader and shorter time constants may govern fatigue behavior along $<001>_C$ orientations. It would be interesting to investigate the microdomains as a function of orientation by TEM.

Fatigue $<111>_C$ orientations involve an asymmetry evolution which is local as indicated by region-to-region changes in bipolar switching strain. This is consistent with the report of region to region freezing of polarization in fatigued thin films.[1] By using atomic force microscopy techniques (AFM) the nature (surface or bulk effect) and the scale of these frozen islands can be revealed. Thermal annealing at temperatures above the Curie range recovered both the asymmetry and polarization but the coercive fields remained large. This may indicate that the defects causing fatigue can be ionic. This is not clear at this moment but by using both thicker and thinner films recovery of E_c can be better understood. Also the role of thermal treatments of crystals need to be studied by thermally annealing the fatigued crystals at different temperatures both below and above T_c. Especially the effect of thermal annealing at temperatures lower than Curie temperatures in ferroelectrics should be understood.

In this study fatigue anisotropy was verified only in rhombohedral compositions. However, it is known form Wada et al.'s work that domain engineering can be realized

also in $[111]_C$-oriented $BaTiO_3$ single crystals.[2] If engineered domain states are important for fatigue anisotropy, tetragonal relaxor ferroelectrics may also demonstrate fatigue resistance along $<111>_C$ orientations. Even though $[111]_C$-oriented tetragonal PZN-PT crystals fatigued in this study, such compositions were not relaxor ferroelectric. This should be studied and contrasted with tetragonal but still relaxor single crystals. This will clarify whether a relaxor nature or domain engineering is critical for fatigue anisotropy and free behavior in certain orientations.

The polarization relaxation observations of this study suggesting anisotropic behavior should be extended to short time scales and also different temperature and ferroelectric phase regions which are influential on fatigue resistance. A more detailed information on switching currents and time distribution as a function of orientation and fatigue history can be obtained through switching current measurements as described in chapter 1.

The fundamental observations made here can be extended to new relaxor based thin films and also textured (grain oriented) ceramics. With good orientation control, ferroelectric films or textured ceramics can be useful for a variety of applications employing polarization reversal. It would be particularly interesting to check the fatigue anisotropy in a tetragonal phase ferroelectric material without microcracking.

7.3 References

[1] E. L. Colla, S. Hong, D. V. Taylor, A. K. Tagantsev, and N. Setter, Appl. Phys. Lett. **72**, 2763 (2000).
[2] S. Wada, S. Suzuki, T. Noma, T. Suzuki, M. Osada, M. Kakihana, S.-E. Park, L. E. Cross, and T. Shrout, Jpn. J. Appl. Phys. **38**, 5505 (1999).

VITA

Metin Ozgul was born in Tokat, Turkey on March 5, 1973.

❖ Education:

- 1993- B.Sc. in Metallurgical Engineering, Istanbul Technical University, Istanbul, Turkey
- 1998- M.S. in Materials Science and Engineering (Ceramics option), Pennsylvania State University, U.S.A.
- 2003- Ph.D. in Materials Science and Engineering (Ceramics option), Pennsylvania State University, U.S.A.

❖ Honors and Awards:

- Scholarship from The Ministry of Turkish National Education to pursue a graduate degree in the U.S.A. (1996)
- American Ceramic Society Electronics Division's year 2003 "Best Student Presentation Award in Oral Presentation." for an invited talk given at the 27th Annual Cocoa Beach Conference and Exposition on Advanced Ceramics & Composites at Cocoa Beach, FL, January 27-30, 2003.

❖ Selected Publications from This Work:

1. K. Takemura, **M. Ozgul**, S. Trolier-McKinstry, and C. A. Randall, "Fatigue Anisotropy in Single Crystal $Pb(Zn_{1/3}Nb_{2/3})O_3$ - $PbTiO_3$", J. Appl. Phys. **88** (12), 7272-7277 (2000).
2. V.Y. Shur, E. L. Rumyantsev, E. V. Nikolaeva, E. I. Shishkin, I. S. Baturin, **M. Ozgul**, C. A. Randall, "Kinetics of Fatigue Effect", Integr. Ferroelectr. **33** (1-4), 117-132 (2001).
3. **M. Ozgul**, K. Takemura, S. Trolier-McKinstry, and C. A. Randall, "Polarization Fatigue in $Pb(Zn_{1/3}Nb_{2/3})O_3$ - $PbTiO_3$ Ferroelectric Single Crystals", J. Appl. Phys. **89** (9), 5100-5106 (2001).
4. **M. Ozgul**, E. Furman, S. Trolier-McKinstry, and C. A. Randall, "Polarization Relaxation Anisotropy in $Pb(Zn_{1/3}Nb_{2/3})O_3$ - $PbTiO_3$ Single Crystals Ferroelectrics as a Function of Fatigue History," *accepted for publication* in J. Appl. Phys.
5. **M. Ozgul**, S. Trolier-McKinstry, and C. A. Randall, "Influence of Electrical Cycling on Polarization Reversal Processes in $Pb(Zn_{1/3}Nb_{2/3})O_3$-$PbTiO_3$ Ferroelectric Single Crystals as a Function of Orientation," *submitted to* J. Appl. Phys.